

# O-Acyl Sugars Protect a Wild Tobacco from Both Native Fungal Pathogens and a Specialist Herbivore<sup>1</sup>

Van Thi Luu, Alexander Weinhold, Chhana Ullah, Stefanie Dressel, Matthias Schoettner, Klaus Gase, Emmanuel Gaquerel, Shuqing Xu, and Ian T. Baldwin\*

Department of Molecular Ecology (V.T.L., S.D., M.S., K.G., S.X., I.T.B.) and Department of Biochemistry (C.U.), Max Planck Institute for Chemical Ecology, Jena 07745, Germany; Department of Molecular Interaction Ecology, German Centre for Integrative Biodiversity Research, Leipzig 04103, Germany (A.W.); and Centre for Organismal Studies, University of Heidelberg, Heidelberg 69120, Germany (E.G.)

ORCID IDs: 0000-0002-0709-2783 (V.T.L.); 0000-0002-8898-669X (C.U.); 0000-0001-7483-4567 (M.S.); 0000-0003-0796-6417 (E.G.); 0000-0001-7010-4604 (S.X.); 0000-0001-5371-2974 (I.T.B.).

O-Acyl sugars (O-AS) are abundant trichome-specific metabolites that function as indirect defenses against herbivores of the wild tobacco *Nicotiana attenuata*; whether they also function as generalized direct defenses against herbivores and pathogens remains unknown. We characterized natural variation in O-AS among 26 accessions and examined their influence on two native fungal pathogens, *Fusarium brachygibbosum* U4 and *Alternaria* sp. U10, and the specialist herbivore *Manduca sexta*. At least 15 different O-AS structures belonging to three classes were found in *N. attenuata* leaves. A 3-fold quantitative variation in total leaf O-AS was found among the natural accessions. Experiments with natural accessions and crosses between high- and low-O-AS accessions revealed that total O-AS levels were associated with resistance against herbivores and pathogens. Removing O-AS from the leaf surface increased *M. sexta* growth rate and plant fungal susceptibility. O-AS supplementation in artificial diets and germination medium reduced *M. sexta* growth and fungal spore germination, respectively. Finally, silencing the expression of a putative branched-chain  $\alpha$ -ketoacid dehydrogenase E1  $\beta$ -subunit-encoding gene (*NaBCKDE1B*) in the trichomes reduced total leaf O-AS by 20% to 30% and increased susceptibility to *Fusarium* pathogens. We conclude that O-AS function as direct defenses to protect plants from attack by both native pathogenic fungi and a specialist herbivore and infer that their diversification is likely shaped by the functional interactions among these biotic stresses.

In nature, plants are often under attack by multiple enemies, including pathogens and herbivores. The co-evolutionary interactions between plants and their natural enemies are thought to have resulted in the extraordinary diversity of plant secondary metabolites (Ehrlich and Raven, 1964). More than 200,000 secondary metabolites are known from plants (Altman, 1997; Haslam, 1998; Wink, 2011), and both presence/absence polymorphisms as well as quantitative variations in the concentration of individual compounds are commonly found (Moore et al., 2014). While many secondary metabolites are involved in defense against either

pathogens or insect herbivores, some provide protection against both and are considered as generalized defense compounds (Biere et al., 2004). For example, iridoid glycosides increase the resistance to both the generalist herbivore *Spodoptera exigua* and the biotrophic fungal pathogen *Diaporthe adunca* (Biere et al., 2004). For these generalized defense compounds, diffuse rather than pairwise coevolutionary interactions are likely to occur among plants and their enemies (Biere et al., 2004). Balancing selection is thought to act on these traits together with other selective forces, such as abiotic stresses and inherent tradeoffs with growth fitness costs (Moore et al., 2014). Consequently, the quantitative variation of a given secondary metabolite is thought to be constrained in a given plant tissue (Moore et al., 2014). For example, for iridoid glycosides, despite their high putative metabolic production costs (Gershenson, 1994), substantial natural variation in iridoid glycoside concentrations has been reported in *Plantago lanceolata*, ranging from 0% to 10% dry mass (Marak et al., 2003).

Approximately 30% of all vascular plants produce glandular trichomes, which provide physical barriers to insect and pathogen attack and function as production and storage places for various secondary metabolites (Calo et al., 2006; Weinhold et al., 2011; Glas et al., 2012). Terpenoids, phenylpropenes, flavonoids, methyl ketones, and O-acyl sugars (O-AS) are all known to be

<sup>1</sup> This work was supported by the Max Planck Society, the European Research Council (grant no. 293926 to I.T.B.), and the Deutsch Forschungsgemeinschaft (grant no. SFB 1127 and grant no. FZT 118 to the German Centre for Integrative Biodiversity Research).

\* Address correspondence to [baldwin@ice.mpg.de](mailto:baldwin@ice.mpg.de).

The author responsible for distribution of materials integral to the findings presented in this article in accordance with the policy described in the Instructions for Authors ([www.plantphysiol.org](http://www.plantphysiol.org)) is: Ian T. Baldwin ([baldwin@ice.mpg.de](mailto:baldwin@ice.mpg.de)).

V.T.L., A.W., K.G., E.G., S.X., and I.T.B. designed the study; V.T.L., A.W., C.U., S.D., M.S., and K.G. carried out experiments; V.T.L., A.W., C.U., S.D., M.S., and K.G. analyzed data; V.T.L., A.W., C.U., S.D., M.S., K.G., E.G., and S.X. prepared the article, which I.T.B. revised.

[www.plantphysiol.org/cgi/doi/10.1104/pp.16.01904](http://www.plantphysiol.org/cgi/doi/10.1104/pp.16.01904)

produced in trichomes (Gang et al., 2001; Fridman et al., 2005; Treutter, 2006; Gershenzon and Dudareva, 2007; Glas et al., 2012). O-AS consist of branched-chain fatty acids (BCFAs) esterified to the hydroxyl groups of glucose (Glc) or sucrose (Suc). Most O-AS harbor monoacyl, diacyl, or triacyl sugars, and acyl groups are esterified to the sugar backbone via O-acylation (Puterka et al., 2003). In tomato (*Solanum lycopersicum*), the O-acylation requires the sequential action of BAHD ACYLTRANSFERASE1 (AT1) to form the first monoacyl sugar and other BAHD acyltransferases (AT2, AT3, and AT4) to add additional BCFAs or acetyl groups to the Suc backbone (Kim et al., 2012; Schillmiller et al., 2012, 2015; Fan et al., 2016). The BCFAs or straight-chained fatty acids incorporated in O-AS are derived from branched-chain amino acids (i.e. Val, Leu, and Ile; Walters and Steffens, 1990). In tobacco (*Nicotiana* spp.) and petunia (*Petunia* spp.), the elongation of BCFAs involves  $\alpha$ -ketoacid elongation (Kroumova and Wagner, 2003). Branched-chain ketoacid molecules are activated as acyl-CoA esters by the branched-chain ketoacid dehydrogenase (BCKD) protein complex, and these acyl-CoA esters are used for O-acylation to produce O-AS (Slocombe et al., 2008). O-AS are found in trichomes of many solanaceous genera, including *Solanum*, *Nicotiana*, *Datura*, and *Petunia* (Chortyk et al., 1997; Kroumova and Wagner, 2003). They accumulate in large amounts in *Solanum pennellii* (approaching 20% leaf dry mass; Fobes et al., 1985). Trichome-specialized metabolites are thought to be particularly evolutionarily variable (Sallaud et al., 2009; Schillmiller et al., 2009; Gonzales-Vigil et al., 2012), as seen among different *S. pennellii* or *S. habrochaites* natural accessions, in which O-AS levels vary in total amounts, the proportion of Suc or Glc backbones, and the types of fatty acid esters to the sugar backbones (Shapiro et al., 1994; Kim et al., 2012). However, the biotic selection pressures that shape these patterns of natural variation remain unknown.

O-AS play important roles in plant defense against insect herbivores. It has been shown that O-AS can deter or repel aphids, beet armyworms, and leaf miners (Goffreda et al., 1989; Hawthorne et al., 1992; Juvik et al., 1994; Puterka et al., 2003). O-AS also were known to be excellent emulsifiers and surfactants that readily adhere to arthropod cuticles and, thereby, can immobilize or suffocate arthropods (Puterka et al., 2003; Wagner et al., 2004). In *Datura wrightii*, a mixture of O-AS was found to be responsible for the delayed development of *Manduca sexta* larvae (Van Dam and Hare, 1998) and moderately deterrent to the feeding of the tobacco flea beetle (*Epitrix hirtipennis*) and a weevil (*Trichobaris compacta*; Hare, 2005). The function of O-AS in defense against pathogens is much less well studied despite a long history of investigations. Kato and Arima (1971) reported that *Escherichia coli* was inhibited by synthetic Suc monolaurate, and later, this activity was extended to other gram-positive bacteria (Kato and Shibasaki, 1975). Marshall and Bullerman (1986) showed that Suc fatty acid ester emulsifiers had antimycotic activity against several fungal genera, including *Penicillium*, *Alternaria*, *Cladosporium*, and

*Aspergillus*. However, none of these studies was conducted with natural O-AS. Chortyk et al. (1993) studied plant-derived O-AS produced by several *Nicotiana* species and demonstrated their antibiotic activities against several gram-positive and gram-negative bacteria. Based on these results, we hypothesized that natural O-AS would have a wide range of antipathogen activities.

O-AS are found in high concentrations in the trichomes of *Nicotiana attenuata*, a wild tobacco plant that grows in the Great Basin Desert of the United States (Roda et al., 2003; Weinhold and Baldwin, 2011; Weinhold et al., 2011). This plant is well known for its fire-chasing germination behavior and growth in the immediate postfire environment, where it faces the pressures of highly variable herbivore and pathogen challenges (Baldwin, 2001). Herbivores from more than 20 different taxa, including both generalists (*Spodoptera litura*) and specialists (*M. sexta*), attack the plant (Baldwin, 2001). O-AS have been shown to function as indirect defenses against the specialist herbivore *M. sexta* (Roda et al., 2003; Weinhold and Baldwin, 2011). Neonate larvae frequently consume the exudates of glandular trichomes as their first meal, and later-stage larvae consume entire trichomes as they ingest shoot materials. When O-AS enter the high-pH environment of the larval midgut, the BCFAs are deesterified to give their bodies and frass a distinctive odor that attracts ground-foraging predators, such as the omnivorous ant *Pogonomyrmex rugosus* (Weinhold and Baldwin, 2011). However, it is unknown whether O-AS produced by *N. attenuata* also can directly affect *M. sexta* growth and development and, thereby, also function as a direct defense. *N. attenuata* is also under attack from native fungal pathogens (Schuck et al., 2014; Luu et al., 2015; Santhanam et al., 2015). *Alternaria* and *Fusarium* species are known to infect *N. attenuata* plants in both native and cultivated plantations (Schuck et al., 2014; Santhanam et al., 2015). The jasmonic acid (JA) signaling pathway has been shown to play an important role in the defense of this plant against *Fusarium* species (Luu et al., 2015). However, whether the trichomes of *N. attenuata* and their secondary metabolites, such as O-AS, play a role in defense against these native fungal pathogens remains unknown.

Here, we demonstrate the generalized function of *N. attenuata* O-AS in direct defenses against both a native herbivore and two native pathogens. We characterized the composition of *N. attenuata* O-AS by ultra-high-performance liquid chromatography/quadrupole time-of-flight mass spectrometry (UHPLC/Q-TOF-MS) analysis and identified 15 different O-AS belonging to three structural classes. Among 26 natural accessions, total leaf O-AS levels varied by 3-fold. By analyzing this natural variation and F2 crosses between high- and low-O-AS ecotypes, we found O-AS in *N. attenuata* leaves to be associated with resistance to both fungal pathogens (*Fusarium brachygibbosum* U4 [*Fusarium*] and *Alternaria* sp. U10 [*Alternaria*]) and the herbivore *M. sexta*. Manipulating O-AS contents in vivo by washing leaves or silencing the expression of a putative

branched-chain  $\alpha$ -ketoacid dehydrogenase E1  $\beta$ -subunit-encoding gene (*NaBCKDE1B*) in trichomes revealed that *O*-AS functions in plant defenses against fungal pathogens. The *in vitro* experiment confirmed that *O*-AS and their BCFA substitutions are detrimental to both herbivores and pathogens. From these results, we conclude that *O*-AS in *N. attenuata* function as direct defenses and infer that these defensive functions shape their natural variation.

## RESULTS

### At Least 15 Different *O*-AS Are Found in *N. attenuata*

To estimate the abundance of *O*-AS in *N. attenuata*, we isolated an *O*-AS extract that, after examination by ultra-high-performance liquid chromatography/time-of-flight mass spectrometry (UHPLC/TOF-MS), was found to be dominated by a complex mixture of *O*-AS (Supplemental Fig. S1). Other leaf metabolites, such as nicotine and 17-hydroxygeranylinalool diterpene glycosides (DTGs), were removed completely with different fractioning steps. We isolated 1.5 mg of *O*-AS per 1 g fresh mass of plant tissues. The concentrations of these *O*-AS are comparable to that of the alkaloid nicotine, which is present at 1 mg g<sup>-1</sup> fresh mass in the plant tissue, and DTGs (2.5 mg g<sup>-1</sup> fresh mass; Snook et al., 1997). This makes *O*-AS one of the most abundant groups of secondary metabolites in *N. attenuata*.

To analyze the *O*-AS structures, the *O*-AS extract was separated by preparative HPLC, resulting in 30 fractions containing different *O*-AS. The separation did not resolve all *O*-AS; some fractions contained more than one *O*-AS, and not all were present in a single fraction. We obtained at least 14 fractions containing three or fewer *O*-AS that were suitable for further tandem mass spectrometry (MS<sup>2</sup>) experiments.

The single fractions were injected into a UHPLC/Q-TOF-MS device for MS<sup>2</sup> experiments. We selected electrospray ionization conditions that favored the formation of single sodium adducts and performed MS<sup>2</sup> experiments on the sodium adducts of the molecular ions (M+Na)<sup>+</sup>. The collision-induced dissociation (CID)-MS<sup>2</sup> spectra clearly showed two different kinds of neutral losses, which could be attributed to the loss of a hexose (mass-to-charge ratio [*m/z*] 162.0528 C<sub>6</sub>H<sub>10</sub>O<sub>5</sub>) and an acetylated hexose (*m/z* 204.0633 C<sub>8</sub>H<sub>12</sub>O<sub>6</sub>; Fig. 1A). In addition, the fragment peaks of an acetylated hexose (*m/z* 205.0707 C<sub>8</sub>H<sub>13</sub>O<sub>6</sub><sup>+</sup>) and that of the sodium adduct of a non-acetylated hexose (*m/z* 185.0420 C<sub>6</sub>H<sub>10</sub>O<sub>5</sub>Na<sup>+</sup>) also were observed in the spectra (Fig. 1A). The identity of the hexose could not be explained by the mass of the neutral losses. Since previous reports have shown that the core molecule of *O*-AS is a Suc molecule (Simonovska et al., 2006), the observed peaks likely corresponded to either fructose (Fru) or Glc.

The sodium adducts of triester or tetraester hexoses (e.g. *m/z* 469.2403 [AS4/AS10] or *m/z* 469.2050 [AS12]) were found (Fig. 1A). Since we did not find peaks reflecting a mixed substitution pattern on both sugar

moieties of the Suc core molecule, we inferred that the observed losses corresponded to either acetylated or nonacetylated Fru and that the BCFAs were esterified to only one of the sugars, most likely the Glc as described previously by Arrendale et al. (1990).

From these esterified sugars, there were three neutral losses of different BCFAs observable at *m/z* 116.0837 C<sub>6</sub>H<sub>12</sub>O<sub>2</sub>, *m/z* 102.0681 C<sub>5</sub>H<sub>10</sub>O<sub>2</sub>, and *m/z* 88.0525 C<sub>4</sub>H<sub>8</sub>O<sub>2</sub>. The first mass corresponds to 3-methyl and 4-methyl pentanoic acid, and the second mass corresponds to either 2-methyl or 3-methyl butanoic acid, as reported previously (Weinhold and Baldwin, 2011). The loss of C<sub>4</sub>H<sub>8</sub>O<sub>2</sub> corresponded to either 2-methyl propanoic acid or butanoic acid. To confirm these inferences about the fatty acid substitutions, we saponified the *O*-AS from an *O*-AS extract and subjected them to gas chromatography-flame ionization detection analysis. By comparison with the retention indices of authentic standards, we identified the four major fatty acids described previously (Weinhold and Baldwin, 2011). In addition, we identified 2-methyl propanoic acid, which we predicted from the neutral losses of *m/z* 88.0525 C<sub>4</sub>H<sub>8</sub>O<sub>2</sub> in the MS<sup>2</sup> spectra (Fig. 1B).

In summary, the MS<sup>2</sup> experiments revealed 15 different *O*-AS in *N. attenuata* (Fig. 1C), which were classified into three classes, class 2 (SE-2; Supplemental Fig. S2; Supplemental Table S3), class 3 (SE-3; Supplemental Fig. S3; Supplemental Table S4), and class 4 (SE-4; Supplemental Fig. S4; Supplemental Table S5), according to the scheme of Arrendale et al. (1990) and Ding et al. (2006). Class 2 is the largest class, with six compounds (AS1–AS6) all lacking acetylations of the Glc or Fru moiety, which makes them (tri-*O*-acyl)- $\alpha$ -D-glucopyranosyl- $\beta$ -D-fructofuranosides. Class 3 contains an acetylated Fru moiety resulting in five tri-*O*-acyl- $\alpha$ -D-glucopyranosyl-(*O*-acetyl)- $\beta$ -D-fructofuranosides (AS7–AS11). Class 4 contains four compounds (AS12–AS15) that are characterized by the acetylation of the Fru and Glc moieties and represent (*O*-acetyl-tri-*O*-acyl)- $\alpha$ -D-glucopyranosyl-(*O*-acetyl)- $\beta$ -D-fructofuranosides.

### *O*-AS Levels Vary 3-Fold among 26 *N. attenuata* Natural Accessions

We examined the natural variation in total *O*-AS contents of leaves from different *N. attenuata* accessions using UHPLC/TOF-MS by summing normalized peak areas of all 15 *O*-AS and expressing the totals relative to UT, the well-characterized inbred line. Among the 26 accessions, total *O*-AS varied 3-fold in their quantities, ranging from 0.48- to 1.44-fold of that found in UT (Fig. 2A). The accession A85 had the highest total *O*-AS content, with 44% more than that found in UT, while A83 and A84 had the lowest total *O*-AS content, with 45% to 50% of the UT levels of *O*-AS. Interestingly, both high- and low-content accessions were collected from the same region (Supplemental Table S1), indicating that *O*-AS contents are highly variable within native *N. attenuata* populations.

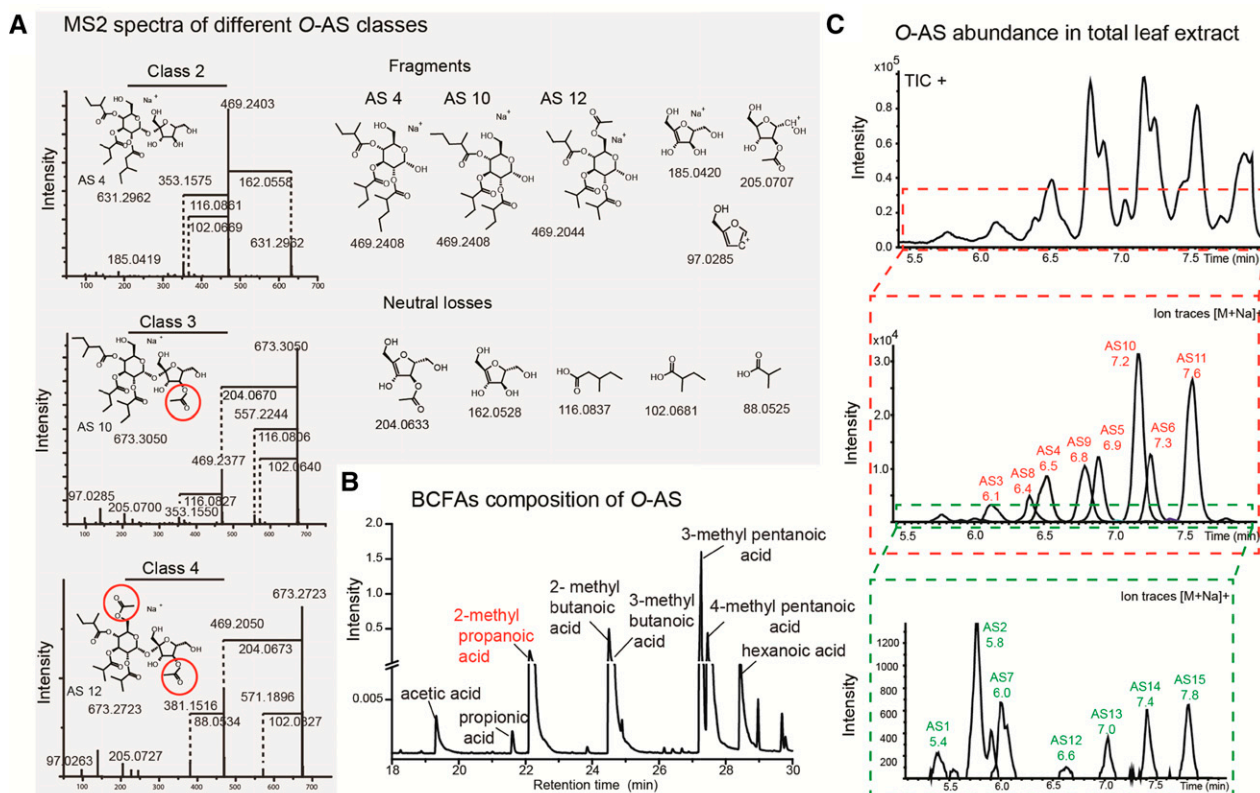


**Figure 1.** *O*-AS composition of *N. attenuata*. A, MS<sup>2</sup> spectra of three *O*-AS sharing the same fragment ion 469 (nominal mass) but belonging to three different structural classes, 2, 3, and 4. Main fragment peaks and neutral losses are annotated. The positions of the fatty acids could not be verified and may vary. MS<sup>2</sup> spectra of all *O*-AS are shown in Supplemental Figures S2 to S4. B, Gas chromatography-flame ionization detection analysis of a saponified *O*-AS extract of *N. attenuata* revealed five major BCFAs: 2-methyl propanoic acid (in red), 2-methyl butanoic acid, 3-methyl butanoic acid, 3-methyl pentanoic acid, and 4-methyl pentanoic acid. Three less abundant acids were identified as acetic acid, propionic acid, and hexanoic acid. C, Total ion current of a positive-mode UHPLC/TOF-MS run (TIC+) from a whole-leaf extract with single ion traces for the sodium adducts [M+Na]<sup>+</sup> of 15 different *O*-AS. Peak annotations correspond to the MS<sup>2</sup> spectral information shown in Supplemental Tables S4 to S6.

Furthermore, we evaluated the variation in *O*-AS composition among the 26 accessions. A heat map showing a hierarchical clustering of the 26 accessions and 15 *O*-AS was created using the MetaboAnalyst 3.0 online software (www.metaboanalyst.ca; Xia et al., 2015). The peak area g<sup>-1</sup> fresh mass data were standardized using autoscaling. The levels of each individual *O*-AS varied significantly among the different accessions (Fig. 2B). For instance, A83, A84, and UT had similar peak areas of AS6 but different peak areas of AS5, AS6, AS10, and AS11 (Fig. 2B; Supplemental Fig. S5). Based on this variation, the 26 natural accessions were classified into three major groups: A, B, and C. UT was grouped together with the high-*O*-AS accessions (group C), such as A179, A176, and A85. A83 and A84 were grouped together with other low-*O*-AS accessions, such as A422, A421, and A278, in group A. The 15 *O*-AS were classed into two groups: group 1 contained *O*-AS class 3 and 4, and group 2 contained all *O*-AS class 1, two *O*-AS class 2, and one *O*-AS class 4 (Fig. 2B). These results indicate that the *O*-AS clustering based on cross-individual expression patterns does not overlap with the *O*-AS classes, suggesting that the variation in

individual *O*-AS differs from the variation in *O*-AS classes. In addition, by plotting the three groups of natural accessions (A, B, and C) on a map, some accessions that belong to different groups were seen to locate near each other (e.g. A331 and A214, A384 and A382, or A83, A84, and A85; Supplemental Fig. S6). This points to a lack of geographic associations among accessions that share similar *O*-AS profiles.

#### Natural Accessions with Lower Levels of *O*-AS Are More Susceptible to Native Herbivore and Fungal Pathogens

Because the genes responsible for *O*-AS composition are not yet elucidated in *N. attenuata*, it was not possible to genetically manipulate specific groups of the *O*-AS chemotype to investigate their ecological functions. Hence, we took advantage of the natural variations in the total *O*-AS pools produced in *N. attenuata* leaves to examine their overall defensive function. We selected two natural accessions, A83 and A84, which had lower levels of *O*-AS compared with UT (Fig. 2A), for herbivore and

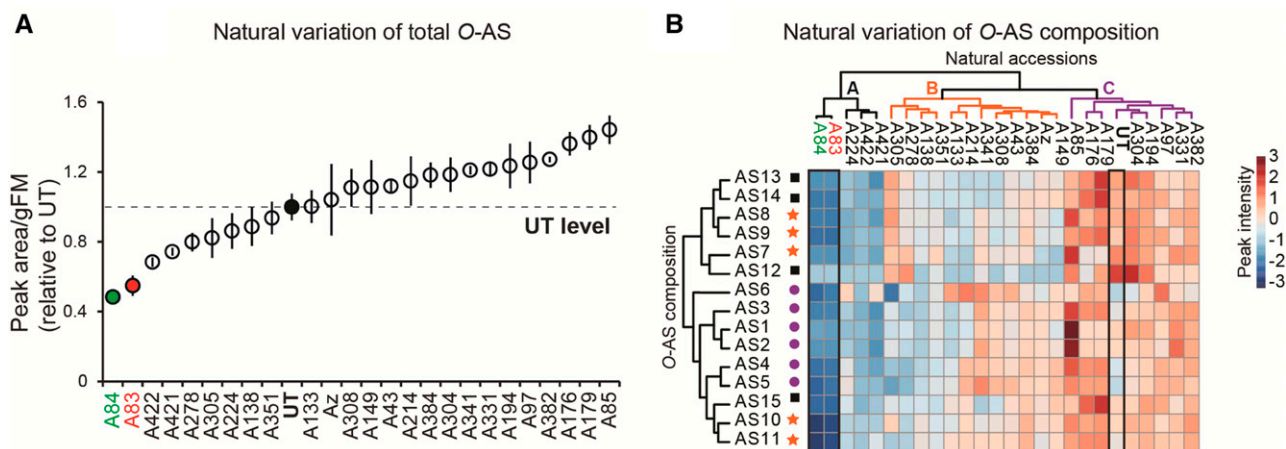


**Figure 2.** Natural variation in *O*-AS levels among 26 natural accessions. A, Relative abundance of total *O*-AS among different accessions. Three biological replicates for each natural accession were used to estimate *O*-AS content. The average peak area per gram fresh mass (peak area/gFM) was normalized to that of the UT accession. B, Heat map showing the hierarchical clustering of 26 accessions and the 15 *O*-AS based on peak area per gram fresh mass data in MetaboAnalyst (distance measure using Euclidean, and clustering algorithm using complete linkage). The degree of peak intensity for each individual *O*-AS is denoted by a different color from blue (low) to red (high). The *O*-AS classes 2, 3, and 4 are indicated by circles, stars, and squares, respectively.

pathogen bioassays. Newly hatched *M. sexta* larvae were allowed to feed on A83, A84, and UT plants. We found that the *M. sexta* larvae that had fed on A83 and A84 plants had larger mass compared with those that fed on UT plants (Supplemental Fig. S7A). A83 and A84 differed from UT not only in *O*-AS levels but also in other traits, such as having a higher trichome density, broader leaves, and smaller stem diameters, and were delayed in bolting and flowering times (Supplemental Fig. S8). Thus, the observed difference in *M. sexta* performance may have resulted from traits in addition to *O*-AS contents.

Because JA signaling is crucial for *N. attenuata*'s herbivore resistance (Baldwin, 1998), we examined the JA signaling pathway in A83 and A84 after mimicking herbivore attack. Oral secretions (OS) of *M. sexta* were immediately applied to leaf puncture wounds, and phytohormones including JA and JA-Ile were measured at 1 h; nicotine, DTGs, and trypsin proteinase inhibitors (TPIs) were measured at 48 h after elicitation. The two natural accessions were not compromised in most of the JA signaling-associated compounds compared with UT (Supplemental Fig. S7B). JA was induced significantly higher in A83 plants compared with UT plants (Student's *t* test,  $P = 0.04$ ), while JA-Ile was significantly higher in both A83 and A84 plants (Student's *t* test,  $P = 0.007$  for A83 and  $P = 0.008$  for A84). These two accessions also had significantly higher levels of TPI compared with UT after OS elicitation (Student's *t* test,  $P = 0.001$  for A83 and  $P = 0.01$  for A84). A83 had higher levels of constitutive and induced DTGs compared with UT (Student's *t* test,  $P = 0.02$ ). While A83 showed no significant difference in nicotine induction, A84 had 38.9% lower levels than UT (Supplemental Fig. S7B). Interestingly, *O*-AS levels of A83, A84, and UT were not changed by OS elicitation, and the two accessions had lower constitutive and induced total

*O*-AS levels compared with UT (Supplemental Fig. S7C). We conclude that the two natural accessions have lower *O*-AS contents but stronger inductions of the JA signaling pathway after OS elicitation.

To assess the herbivore and pathogen susceptibility of the two natural accessions while minimizing the side effect of induced defenses, we used detached leaves to feed *M. sexta* larvae and inoculate with native fungal pathogens. *M. sexta* fed on A83 and A84 detached leaves attained greater mass than those fed on UT plants after 12 d of feeding (DOF; Student's *t* test,  $P = 0.028$  for A83 and  $P = 0.037$  for A84; Fig. 3A). Both *Fusarium* and *Alternaria* caused significantly larger necrotic lesions on A83 and A84 than on UT detached leaves at 5 d post inoculation (DPI; Student's *t* test,  $P < 0.001$  for both *Fusarium* and *Alternaria*; Fig. 3, B and C). From these results, we conclude that the two accessions A83 and A84 are more susceptible to *M. sexta* and fungal pathogens than UT. In conclusion, the natural accessions A83 and A84 are more susceptible to herbivore and pathogen attack while containing lower levels of total leaf *O*-AS but higher levels of herbivore-induced defenses, with the exception of nicotine.

## F2 Crosses Reveal That the Overall *O*-AS Pool Is Associated with Resistance against Both Fungal Pathogens and Herbivores

While the two natural accessions A83 and A84 were more susceptible to an herbivore and pathogens, they also differed in morphology as well as defense-related traits, pointing to genetic differences. To segregate their genetic backgrounds via natural recombination, we created F2 genetic crosses between UT and A84. Thirty independent crosses were made, and a pooled population of F2 individuals was created (Fig. 4A). We measured

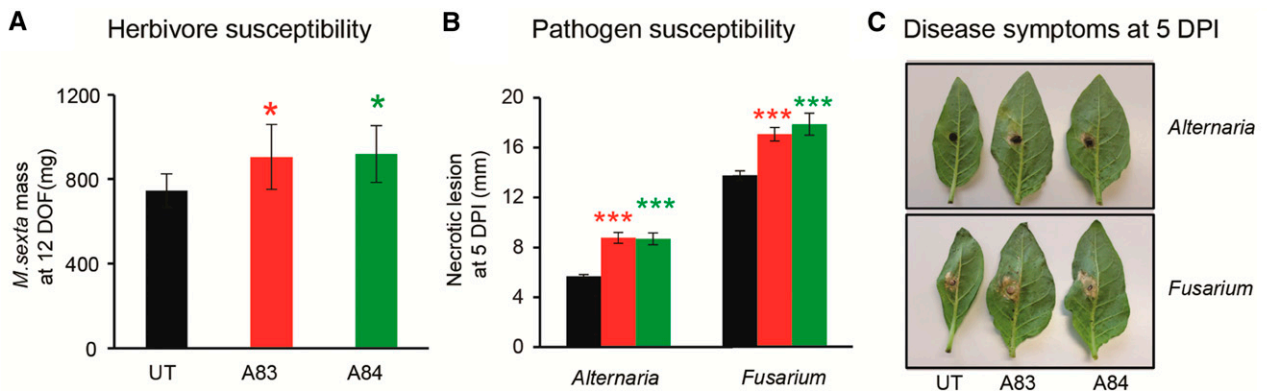


**Figure 3.** Two low-*O*-AS accessions were more susceptible to a native herbivore and pathogens. A, *M. sexta* larvae fed on A83 (red bar) and A84 (green bar) plants gained more mass than those fed on UT (black bar) plants after 12 DOF (days of feeding). B, *Fusarium* and *Alternaria* infection resulted in larger necrotic lesions on leaves of A83 and A83 than UT at 5 DPI (days post inoculation). Error bars represent SE ( $n = 30$ ). Asterisks indicate significant differences between A83 (red asterisks) or A84 (green asterisks) and UT at a given treatment (Student's *t* test: \*\*\*,  $P \leq 0.001$  and \*,  $P \leq 0.05$ ). C, Necrotic lesions caused by *Alternaria* and *Fusarium* on detached leaves of UT, A83, and A84 at 5 DPI.

*O*-AS contents among 162 F2 individuals and selected 30 individuals that had similar *O*-AS levels to UT (UT-like) and 30 individuals that had similar *O*-AS levels to A84 (A84-like) for herbivore and pathogen bioassay. *M. sexta* larvae that had fed on detached leaves of A84-like gained more mass than those that fed on UT-like at 9 DOF (Student's *t* test,  $P < 0.001$ ; Fig. 4B). The caterpillars also developed faster on A84-like than on UT-like as they reached higher instar stages at 9 DOF (*G* test,  $P = 0.004$ ). This indicates that the A84-like group is more susceptible to *M. sexta* than the UT-like group. Furthermore, both *Fusarium* and *Alternaria* challenge resulted in larger necrotic lesions on A84-like than on UT-like plants at 5 DPI (Student's *t* test,  $P = 0.011$  for *Fusarium* and  $P = 0.015$  for *Alternaria*; Fig. 4C), indicating that A84-like individuals are more susceptible to these fungal pathogens than UT-like individuals. Since the 30 individuals in each group were segregated in their genetic backgrounds but were similar in *O*-AS contents, we conclude that the level of total *O*-AS in leaf is associated with defenses against both fungal pathogens and herbivore.

#### Removing *O*-AS from Leaf Surfaces Increased Caterpillar Growth and Fungal Necrotic Lesions

To further explore the involvement of *O*-AS in *N. attenuata*'s defense against insects and pathogens, we manipulated the leaf *O*-AS content by removing them from the leaf surfaces via leaf washing. To test whether washing with water was a suitable method to remove *O*-AS, leaf discs were punched from UT leaves and sonicated in water for 10 min. The first and second washes were analyzed separately. We observed that this washing method removed the trichome droplets without destroying the trichome structure (Fig. 5A). The first water wash is sufficient to remove most of the leaf surface metabolites (Fig. 5B). Compared with

whole-leaf extracts (Supplemental Fig. S1), the nicotine peak intensity in the first water wash was relatively low, indicating that washing by water removed mainly *O*-AS. Using the same washing technique, washes of A83 and A84 leaves showed lower total *O*-AS compared with those of UT (Supplemental Fig. S9), suggesting that this method also is suitable for comparing total *O*-AS among different genotypes. To be able to wash a large number of leaves for feeding and pathogen assays, we simply soaked leaves with an excess of water for 30 s. The washed leaves contained only 25% of their total *O*-AS by this method (Fig. 5C).

To evaluate whether removing *O*-AS from the leaf surface alters plant defenses, we performed herbivore and pathogen bioassays on *N. attenuata* washed leaves. We found that *M. sexta* larvae that fed on washed leaves were significantly heavier than those that fed on unwashed leaves (Student's *t* test,  $P < 0.001$ ; Fig. 5D). Necrotic lesions caused by *Fusarium* or *Alternaria* were significantly larger on washed leaves in comparison with unwashed leaves (Student's *t* test,  $P < 0.001$  for *Fusarium* and  $P = 0.017$  for *Alternaria*). These data demonstrate that removing *O*-AS from leaf surfaces increases *N. attenuata* susceptibility to herbivore and fungal pathogens.

#### Silencing *NaBCKDE1B* in Trichomes Led to 20% to 30% Reductions in Total Leaf *O*-AS and Increased Susceptibility to *Fusarium* Fungal Pathogen

To genetically manipulate the *O*-AS content of *N. attenuata* in vivo, we searched for candidate genes that may control *O*-AS biosynthesis in this plant. The BCKD complex is known to control the production of BCFAs that are used for *O*-AS production (Fig. 6A; Slocombe et al., 2008). Using virus-induced gene silencing, Slocombe et al. (2008) demonstrated that silencing a

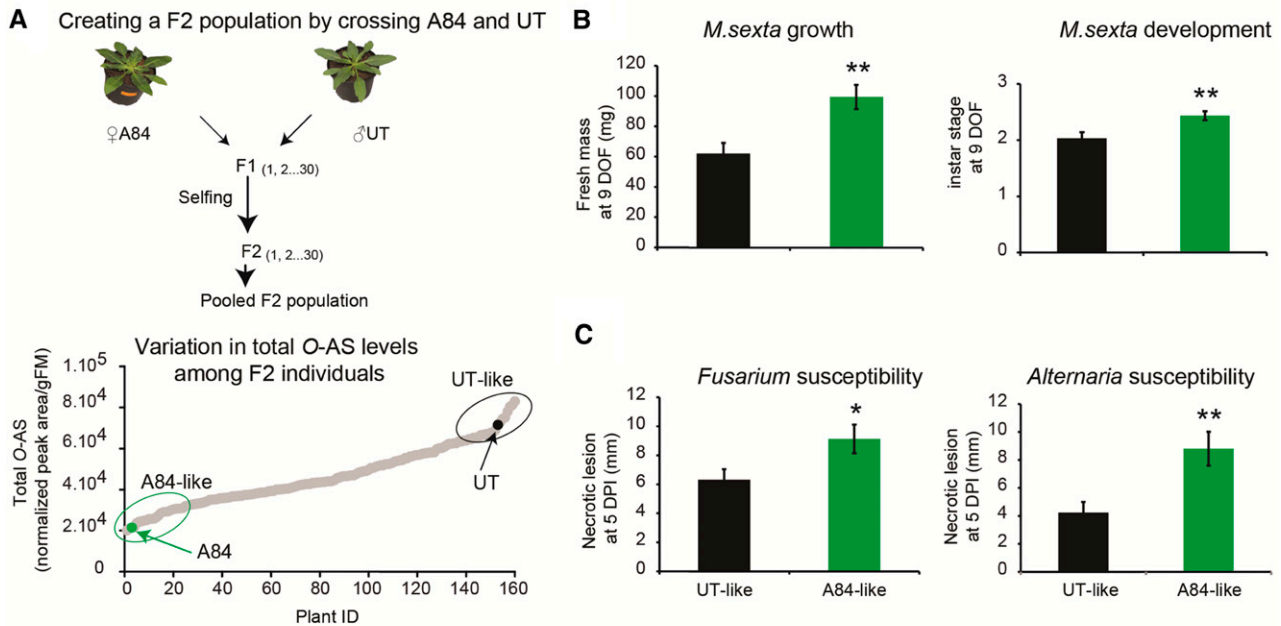


**Figure 4.** O-AS levels were associated with growth rates of *M. sexta* and fungal susceptibilities. A, Diagram showing how the genetic crosses for the F2 population were created, from which two groups of plants ( $n = 30$ ) were selected based on their O-AS contents. B, *M. sexta* larvae that fed on UT-like plants showed reduced mass and delayed development in comparison with those that fed on A84-like plants after 9 DOF (days of feeding). C, *Fusarium* and *Alternaria* caused larger necrotic lesions on A84-like plants than on UT-like plants at 5 DPI (days post inoculation). Error bars indicate se. Asterisks indicate significant differences between A84-like and UT-like plants (Student's *t* test for all but *G* test for *M. sexta* development: \*\*,  $P \leq 0.01$  and \*,  $P \leq 0.05$ ).

gene encoding an E1  $\beta$ -subunit of this enzyme complex (*NbBCKDE1B*) reduced total O-AS in *Nicotiana benthamiana* by 70%. In the *N. attenuata* genome, we identified a homolog of this gene with a length of 1,092 bp (Supplemental Fig. S10), named *NaBCKDE1B*. This gene had significantly lower transcript abundance in trichomes of A83 but not in A84, in comparison with UT trichomes (Student's *t* test,  $P = 0.004$ ; Supplemental Fig. S11). Because both A83 and A84 contain less O-AS in comparison with UT, this result suggested the potential involvement of *NaBCKDE1B* and other unknown genes in controlling O-AS level in *N. attenuata*.

To reduce the total O-AS level in *N. attenuata* leaves, we used RNA interference (RNAi) gene silencing via *Agrobacterium tumefaciens* transformation to silence the *NaBCKDE1B* gene. Because O-AS are known to be synthesized in trichomes (Kandra and Wagner, 1988; Kroumova and Wagner, 2003) and to avoid the pleiotropic effect of silencing this gene ectopically, we aimed to silence this gene specifically in trichomes. A trichome-specific promoter from tomato (SIAT2 promoter), described by Schilmiller et al. (2012), was used to drive the expression of a GFP-GUS fusion protein in *N. attenuata* plants (Supplemental Fig. S12A). We checked three independent T1 lines (A-14-175, A-14-181, and A-14-182) for the GUS expression and found that, in two independent T1 lines (A-14-181 and A-14-175), the GUS signals were localized specifically in the tip cells

of trichomes (Supplemental Fig. S12B), which indicated that the SIAT2 promoter could drive the trichome-specific expression of RNAi constructs in *N. attenuata*.

Silencing of the *NaBCKDE1B* gene using the SIAT2 trichome-specific promoter was carried out using an inverted repeat (ir) RNAi construct of *NaBCKDE1B* (Supplemental Fig. S13B). Twelve independent T0 lines were used for screening. Two independently irBCKDE1B T2 transformed lines (A-15-132-10 and A-15-147-2) were found to harbor a single T-DNA insertion (Supplemental Fig. S13A). They also had more than a 78% reduction of *NaBCKDE1B* transcript abundance in trichomes (Fig. 6B) and more than a 40% reduction in leaves (Fig. 6C). The transformed plants had similar morphology (Supplemental Fig. S13D) and trichome density to wild-type plants (Supplemental Fig. S13C). These results indicate that the specific silencing of this gene in *N. attenuata* trichomes does not dramatically influence overall plant physiology. However, total O-AS in these two transgenic lines was reduced by only 20% to 30% in leaf washes (Fig. 6D) and in the whole leaf (Fig. 6E), while the proportion of each O-AS was unaffected (Supplemental Fig. S13F). These data suggest that specific silencing of *NaBCKDE1B* in trichomes does not result in a major change in total O-AS in leaves of *N. attenuata*. As a consequence, although there was a trend for *M. sexta* larvae to attain greater mass when fed on the two irBCKDE1B lines as well as larger necrotic lesions caused

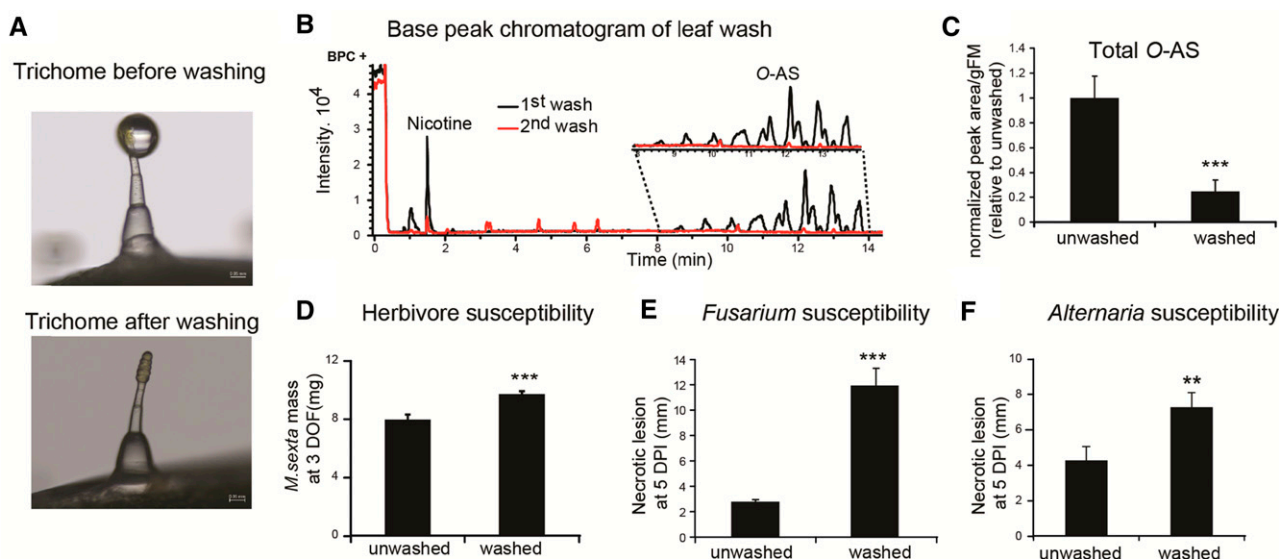


**Figure 5.** Removing *O*-AS from leaf surfaces increased herbivore and fungal susceptibility. A, Images of an *N. attenuata* trichome before and after washing with water. Photographs were taken with an Axio Zoom.V16 stereomicroscope at 180 $\times$  magnification. B, Base peak chromatogram (BPC+) of a positive-mode UHPLC/TOF-MS analysis revealed that leaf washing can efficiently remove most of the leaf trichome *O*-AS. First wash and second wash are indicated by black and red lines, respectively. C, Washing by water removed about 75% of the total leaf *O*-AS. D, *M. sexta* fed on washed leaves gained more mass than those fed on unwashed leaves at 3 DOF (day of feeding) ( $n = 30$ ). E and F, Larger necrotic lesions on washed leaves compared with unwashed leaves caused by *Fusarium* (E) and *Alternaria* (F) at 5 DPI (days post inoculation;  $n = 10$ ). Error bars represent se. Asterisks indicate significant differences between washed and unwashed leaves in a given treatment (Student's *t* test: \*\*\*,  $P \leq 0.001$  and \*\*,  $P \leq 0.01$ ).

by *Alternaria* on these lines, no significant difference was found (Fig. 6, F and H; Supplemental Fig. S14). In the case of *Fusarium*, there was a significant increase in necrotic lesions caused by this fungus on irBCKDE1B lines compared with those on the wild type at 8 DPI (Student's *t* test,  $P < 0.001$  for both 132-10 and 147-2; Fig. 6G). This result indicates that specific silencing of *NaBCKDE1B* in trichomes increases susceptibility to *Fusarium*.

#### Adding *O*-AS or a Mixture of the Four Main BCFAs to Artificial Diet or Medium Reduced *M. sexta* Growth, *Fusarium* and *Alternaria* Spore Germination, and Mycelium Growth

To test whether *O*-AS has direct detrimental effects on both the herbivore and pathogens, an *O*-AS extract from an *N. attenuata* plant was added to artificial diets for *M. sexta* and germination medium for *Fusarium* and *Alternaria*. To mimic the normal *O*-AS concentrations found in plants ( $1.5 \text{ mg g}^{-1}$  fresh mass), we produced artificial diets with the *O*-AS concentration of  $1.2 \text{ mg g}^{-1}$  diet. For spore germination, the concentration of *O*-AS was tested within a range of  $0.187$  to  $3 \text{ mg mL}^{-1}$  to see concentration-dependent effects. As a result, *M. sexta* larvae that fed on *O*-AS-containing artificial diets showed significant reductions in their mass compared with those that fed on *O*-AS-free artificial diets (Student's *t* test,  $P = 0.002$  at 12 DOF; Fig. 7A). *Fusarium* germination and hyphal growth were strongly inhibited by *O*-AS, which was already seen at the lowest concentration tested,  $0.375 \text{ mg mL}^{-1}$  (ANOVA,  $F_{4,88} = 244.51$ ,  $P < 0.001$ ). This inhibition

effect increased with increasing *O*-AS concentrations in the germination medium (Fig. 7B; Supplemental Fig. S15). For *Alternaria*, *O*-AS at the concentration of  $0.375 \text{ mg mL}^{-1}$  significantly reduced their hyphal length (ANOVA,  $F_{4,612} = 85.62$ ,  $P < 0.001$ ) but not the percentage of germinated spores. Higher *O*-AS concentrations ( $1.5 \text{ mg mL}^{-1}$ ) were required to significantly reduce the number of *Alternaria* germinated spores (ANOVA,  $F_{4,111} = 12.53$ ,  $P < 0.001$ ). These results indicate that spore germination and growth of *Fusarium* are more sensitive than those of *Alternaria* to *O*-AS. In summary, we conclude that *N. attenuata* *O*-AS strongly inhibit caterpillar growth as well as fungal germination and growth.

In *N. attenuata*, *O*-AS consist of BCFAs esterified to a Suc core molecule. To get insights into the mechanisms of their toxicity, we tested the effect of BCFAs on *M. sexta* growth as well as fungal pathogen germination and growth. A mixture of the four main BCFAs produced in *N. attenuata*, 2-methyl butanoic acid, 3-methyl butanoic acid, 3-methyl pentanoic acid, and 4-methyl pentanoic acid, was created with the proportion of each BCFA reflecting its proportion released from *M. sexta* frass and bodies after *O*-AS ingestion as described by Weinhold and Baldwin (2011; Supplemental Table S7). To compare its effect with *O*-AS, a BCFA mixture of  $1.2 \text{ mg g}^{-1}$  diet was added to the artificial diets, and a range of concentrations (from  $0.187$  to  $3 \text{ mg mL}^{-1}$ ) was added into fungal germination medium. Interestingly, this mixture of BCFAs showed a strong effect on *M. sexta* growth (Student's *t* test,  $P < 0.001$  at 12 DOF; Fig. 7C). Moreover, *Alternaria* and *Fusarium* hyphal length was inhibited significantly at the lowest

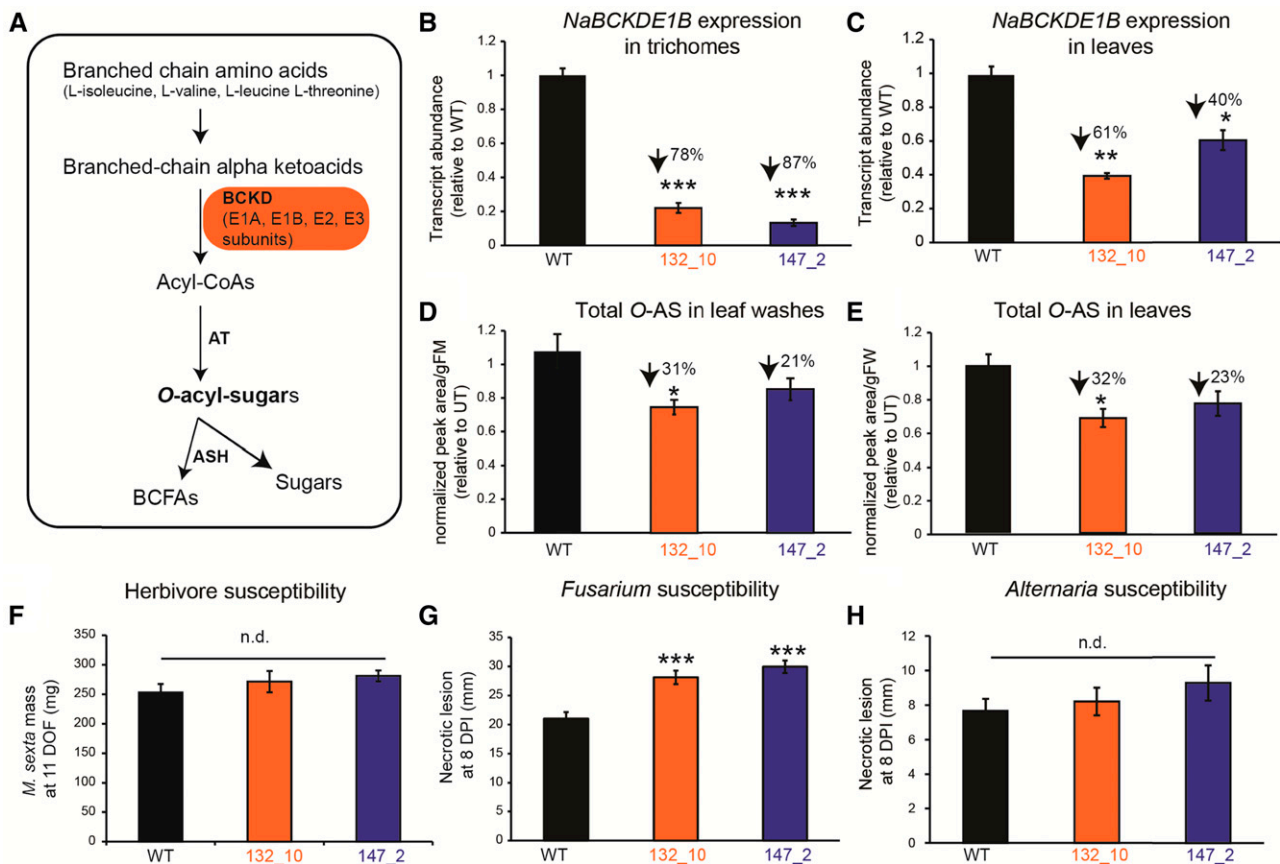


**Figure 6.** Silencing *NaBCKDE1B* in trichomes reduced total leaf O-AS by 20% to 30% and increased susceptibilities to *Fusarium*. A, Diagram shows the simplified model of O-AS biosynthesis in solanaceous plants based on current knowledge. B and C, Trichome-specific silencing of *NaBCKDE1B* resulted in 78% to 87% and 40% to 61% reductions of its transcript abundance in trichomes and whole leaves, respectively ( $n = 6$  for gene expression in leaf,  $n = 3$  [two pooled samples per replicate] for gene expression in trichomes). D and E, Trichome-specific silencing of *NaBCKDE1B* reduced O-AS content to 21% to 31% and 23% to 32% in leaf washes ( $n = 6$ ) and total leaf extracts ( $n = 6$ ), respectively. F, *M. sexta* larvae that fed on detached leaves of wild-type (WT) and irBCKDE1B plants grew similarly at 11 DOF (day of feeding) ( $n = 30$ ). G and H, Necrotic lesions caused by *Fusarium* and *Alternaria* on irBCKDE1B and wild-type detached leaves at 8 DPI, respectively ( $n = 30$ ). Error bars represent se. Asterisks indicate significant differences between the wild type and individual irBCKDE1B lines (Student's *t* test: \*\*\*,  $P \leq 0.001$ ; \*\*,  $P \leq 0.01$ ; and \*,  $P \leq 0.05$ ), n.d. not different.

concentrations tested, 0.187 and 0.375 mg mL<sup>-1</sup>, respectively (ANOVA,  $F_{5,149} = 83.03$  and  $P < 0.001$  for *Alternaria*,  $F_{4,125} = 59.67$  and  $P < 0.001$  for *Fusarium*; Fig. 7D; Supplemental Fig. S16). Spore germination of *Alternaria* and *Fusarium* was reduced significantly at concentrations of 0.375 and 0.75 mg mL<sup>-1</sup>, respectively (ANOVA,  $F_{5,79} = 121.01$  and  $P < 0.001$  for *Alternaria*,  $F_{4,65} = 1,639.2$  and  $P < 0.001$  for *Fusarium*; Fig. 7D). These results indicate that the mixture of four main BCFAs is detrimental to *M. sexta*, *Fusarium*, and *Alternaria*, suggesting that the detrimental effect of O-AS toward the herbivore and the fungal pathogen is due to their BCFA substitutions.

## DISCUSSION

In this study, we characterized 15 O-AS from three structural classes whose concentrations varied 3-fold among natural accessions in *N. attenuata* and demonstrated

their generalized function in defense against a native herbivore and two fungal pathogens. The contents of O-AS in *N. attenuata* natural accessions were associated with plant resistance to two fungal pathogens and a specialist herbivore. In vivo manipulations of O-AS contents via leaf washing or silencing the *NaBCKDE1B* gene in trichomes revealed a crucial role of O-AS in defenses against native fungal pathogens. In vitro experiments confirmed that O-AS and their BCFA substitutions were detrimental to *M. sexta* and fungal pathogens. Hence, this work establishes a direct defense function of O-AS in *N. attenuata* against a specialist herbivore and two native pathogens, which complements the previously established function of O-AS as indirect defenses (Weinhold and Baldwin, 2011).

In *N. attenuata*, total O-AS varied up to 3-fold among 26 natural accessions, which is similar to that reported from *S. pennellii* (2- to 4-fold; Shapiro et al., 1994) but less than that reported from *S. habrochaites* (8-fold;

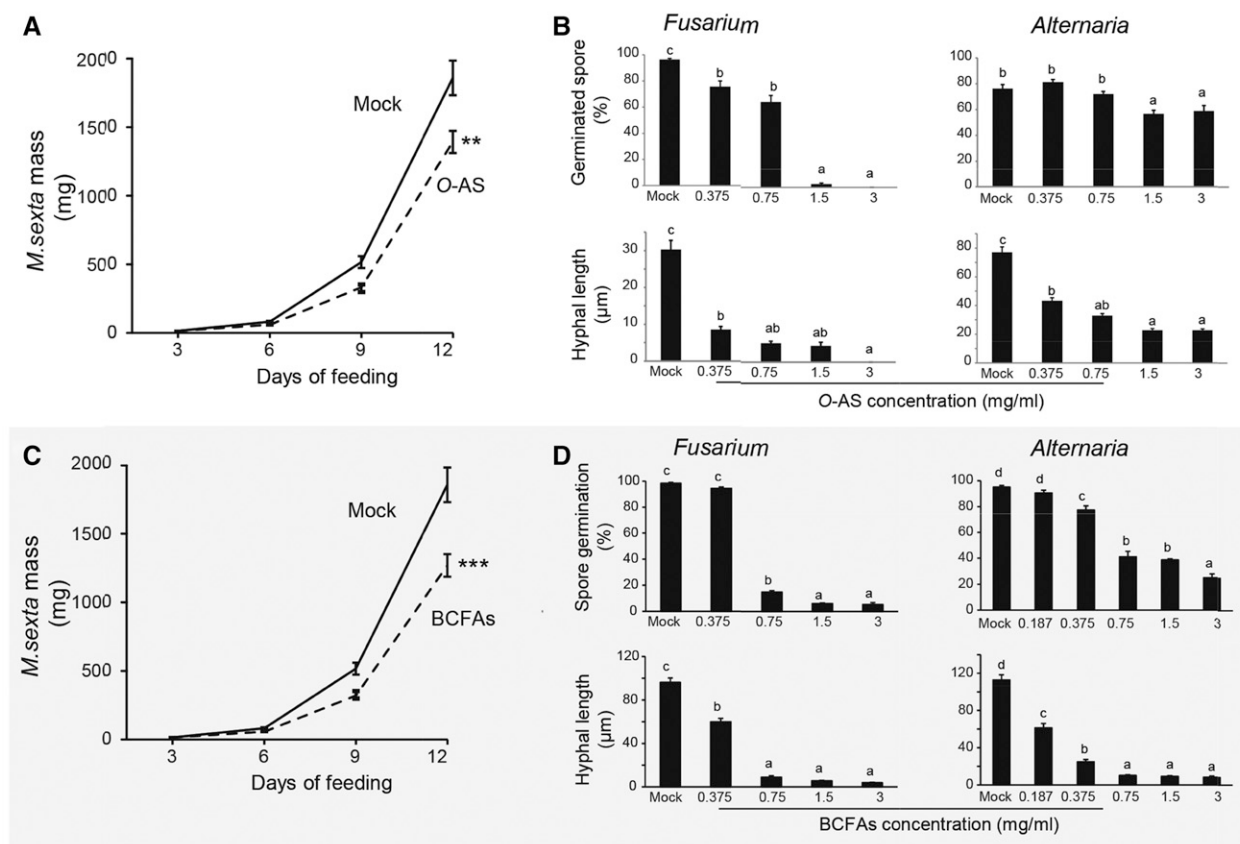


**Figure 7.** Both *O*-AS extracts and a mixture of the four BCFAs suppressed *M. sexta* growth and fungal pathogen germination in vitro. A and C, *M. sexta* larvae grow slower when they are fed artificial diets amended with *O*-AS extracts or a mixture of the four main BCFAs in comparison with those fed a mock diet. Solid lines indicate mock diet, and dashed lines indicate diet amended with *O*-AS extract or the mixture of four BCFAs. Asterisks indicate significant differences between two treatments (Student's *t* test: \*\*\*,  $P \leq 0.001$  and \*\*,  $P \leq 0.01$ ). B and D, Spore germination and hyphal length of *Fusarium* and *Alternaria* fungal on plain agar supplemented with *O*-AS extract or the mixture of four BCFAs with different concentrations. Different letters (a and b) indicate significantly different data groups determined by one-way ANOVA with the Bonferroni posthoc test ( $P \leq 0.05$ ). Error bars indicate SE.

Kim et al., 2012). We also found that accessions collected from the same location have different *O*-AS contents and composition. This large variation in *O*-AS levels within *N. attenuata* populations is consistent with the metabolomic variation within populations reported previously by Li et al. (2015) and likely results from the high genetic variation within *N. attenuata* populations, which, in turn, is associated with the plant's long-lived seed banks and fire-chasing behavior (Bahulikar et al., 2004).

The structural variation found among the 26 natural accessions can be organized into three different groups that differ in the acetylations of the Glc/Fru components of the Suc core. The *O*-AS clustering based on cross-individual expression patterns did not overlap with these *O*-AS classes, indicating that the variation in individual *O*-AS differed from the variation in *O*-AS classes. Interestingly, in *S. habrochaites*, the variation of *O*-AS classes results from variation in a single gene encoding ACYLTRANSFERASE2 and duplication of ACYLSUGAR ACYLTRANSFERASE3 (Kim et al., 2012; Schillmiller et al., 2015). For *N. attenuata*, the mechanisms

responsible for the variation in *O*-AS individual or class remain unknown. As a consequence, the ecological functions of the different classes remain elusive. To gain more knowledge about the functions of individual *O*-AS, fraction-guided bioassays can be used. A prerequisite for such an approach will be the purification of individual *O*-AS, which could be obtained with further modifications of the reverse-phase HPLC method used in this study, such as developing longer or more aggressive mobile phase gradients, as done by Ghosh et al. (2014). Since each *O*-AS has a particular combination of BCFAs, we speculate that the functions of individual *O*-AS depend on the proportion and composition of BCFA chains, whereby a larger number of acidic substituents increases the lipophilicity of a given *O*-AS. Since *O*-AS are important leaf surface chemicals exuded by trichomes, increased lipophilicity might be advantageous for the exudation and surface adherence process. Furthermore, *O*-AS are thought to damage the membranes of soft-bodied insects and cause their death by desiccation (Puterka et al., 2003). According

to this scenario, a greater lipophilicity could increase the defensive function of *O*-AS. In this study, the mixture of the four main BCFAs, 2-methyl butanoic acid, 3-methyl butanoic acid, 3-methyl pentanoic acid, and 4-methyl pentanoic acid, alone is detrimental to *M. sexta*, suggesting that BCFAs that are released after *O*-AS digestion are detrimental compounds. We also observed a detrimental effect on both *Fusarium* and *Alternaria*.

For pathogens, BCFAs are well known to disrupt the cell membrane, inhibit the myristoylation of proteins, inhibit  $\beta$ -oxidation, triacylglycerol synthesis, and sphingolipid synthesis, and to have topoisomerase activity, as reviewed by Pohl et al. (2011). For caterpillars, the antifeedant function of BCFAs could involve changes in the artificial diet. However, many other possibilities exist. They may affect the metabolism of the insect, resulting in lower growth rates, inhibit microbial symbionts of the insect, or even function as metabolic toxins. To address these open questions, further experiments, such as Waldbauer assay (Waldbauer, 1968) or food labeling, can be used to quantitatively measure the amount of food assimilated by caterpillars as well as the BCFA flux through the insects. It is also unknown whether an increase in the acyl chain length of *O*-AS is needed to increase insecticidal/fungicidal activities. To answer this question, one could examine the effects of each of the free BCFAs in the mixture individually and in different combinations of BCFAs representing their native mixtures according to the different *O*-AS patterns. Interestingly, in our experiment, we observed that the detrimental effects of BCFAs on *M. sexta* and the pathogens seemed to be greater than the effects of the *O*-AS mixture. We do not know yet whether this is due to the proportion or composition of BCFAs in the reconstructed mixture or to other differences between free BCFAs and esterified BCFAs. Furthermore, if BCFAs are actually the basis of a plant's resistance to both pathogens and herbivores, then why do plants produce BCFAs in their esterified form with the sugar backbone? Weinhold and Baldwin (2011) demonstrated that trichome secretions were frequently the first meal of neonate caterpillars, and the Suc core of *O*-AS could provide a sweet enticement for their ingestion, so that larvae could be olfactory tagged for predation, as an indirect defense. The esterification of BCFAs to sugars also could function as a stable delivery mechanism for these highly volatile BCFAs. As a consequence, for tests of their defense function, it is more relevant to test the function of each *O*-AS rather than each BCFA individually.

To examine the *in vivo* function of *O*-AS, we manipulated the *O*-AS contents by washing the leaf surface with water. About 75% of the total *O*-AS in leaves was removed, and so was nicotine. We do not know yet whether *O*-AS and nicotine function synergistically to enhance plant defense. However, we observed that A84 plants had not only lower *O*-AS contents but also lower nicotine inductions after simulated herbivore attack. We speculate that nicotine-*O*-AS synergisms

are responsible for the greater *M. sexta* larvae growth on the A84 plants compared with those fed on A83 or UT plants. The washing treatment also could damage trichomes and leaf surfaces, resulting in wound responses that increase flavonol content, which may influence herbivore and pathogen susceptibility (Malhotra et al., 1996; Faini et al., 1997; Roda et al., 2003). Therefore, the differences in herbivore and pathogen susceptibility cannot be attributed solely to the difference in *O*-AS contents between washed and unwashed leaves. Further studies on the interactions of *O*-AS with other herbivore and pathogen defensive compounds could significantly further our general understanding of plant biology and physiology. Such studies, however, require knowledge not only about *O*-AS biosynthetic pathways but also those of other defensive compounds.

To provide a cleaner manipulation of *O*-AS contents *in vivo*, we stably silenced the expression of *NaBCKDE1B* in *N. attenuata*. To avoid the pleiotropic effect of silencing this gene throughout the plant via its function in branched-chain amino acid catabolism in different tissues (Peng et al., 2015), we specifically silenced this gene in *N. attenuata* trichomes, which are known to be an important location of *O*-AS biosynthesis in solanaceous species (Kandra and Wagner, 1988; Kroumova and Wagner, 2003). In *N. attenuata*, staining *O*-AS with Rhodamine B also showed that *O*-AS are highly accumulated in trichomes (Weinhold and Baldwin, 2011). Therefore, we expected that silencing a gene controlling *O*-AS levels in trichomes would reduce total leaf *O*-AS. We obtained two independent transgenic lines with more than 78% reduction of *NaBCKDE1B* transcript abundance in trichomes and no influence on trichome density and plant morphology. However, the specific silencing of *NaBCKDE1B* in trichomes only resulted in a 20% to 30% reduction of the total *O*-AS in *N. attenuata* leaves. It is possible that the remaining *NaBCKDE1B* protein was sufficient to maintain the activity of the *NaBCKDH* complex. Hence, a complete knockout would be a better tool for tests of the role of this gene. The use of the *SLAT2* promoter in our silencing construct also may explain the anemic reductions in total *O*-AS levels. This promoter specifically drives gene expression in the tip cell of trichomes. While the entire *N. attenuata* trichome contains two to six cells (Fig. 5A; Supplemental Fig. S12), it is unknown whether this gene is expressed only in *N. attenuata*'s trichome tip cell or also is expressed in other trichome cells. Hence, silencing *NaBCKDE1B* only in the trichome tip cells may have minor effects on total *O*-AS levels if *O*-AS also are synthesized in the other trichome cells. In addition, *O*-AS precursors may be transported from leaf mesophyll cells to trichomes to provide BCFA precursors for *O*-AS synthesis in *NaBCKDE1B*-silenced trichomes. Consistent with the existence of a transport system of *O*-AS precursors throughout the plant, Slocombe et al. (2008) demonstrated that transiently silencing *NbBCKDE1B* by virus-induced gene silencing resulted in a 70% reduction in the total *O*-AS in *N. benthamiana*. Since the virus-induced gene silencing was done on the whole plant instead of specifically

targeting trichomes and as it affects *BCKDE1B* transcript abundance in all cells, this procedure could result in a greater reduction in O-AS precursors transported into trichomes to support O-AS biosynthesis. An in vitro synthesis of O-AS using isolated trichomes or detached leaves and  $^{14}\text{C}$ -labeled precursors coupled with the nondestructive O-AS analysis by NMR spectroscopy could be used to test this idea. However, the elucidation of the O-AS biosynthetic pathway and the genes involved in different steps of O-AS biosynthesis would be required for such an experiment.

Recently, the tomato O-AS metabolic network was successfully reconstructed in vitro, where O-AS assembly begins by adding a five-carbon acyl chain to the pyranose ring of Suc by AT1 and followed by the addition of a second acyl chain by AT2 (Fan et al., 2016). AT3 adds the third acyl chain to create triacylsucrose (Schillmiller et al., 2015), and finally, AT4 adds an acetyl group to the pyranose ring of a triacylsucrose acceptor (Kim et al., 2012; Schillmiller et al., 2012). The synthesized O-AS can be hydrolyzed by ACYL SUGAR ACYLHYDROLASE1 (ASH1) and ASH2 (Schillmiller et al., 2016). All of these newly discovered genes involved in O-AS biosynthesis could potentially influence the total O-AS content in the plant, in particular, the first committed step mediated by AT1 and the hydrolysis step of ASH1 and ASH2. In addition, the more upstream genes involving BCFA production, elongation, and activation, such as genes encoding the three subunits of the BCKD complex, Thr deaminase, acetolactate synthase, isopropyl malate synthase, isopropyl malate dehydrogenase, and isopropylmalate dehydratase (Slocombe et al., 2008), also could be considered for their contributions to total O-AS content in the plant. Our gene expression analysis of *N. attenuata* homologs encoding one  $\beta$ -subunit (E1B) and two  $\alpha$ -subunits (E1A) of BCKD (*NaBCKDE1B*, *NaBCKDE1A\_1*, and *NaBCKDE1A\_2*), acyltransferases (*NaAT1* and *NaAT2*), and acyl sugar acylhydrolases (*NaASH1* and *NaASH2*) in the trichomes of two low-O-AS-containing natural accessions, A83 and A84 (Supplemental Fig. S11), suggested that not only genes involved in O-AS synthesis (*NaBCKDE1B*, *NaBCKDE1A\_2*, *NaAT1*, and *NaAT2*) but also genes involved in O-AS degradation (*NaASH2*) potentially control the total O-AS content in *N. attenuata*. In addition, in *N. attenuata*, trichomes may not be the only location of O-AS production; we found high transcript abundance of not only *NaBCKDE1B* but also *NaAT1*, *NaAT2*, *NaASH1*, and *NaASH2* in other tissues, particularly in flower tissues, including corollas, stigmas, ovaries, styles, and nectaries (Supplemental Table S8). At the metabolite level, O-AS are found to be highly accumulated in flower tissues as well as in the root of *N. attenuata* (Li et al., 2016). Therefore, we suspect that, in *N. attenuata*, O-AS or O-AS precursors may be produced or transported among different plant parts. Hence, a detailed O-AS metabolic network for *N. attenuata* would enhance our understanding of O-AS biosynthesis and provide a more efficient means of manipulating O-AS contents in this plant.

Although silencing *NaBCKDE1B* expression in trichomes led only to a 20% to 30% reduction in total leaf O-AS, this modest reduction resulted in a significantly higher susceptibility of the transgenic lines to *Fusarium* but not *Alternaria* challenges. From these results, we infer that *Fusarium* is more sensitive to O-AS compared with *Alternaria*. In our in vitro test, we observed that *Fusarium* spore germination could be inhibited at the low O-AS concentration of  $0.375\text{ mg mL}^{-1}$ , while to inhibit *Alternaria*, the higher concentration of  $1.5\text{ mg mL}^{-1}$  was required. Based on our O-AS extraction results, the O-AS concentration in *N. attenuata* is normally about  $1.5\text{ mg g}^{-1}$  fresh mass. The 20% to 30% reduction of this concentration results in a difference of 0.3 to  $0.45\text{ mg g}^{-1}$  fresh mass, which is equal to  $0.3\text{ to }0.45\text{ mg mL}^{-1}$  O-AS used for the fungal inhibition test. This O-AS range is already sufficient for an in vitro reduction in fungal spore germination and growth of *Fusarium* but not *Alternaria*. A further analysis of the interaction of these fungal pathogens and O-AS could answer the question of why *Fusarium* is more sensitive to O-AS than *Alternaria*. In nature, fungal spores can be dispersed via air and rainfall to land on the leaf surface, where they wait to germinate (Timmer et al., 2003); hence, spores are in direct contact with excreted O-AS on the leaf surface. We speculate that fungal spores can be fully covered by O-AS due to their small size, which makes their germination exquisitely sensitive to O-AS. Recently, it was shown that trichomes can serve as entry points for *Fusarium* infection (Nguyen et al., 2016); hence, not only excreted O-AS but also O-AS retained inside trichomes could act as the first layer of defense against fungal pathogen infections.

In contrast to the small size of fungal pathogens, chewing herbivores such as *M. sexta* have large bodies and, hence, reduced exposures to O-AS. We observed that the effect of O-AS in the artificial diet on *M. sexta*'s mass can be seen already after 6 d of feeding. Thus, we hypothesize that the early developmental stages of caterpillars are more sensitive to O-AS and that O-AS may act as lipophilic exudates that enhance the penetration of other toxic agents into caterpillar via skin contact. To grow, chewing insects need to consume large amounts of leaf tissue. While silencing *NaBCKDE1B* in trichomes led to a reduction of O-AS in the leaf, we do not know if silencing this gene also alters leaf nutrient contents that compromise larval performance on the transgenic lines. In addition, the sensitivity of *M. sexta* to O-AS also may be concentration dependent, and a reduction of 0.3 to  $0.45\text{ mg g}^{-1}$  fresh mass may not be sufficient to result in significant differences in caterpillar growth.

In native environments, *N. attenuata* seeds remain dormant for the long between-fire intervals and germinate when the smoke signal is sensed and leaf litter is removed or pyrolyzed (Baldwin and Morse, 1994); thus, the locations of *N. attenuata* populations, as well as their herbivores and pathogens, are unpredictable. This unpredictability likely accounts for *N. attenuata*'s remarkable plasticity in herbivore and pathogen defense

strategies. Here, we show a substantial variation of *O*-AS among 26 natural accessions, in both total amounts and composition. However, the biotic selection pressures that shape this natural variation remain unknown. A long-standing hypothesis is that the *O*-AS diversity results from the plant-herbivore or plant-pathogen co-evolutionary process. In this study, we provide evidence for a direct defense function of *O*-AS against *M. sexta*, which complements their previously established function as indirect defenses (Weinhold and Baldwin, 2011) and identify *M. sexta* as an important herbivore that may have shaped the *O*-AS natural variation in *N. attenuata*. Furthermore, we show how *O*-AS also function in the resistance against native fungal pathogens, indicating that *N. attenuata* *O*-AS can be considered as generalized defense compounds that play roles in defense against both native pathogens and herbivores. Hence, we suggest that the *N. attenuata* *O*-AS natural variation results from selection pressures from both herbivores and pathogens. Furthermore, the variation in *O*-AS production also can be shaped by other selective forces, such as abiotic stresses, competition effects, and ecological fitness tradeoffs, all of which will require additional research. Answering these questions would help us to understand how the balancing selection is generated and how this selection likely accounts for the great diversity of *O*-AS concentrations and composition in natural accessions.

## MATERIALS AND METHODS

### Plant, Caterpillar, and Fungal Materials and Growth Conditions

We used 26 *Nicotiana attenuata* natural accessions that were collected over the last 20 years in the southwestern United States (Supplemental Table S1). The accessions UT, A83, and A84 were collected from the same region (UT, 37°19'36.26''N, 113°57'53.05''W; A83 and A84, 37°19'34''N, 113°57'38''W). The UT accession used as a control for comparison was inbred for 30 generations, and A83 and A84 were inbred for five generations under glasshouse conditions in Jena, Germany. Seed germination and growth conditions were as described by Krugel et al. (2002).

*Manduca sexta* eggs were from our in-house colony. *M. sexta* eggs were kept in a growth chamber (Snijders Scientific) for 16 h of light at 26°C, 8 h of dark at 24°C, and 65% relative humidity until the larvae hatched. Newly hatched neonates were used for all feeding experiments.

Phytopathogens used in this study were *Fusarium brachygibbosum* U4 and *Alternaria* sp. U10, which were originally isolated from diseased plants grown in a native population in Utah in the United States (Schuck et al., 2014) and shown to be a suitable system for studying *N. attenuata*'s defense against native pathogens (Luu et al., 2015). The fungus was cultured and maintained as described by Luu et al. (2015).

### *O*-AS Isolation and Characterization

To isolate *O*-AS from *N. attenuata* plants, we used a protocol similar to that of Van Dam and Hare (1998). All plant parts except the flowers and roots were harvested. After extraction, the glue-like, brownish-yellow residue was obtained and kept under argon at 4°C until further use for bioassay and MS<sup>2</sup> experiments. A small portion was dissolved in 40% (v/v) methanol and analyzed by UHPLC/TOF-MS to verify the extraction. For details, see Supplemental Methods S1.

To fractionate the *O*-AS for MS<sup>2</sup> experiments, extracted *O*-AS were dissolved in acetonitrile at a concentration of 1 mg mL<sup>-1</sup>. An Agilent 1100 HPLC system equipped with a diode-array detector (DAD) was used, and the fractions were

collected with a Foxy fraction collector (Isco) in 20-mL glass reaction tubes (Schott). Forty fractions of 30 s were cut starting 5 min after injection. The fractions were transferred to scintillation vials, and the solvent was evaporated in a vacuum centrifuge (Eppendorf). The single fractions were then analyzed for their content by injection into the UHPLC/TOF-MS system with conditions described by Weinhold and Baldwin (2011). For details, see Supplemental Methods S1.

For MS<sup>2</sup> experiments, 1 μL of each fraction was separated using the Dionex RSLC system with a Dionex Acclaim RSLC 120 C-18 column (150 × 2.1 mm, 2.2 μm). Mass spectrometry detection was carried out with the UHPLC/Q-TOF-MS system (BrukerDaltonik) operated in positive electrospray ionization mode. Mass calibration was performed using sodium formate clusters (10 mM solution of NaOH in 50:50 [v/v] isopropanol:water containing 0.2% [v/v] formic acid). Elemental formula and mass were calculated with the ACD/Labs 12 ChemSketch calculating tool. For details, see Supplemental Methods S1.

The analysis of *O*-AS BCFA composition was done using a Varian 3800 gas chromatograph equipped with a ZB-Wax-plus column (30 m × 0.25 mm × 0.25 μm; Restek) and a flame ionization detector (Agilent). The identities of the BCFAs were verified by the injection of authentic standards at a concentration of 50 ng μL<sup>-1</sup>. Retention indices were calculated in reference to an alkane standard mixture (C8-C20; Sigma-Aldrich). For more details, see Supplemental Methods S1.

### *O*-AS Relative Comparison Analysis

To cross-compare *O*-AS levels among different accessions or genotypes, we extracted leaf or trichome *O*-AS using a method described by Gaquerel et al. (2010) with some modifications. After extraction, 1-μL supernatants were separated using the Dionex RSLC system with a Dionex Acclaim RSLC 120 C-18 column (150 × 2.1 mm, 2.2 μm). Mass spectrometry detection was carried out with the UHPLC/TOF-MS system operated in positive electrospray mode. Typical instrument settings were described by Gilardoni et al. (2011) and were used with some modification. The peak areas were integrated using extracted ion traces for the sodium adduct [M+Na]<sup>+</sup> of each individual *O*-AS in the QuantAnalysis software version 2.0 SP1 (BrukerDaltonik). The amount was normalized with Suc monolaurate (Sigma) as an internal standard and the fresh mass of the tissue. Total *O*-AS was calculated by summing the normalized peak areas of all 15 *O*-AS. The 15 *O*-AS together with their *m/z* values and retention times are listed in Supplemental Table S2. For details, see Supplemental Methods S1.

To compare *O*-AS in leaf wash among different genotypes, leaf discs of 18 mm diameter was punched from *N. attenuata* fully developed leaves at the rosette stage and placed into a 50-mL Falcon tube. Ten milliliters of MilliQ water containing Suc monolaurate as an internal standard was used to wash the leaf discs by sonication for 10 min. The leaf wash was filtered through paper filters (Whatman), 2 mL of filtered wash was evaporated using a rotary evaporator connected with a CentriVap concentration systems (Labconco) and dissolved in 100 μL of 40% (v/v) methanol, and 1 μL of this extract was analyzed by UHPLC/TOF-MS with conditions as described above.

### Extraction and Analysis of Phytohormones, Secondary Metabolites, and Trypsin Protein Inhibitors

To identify whether A83 and A84 are compromised in the JA signaling pathway in response to herbivory, we evaluated the induction of JA, JA-Ile phytohormones, and their associated secondary metabolites and proteins such as nicotine, DTGs, and TPIs after mimicking *M. sexta* attack. Rosette leaves were wounded using a fabric pattern wheel with three rows of puncture onto each side of the midvein and by directly applying 20 μL of a 1:5 (v/v) MilliQ water-diluted *M. sexta* OS solution. The intact plants were used as a control. The treated leaves were harvested at 1 h after the treatment for phytohormone measurement and at 48 h after induction for secondary metabolites and protein measurement. Five to six biological replicates were used for each treatment.

Phytohormone extraction and quantification were carried out as described by Gilardoni et al. (2011). JA and JA-Ile were quantified by comparing their peak areas with the peak areas of their respective internal standards as described by Wu et al. (2007) and calculated per gram fresh mass. For details, see Supplemental Methods S1.

Nicotine and DTGs were extracted as described above for *O*-AS extraction. Analysis of these metabolites was done using HPLC-diode-array detection as described previously by Keinänen et al. (2001) with some modification (for details, see Supplemental Methods S1). The peak areas were integrated using Chromeleon software (Thermo Fisher), and nicotine in plant tissue was

quantified using an external dilution series of standard mixtures of nicotine. The peak areas were quantified to estimate total DTG contents and normalized to tissue fresh mass. The method was described previously by Kaur et al. (2010)

The qualitative determination of TPI activities was performed by radial diffusion assay relative to protein content as described previously by Van Dam et al. (2001).

## Caterpillar and Fungal Bioassays

The *M. sexta* feeding assay was performed by placing newly hatched *M. sexta* neonates on fully expanded intact or detached leaves from 30-d-old plants. *M. sexta* mass was recorded to assess the performance of larvae.

For *M. sexta* feeding on artificial diet, the artificial diet was prepared as described by Grosse-Wilde et al. (2010). The method of adding *O*-AS into artificial diet was adapted from Van Dam and Hare (1998). While the diet was still liquid and cooling (about 50°C), 600 mg of extracted *O*-AS was dissolved in 5 mL of dichloromethane (DCM) and added into 500 g of diet to achieve a final concentration of 1.2 mg g<sup>-1</sup> diet, which is similar to the concentration of *O*-AS in planta (1.5 mg g<sup>-1</sup> fresh mass, in this study). As a control, 5 mL of pure DCM was added into the medium. The diets were heated and stirred on a hot plate until the DCM had evaporated. The diet was placed in plastic boxes and kept at 5°C until use. To supplement the artificial diet with a mixture of BCFAs, a 600-μL mixture of the four main BCFAs, 2-methyl butanoic acid (19.26 μL), 3-methyl butanoic acid (63.69 μL), 3-methyl pentanoic acid (493.05 μL), and 4-methyl pentanoic acid (23.99 μL), was prepared (Supplemental Table S7). This mixture was added directly to the artificial diet and mixed thoroughly. Freshly hatched *M. sexta* larvae were transferred to plastic containers containing pieces of artificial diet. Thirty plates per diet type and two to three larvae per plate were fed ad libitum in a climate chamber (50% relative humidity, 26°C during days, and 24°C during nights under 12 h of light). Larval mass was measured every 3 d until 12 d.

To test the fungal susceptibility of different plant accessions or genotypes, we used the detached leaf assay that was described by Schuck et al. (2014). At 5, 8, and 10 DPI, the diameters of the smallest and largest necrotic lesions were measured using a caliper. The average of necrotic lesions was calculated and presented as an indicator of plant susceptibility to pathogens.

To test the effect of *O*-AS on fungal spore germination and mycelial growth in vitro, 30 mg of extracted *O*-AS and 30 μL of BCFA mixture were dissolved in 1 mL of DCM and added in 10 mL of spore germination medium, which was composed of 1.2% (w/v) plant agar and 10 mM MgCl<sub>2</sub>. The control medium contained only 1 mL of DCM. The medium was heated in a water bath until the DCM was evaporated. The medium was diluted to attain final concentrations of 3, 1.5, 0.75, and 0.375 mg mL<sup>-1</sup> for *O*-AS and 3, 1.5, 0.75, 0.375, and 0.187 mg mL<sup>-1</sup> for BCFAs. Fungal spores were harvested from 14-d-old cultures as described by Luu et al. (2015). Approximately 2.5 mL of spore germination medium was spread onto microscope glass slides and allowed to solidify. Then, 10 μL of spore suspension (concentration, 10<sup>8</sup>) was placed on the solid germination medium and spread with an inoculation loop. Eight glass slides were prepared for each treatment, and each of them was kept in a sterile petri dish (9 cm diameter) with moist Whatman paper filters (1 mL of sterile water was added) to maintain the high humidity required for spore germination. The petri dishes were incubated in a dark chamber at 25°C, and spore germination was monitored every 1 h with an inverted light microscope (Axiovert 200; Carl Zeiss Microscopy) coupled with a camera (AxioVision). The spore germination rate was determined after 6 and 12 h for *Alternaria* and *Fusarium*, respectively. Three microscopic fields per slide were photographed randomly and considered as technical replicates. The percentage of germinated spores was calculated based on numbers of spores germinated divided by the total number of spores observed per microscopic field. The hyphal length of the germinated spore in each microscopic field was measured by ImageJ software (Wayne Rasband, National Institutes of Health).

## Trichome-Specific Silencing of *N. attenuata* BCKDE1B Using *Agrobacterium tumefaciens*

Comparing publicly available sequences at the National Center for Biotechnology Information for genes encoding BCKDE1B from *Arabidopsis* (*Arabidopsis thaliana*) and closely related solanaceous species, including *Solanum pennellii* and *Nicotiana tabacum*, with the *N. attenuata* 454 transcriptome (Gase and Baldwin, 2012) and the *Nicotiana attenuata* Data Hub (Brockmüller et al., 2017), we identified one homolog (NIATv7\_g34895) in *N. attenuata*.

To elucidate the role of this NIATv7\_g34895 gene in controlling *O*-AS levels in *N. attenuata*, we used RNAi-mediated gene silencing with stable *A. tumefaciens* transformation developed by Krugel et al. (2002). To avoid the pleiotropic

effects of silencing this gene on plant performance, we specifically silenced this gene in trichomes using a trichome-specific promoter, tomato (*Solanum lycopersicum*) SIAT2, as discovered previously by Schillmiller et al. (2012), to drive the expression of a GFP-GUS fusion protein in *N. attenuata* plants. *N. attenuata* 30th inbred plants were transformed using the LBA4404 strain of *A. tumefaciens* as described by Krugel et al. (2002). Three independent T1 transgenic lines (A-14-175, A-14-181, and A-14-182) were selected based on hygromycin resistance, and all showed GUS staining in the tip cell of trichomes, regardless of what type of tissue they were located on (i.e. hypocotyl, cotyledon, stem, leaf, etc.). No GUS staining was seen in other parts of the plant.

To generate irBCKDE1B plants, we cloned a 351-bp fragment of the *NaBCKDE1B* gene (for the sequence, see Supplemental Methods S1) as an inverted repeat construct into pRESC8TRCAS transformation vector containing a hygromycin resistance gene (*hptII*) as a selection marker and the tomato SIAT2 promoter to specifically silence this gene in the trichome. *N. attenuata* 30th inbred plants were transformed using the LBA4404 strain of *A. tumefaciens* as described by Krugel et al. (2002). Homozygous transgenic lines were selected by screening T2 generation seeds that showed hygromycin resistance, and T-DNA insertions were confirmed by Southern-blot hybridization, using genomic DNA from selected lines and <sup>32</sup>P-labeled PCR fragments of the *hptII* gene as a hybridization probe (Supplemental Fig. S13A) according to Gase et al. (2011). Quantitative real-time PCR was used to select the best silenced transgenic lines: irBCKDE1-132-10 and irBCKDE1147-2. Detailed methods for RNA extraction, cDNA synthesis, and quantitative real-time PCR, as well as primers used, are provided in Supplemental Methods S1.

## GUS Staining

Histochemical staining with 5-bromo-4-chloro-3-indolyl glucuronide was done using the protocol described by Jefferson et al. (1987). GUS staining was observed with the Zeiss SV 11 stereomicroscope at 4× magnification.

## Trichome Density Determination

Trichome density was determined by counting trichomes on the adaxial and abaxial sides of leaf discs of three different laminar positions that span the length of the leaf with the Zeiss Axio Zoom.V16 stereomicroscope at 32× magnification. Trichome densities were calculated as the number of trichomes per mm<sup>2</sup> of leaf area.

## Trichome Harvesting Method

Trichomes were harvested by cutting stems and branches into small pieces of about 5 cm, placed into a 50-mL Falcon tube, and frozen in liquid N<sub>2</sub>. Frozen tissues were shaken thoroughly for 30 s, and dislodged trichomes were collected into a 2-mL Eppendorf tube and ground for RNA extraction.

## Statistical Analysis

Statistics were performed using Excel (Microsoft; <http://www.microsoft.com>) and the SPSS software version 17.0 ([www.spss.com](http://www.spss.com)). Statistical significance was evaluated using one-way ANOVA at the 0.05 level, and means were compared by the Bonferroni posthoc test. For analysis of differences in plant performance, Student's *t* test was used with the two-tailed distribution of two sets of samples. The number of replicates (*n*) used in each experiment is detailed in the figure legends.

## Accession Numbers

The coding sequences have been submitted to the GenBank/EMBL data libraries as locus tags A4A49\_34895 (NIATv7\_g34895), A4A49\_19321 (NIATv7\_g19321), A4A49\_12742 (NIATv7\_g12742), A4A49\_04553 (NIATv7\_g04553), A4A49\_42350 (NIATv7\_g42350), A4A49\_11346 (NIATv7\_g11346), and A4A49\_41468 (NIATv7\_g41468).

## Supplemental Data

The following supplemental materials are available.

**Supplemental Figure S1.** Total ion chromatogram of a positive-mode UHPLC/TOF-MS run of a whole-leaf extract compared with an *O*-AS extract.

**Supplemental Figure S2.** MS<sup>2</sup> spectra of class 2 *O*-AS and the annotation of the main fragment peaks and neutral losses.

- Supplemental Figure S3.** MS<sup>2</sup> spectra of class 3 O-AS and the annotation of the main fragment peaks and neutral losses.
- Supplemental Figure S4.** MS<sup>2</sup> spectra of class 4 O-AS and the annotation of the main fragment peaks and neutral losses.
- Supplemental Figure S5.** O-AS composition of A83, A84, and UT plants.
- Supplemental Figure S6.** Locations of the collection sites of 26 accessions in Utah, Nevada, Arizona, and California.
- Supplemental Figure S7.** Two low-O-AS accessions are not compromised in JA signaling but more susceptible to the specialist herbivore.
- Supplemental Figure S8.** Morphological differences between UT, A83, and A84 plants.
- Supplemental Figure S9.** A83 and A84 show less O-AS in the water wash compared with UT.
- Supplemental Figure S10.** Phylogenetic relationships of genes encoding NaBCKDE1B among *N. attenuata* and other closely related species.
- Supplemental Figure S11.** Gene expression in trichomes of UT in comparison with A83 and A84.
- Supplemental Figure S12.** Expression specificity of the tomato trichome-specific promoter in *N. attenuata*.
- Supplemental Figure S13.** Creating irBCKDE1B transgenic lines using *A. tumefaciens* transformation.
- Supplemental Figure S14.** Detached leaf assay on irBCKDE1B transgenic lines.
- Supplemental Figure S15.** Effects of O-AS on fungal pathogens.
- Supplemental Figure S16.** Effects of BCFAs on fungal pathogens.
- Supplemental Table S1.** GPS coordinates of 26 natural accessions.
- Supplemental Table S2.** List of *m/z* and retention times used to identify and measure O-AS.
- Supplemental Table S3.** BCFAs compositions of *N. attenuata* O-AS.
- Supplemental Table S4.** MS<sup>2</sup> spectral data showing the annotation of class 2 O-AS elemental formulas, their calculated monoisotopic mass, the elemental formula of fragment ions, and their annotations, intensity, and *m/z* values compared with the calculated *m/z* values.
- Supplemental Table S5.** MS<sup>2</sup> spectral data showing the annotation of class 3 O-AS elemental formulas, their calculated monoisotopic mass, the elemental formula of fragment ions, and their annotations, intensity, and *m/z* values compared with the calculated *m/z* values.
- Supplemental Table S6.** MS<sup>2</sup> spectral data showing the annotation of class 4 O-AS elemental formulas, their calculated monoisotopic mass, the elemental formula of fragment ions, and their annotations, intensity, and *m/z* values compared with the calculated *m/z* values.
- Supplemental Table S7.** Concentration of each BCFA released from *M. sexta* frass and bodies as described by Weinhold and Baldwin (2011) and in the reconstructed mixture for the artificial diet and spore germination medium.
- Supplemental Table S8.** Relative transcript abundance of O-AS biosynthesis genes among different tissue-specific RNA sequencing libraries.
- Supplemental Methods S1.**

## ACKNOWLEDGMENTS

We thank Dr. Robert Last for providing the SLAT2 promoter; Lucas Cortes Llorca for support with the testing of the trichome-specific promoter in *N. attenuata*; Sven Heiling, Dapeng Li, and Thomas Hahn for analytical technical support; Celia Diezel, Eva Rothe, and Wibke Kroeber for plant transformation; Veit Grabe for Zoom.V16 microscopy instruction; and the Max Planck Institute for Chemical Ecology glasshouse team for nurturing the plants in the glasshouse.

Received December 14, 2016; accepted March 6, 2017; published March 8, 2017.

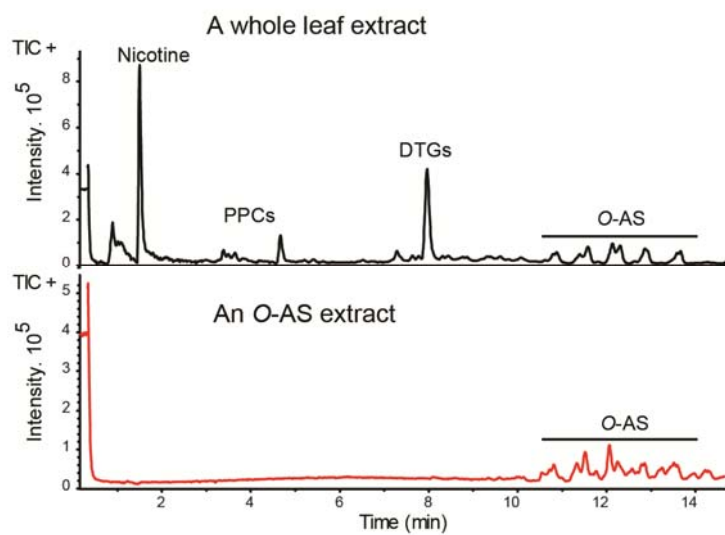
## LITERATURE CITED

- Altman A (1997) Agricultural Biotechnology. CRC Press, Boca Raton, FL
- Arrendale RF, Severson RF, Sisson VA, Costello CE, Leary JA, Himmelsbach DS, Vanhalbeek H (1990) Characterization of the sucrose ester fraction from *Nicotiana glutinosa*. *J Agric Food Chem* **38**: 75–85
- Bahulikar RA, Stanculescu D, Preston CA, Baldwin IT (2004) ISSR and AFLP analysis of the temporal and spatial population structure of the post-fire annual, *Nicotiana attenuata*, in SW Utah. *BMC Ecol* **4**: 12
- Baldwin IT (1998) Jasmonate-induced responses are costly but benefit plants under attack in native populations. *Proc Natl Acad Sci USA* **95**: 8113–8118
- Baldwin IT (2001) An ecologically motivated analysis of plant-herbivore interactions in native tobacco. *Plant Physiol* **127**: 1449–1458
- Baldwin IT, Morse L (1994) Up in smoke. II. Germination of *Nicotiana attenuata* in response to smoke-derived cues and nutrients in burned and unburned soils. *J Chem Ecol* **20**: 2373–2391
- Biere A, Marak HB, van Damme JMM (2004) Plant chemical defense against herbivores and pathogens: generalized defense or trade-offs? *Oecologia* **140**: 430–441
- Brockmöller T, Ling Z, Li D, Gaquerel E, Baldwin IT, Xu S (2017) *Nicotiana attenuata* Data Hub (NaDH): an integrative platform for exploring genomic, transcriptomic and metabolomic data in wild tobacco. *BMC Genomics* **18**: 79
- Calo L, Garcia I, Gotor C, Romero LC (2006) Leaf hairs influence phytopathogenic fungus infection and confer an increased resistance when expressing a trichoderma alpha-1,3-glucanase. *J Exp Bot* **57**: 3911–3920
- Chortyk OT, Kays SJ, Teng Q (1997) Characterization of insecticidal sugar esters of *Petunia*. *J Agric Food Chem* **45**: 270–275
- Chortyk OT, Severson RF, Cutler HC, Sisson VA (1993) Antibiotic activities of sugar esters isolated from selected *Nicotiana* species. *Biosci Biotechnol Biochem* **57**: 1355–1356
- Ding L, Xie FW, Zhao MY, Xie JP, Xu GW (2006) Rapid characterization of the sucrose esters from oriental tobacco using liquid chromatography/ion trap mass spectrometry. *Rapid Commun Mass Spectrom* **20**: 2816–2822
- Ehrlich PR, Raven PH (1964) Butterflies and plants: a study in coevolution. *Evolution* **18**: 586–608
- Faini F, Labbe C, Salgado I, Coll J (1997) Chemistry, toxicity and anti-feedant activity of the resin of *Flourensia thurifera*. *Biochem Syst Ecol* **25**: 189–193
- Fan PX, Miller AM, Schillmiller AL, Liu XX, Ofner I, Jones AD, Zamir D, Last RL (2016) In vitro reconstruction and analysis of evolutionary variation of the tomato acylsucrose metabolic network. *Proc Natl Acad Sci USA* **113**: E239–E248
- Fobes JF, Mudd JB, Marsden MPF (1985) Epicuticular lipid-accumulation on the leaves of *Lycopersicon pennellii* (Corr.) D'Arcy and *Lycopersicon esculentum* Mill. *Plant Physiol* **77**: 567–570
- Fridman E, Wang JH, Iijima Y, Froehlich JE, Gang DR, Ohlrogge J, Pichersky E (2005) Metabolic, genomic, and biochemical analyses of glandular trichomes from the wild tomato species *Lycopersicon hirsutum* identify a key enzyme in the biosynthesis of methylketones. *Plant Cell* **17**: 1252–1267
- Gang DR, Wang JH, Dudareva N, Nam KH, Simon JE, Lewinsohn E, Pichersky E (2001) An investigation of the storage and biosynthesis of phenylpropenes in sweet basil. *Plant Physiol* **125**: 539–555
- Gaquerel E, Heiling S, Schoettner M, Zurek G, Baldwin IT (2010) Development and validation of a liquid chromatography-electrospray ionization-time-of-flight mass spectrometry method for induced changes in *Nicotiana attenuata* leaves during simulated herbivory. *J Agric Food Chem* **58**: 9418–9427
- Gase K, Baldwin IT (2012) Transformational tools for next-generation plant ecology: manipulation of gene expression for the functional analysis of genes. *Plant Ecol Divers* **5**: 485–490
- Gase K, Weinhold A, Bozorov T, Schuck S, Baldwin IT (2011) Efficient screening of transgenic plant lines for ecological research. *Mol Ecol Resour* **11**: 890–902
- Gershenzon J (1994) Metabolic costs of terpenoid accumulation in higher plants. *J Chem Ecol* **20**: 1281–1328
- Gershenzon J, Dudareva N (2007) The function of terpene natural products in the natural world. *Nat Chem Biol* **3**: 408–414
- Ghosh B, Westbrook TC, Jones AD (2014) Comparative structural profiling of trichome specialized metabolites in tomato (*Solanum lycopersicum*) and *S. habrochaites*: acylsugar profiles revealed by UHPLC/MS and NMR. *Metabolomics* **10**: 496–507

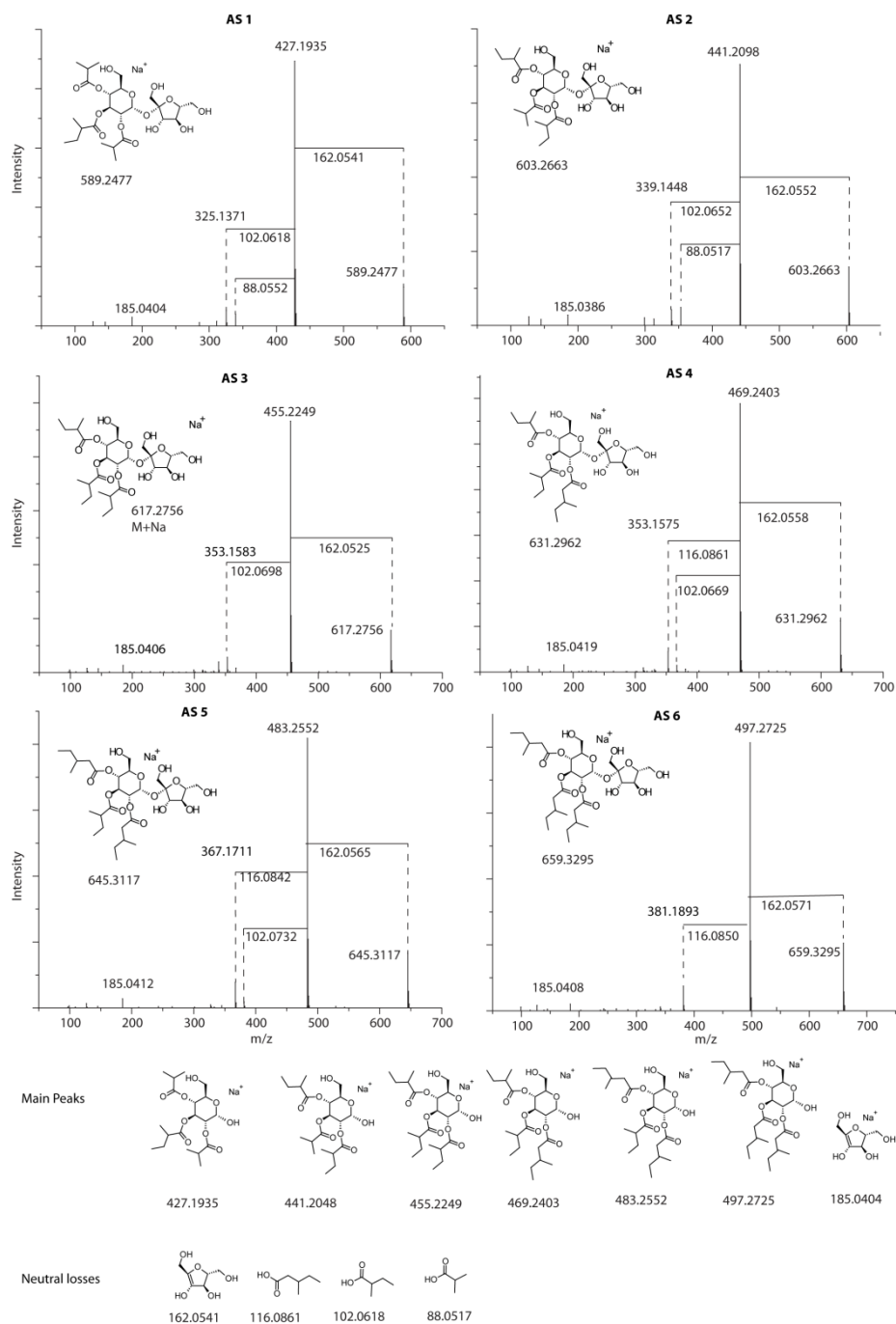
- Gilardoni PA, Hettenhausen C, Baldwin IT, Bonaventure G (2011) *Nicotiana attenuata* LECTIN RECEPTOR KINASE1 suppresses the insect-mediated inhibition of induced defense responses during *Manduca sexta* herbivory. *Plant Cell* **23**: 3512–3532
- Glas JJ, Schimmel BCJ, Alba JM, Escobar-Bravo R, Schuurink RC, Kant MR (2012) Plant glandular trichomes as targets for breeding or engineering of resistance to herbivores. *Int J Mol Sci* **13**: 17077–17103
- Goffreda JC, Mutschler MA, Ave DA, Tingey WM, Steffens JC (1989) Aphid deterrence by glucose esters in glandular trichome exudate of the wild tomato, *Lycopersicon pennellii*. *J Chem Ecol* **15**: 2135–2147
- Gonzales-Vigil E, Hufnagel DE, Kim J, Last RL, Barry CS (2012) Evolution of TPS20-related terpene synthases influences chemical diversity in the glandular trichomes of the wild tomato relative *Solanum habrochaites*. *Plant J* **71**: 921–935
- Grosse-Wilde E, Stieber R, Forstner M, Krieger J, Wicher D, Hansson BS (2010) Sex-specific odorant receptors of the tobacco hornworm *Manduca sexta*. *Front Cell Neurosci* **4** doi/10.3389/fncel.2010.00022
- Hare JD (2005) Biological activity of acyl glucose esters from *Datura wrightii* glandular trichomes against three native insect herbivores. *J Chem Ecol* **31**: 1475–1491
- Haslam E (1998) Practical Polyphenolics: From Structure to Molecular Recognition and Physiological Action. Cambridge University Press, Cambridge, UK
- Hawthorne DJ, Shapiro JA, Tingey WM, Mutschler MA (1992) Trichome-borne and artificially applied acylsugars of wild tomato deter feeding and oviposition of the leafminer *Liriomyza trifolii*. *Entomol Exp Appl* **65**: 65–73
- Jefferson RA, Kavanagh TA, Bevan MW (1987) Gus fusions: beta-glucuronidase as a sensitive and versatile gene fusion marker in higher plants. *EMBO J* **6**: 3901–3907
- Juvik JA, Shapiro JA, Young TE, Mutschler MA (1994) Acylglucosides from wild tomatoes alter behavior and reduce growth and survival of *Helicoverpa zea* and *Spodoptera exigua* (Lepidoptera, Noctuidae). *J Econ Entomol* **87**: 482–492
- Kandra L, Wagner GJ (1988) Studies of the site and mode of biosynthesis of tobacco trichome exudate components. *Arch Biochem Biophys* **265**: 425–432
- Kato A, Arima K (1971) Inhibitory effect of sucrose ester of lauric acid on the growth of *Escherichia coli*. *Biochem Biophys Res Commun* **42**: 596–601
- Kato N, Shibasaki I (1975) Comparison of antimicrobial activities of fatty acids and their esters. *J Ferment Technol* **53**: 793–801
- Kaur H, Heinzl N, Schottner M, Baldwin IT, Galis I (2010) R2R3-NaMYB8 regulates the accumulation of phenylpropanoid-polyamine conjugates, which are essential for local and systemic defense against insect herbivores in *Nicotiana attenuata*. *Plant Physiol* **152**: 1731–1747
- Keinanen M, Oldham NJ, Baldwin IT (2001) Rapid HPLC screening of jasmonate-induced increases in tobacco alkaloids, phenolics, and di-terpene glycosides in *Nicotiana attenuata*. *J Agric Food Chem* **49**: 3553–3558
- Kim J, Kang K, Gonzales-Vigil E, Shi F, Jones AD, Barry CS, Last RL (2012) Striking natural diversity in glandular trichome acylsugar composition is shaped by variation at the acyltransferase2 locus in the wild tomato *Solanum habrochaites*. *Plant Physiol* **160**: 1854–1870
- Kroumova AB, Wagner GJ (2003) Different elongation pathways in the biosynthesis of acyl groups of trichome exudate sugar esters from various solanaceous plants. *Planta* **216**: 1013–1021
- Krugel T, Lim M, Gase K, Halitschke R, Baldwin IT (2002) *Agrobacterium*-mediated transformation of *Nicotiana attenuata*, a model ecological expression system. *Chemoecology* **12**: 177–183
- Li D, Baldwin IT, Gaquerel E (2015) Navigating natural variation in herbivory-induced secondary metabolism in coyote tobacco populations using MS/MS structural analysis. *Proc Natl Acad Sci USA* **112**: E4147–E4155
- Li D, Heiling S, Baldwin IT, Gaquerel E (2016) Illuminating a plant's tissue-specific metabolic diversity using computational metabolomics and information theory. *Proc Natl Acad Sci USA* **113**: E7610–E7618
- Luu VT, Schuck S, Kim SG, Weinhold A, Baldwin IT (2015) Jasmonic acid signalling mediates resistance of the wild tobacco *Nicotiana attenuata* to its native *Fusarium*, but not *Alternaria*, fungal pathogens. *Plant Cell Environ* **38**: 572–584
- Malhotra B, Onyiah JC, Bohm BA, Towers GHN, James D, Harborne JB, French CJ (1996) Inhibition of tomato ringspot virus by flavonoids. *Phytochemistry* **43**: 1271–1276
- Marak HB, Biere A, Van Damme JMM (2003) Fitness costs of chemical defense in *Plantago lanceolata* L.: effects of nutrient and competition stress. *Evolution* **57**: 2519–2530
- Marshall DL, Bullerman LB (1986) Antimicrobial activity of sucrose fatty acid ester emulsifiers. *J Food Sci* **51**: 468–470
- Moore BD, Andrew RL, Kulheim C, Foley WJ (2014) Explaining intra-specific diversity in plant secondary metabolites in an ecological context. *New Phytol* **201**: 733–750
- Nguyen TTX, Dehne HW, Steiner U (2016) Maize leaf trichomes represent an entry point of infection for *Fusarium* species. *Fungal Biol* **120**: 895–903
- Peng C, Uygun S, Shiu SH, Last RL (2015) The impact of the branched-chain ketoacid dehydrogenase complex on amino acid homeostasis in *Arabidopsis*. *Plant Physiol* **169**: 1807–1820
- Pohl CH, Kock JLE, Thibane VS (2011) Antifungal free fatty acids: a review. In A. Méndez-Vilas, ed., *Science Against Microbial Pathogens: Communicating Current Research and Technological Advances*. Microbiology Book Series, Number 3. Formatex Research Center, Spain, pp 61–71
- Puterka GJ, Farone W, Palmer T, Barrington A (2003) Structure-function relationships affecting the insecticidal and miticidal activity of sugar esters. *J Econ Entomol* **96**: 636–644
- Roda AL, Oldham NJ, Svatos A, Baldwin IT (2003) Allometric analysis of the induced flavonols on the leaf surface of wild tobacco (*Nicotiana attenuata*). *Phytochemistry* **62**: 527–536
- Sallaud C, Rontein D, Onillon S, Jabes F, Duffe P, Giacalone C, Thoraval S, Escoffier C, Herbette G, Leonhardt N, et al (2009) A novel pathway for sesquiterpene biosynthesis from Z,Z-farnesyl pyrophosphate in the wild tomato *Solanum habrochaites*. *Plant Cell* **21**: 301–317
- Santhanam R, Luu VT, Weinhold A, Goldberg J, Oh Y, Baldwin IT (2015) Native root-associated bacteria rescue a plant from a sudden-wilt disease that emerged during continuous cropping. *Proc Natl Acad Sci USA* **112**: E5013–E5020
- Schilmiller AL, Charbonneau AL, Last RL (2012) Identification of a BAHD acetyltransferase that produces protective acyl sugars in tomato trichomes. *Proc Natl Acad Sci USA* **109**: 16377–16382
- Schilmiller AL, Gilgallon K, Ghosh B, Jones AD, Last RL (2016) Acylsugar acylhydrolases: carboxylesterase-catalyzed hydrolysis of acylsugars in tomato trichomes. *Plant Physiol* **170**: 1331–1344
- Schilmiller AL, Moghe GD, Fan PX, Ghosh B, Ning J, Jones AD, Last RL (2015) Functionally divergent alleles and duplicated loci encoding an acyltransferase contribute to acylsugar metabolite diversity in *Solanum* trichomes. *Plant Cell* **27**: 1002–1017
- Schilmiller AL, Chauvinhold I, Larson M, Xu R, Charbonneau AL, Schmidt A, Wilkerson C, Last RL, Pichersky E (2009) Monoterpenes in the glandular trichomes of tomato are synthesized from a neryl diphosphate precursor rather than geranyl diphosphate. *Proc Natl Acad Sci USA* **106**: 10865–10870
- Schuck S, Weinhold A, Luu VT, Baldwin IT (2014) Isolating fungal pathogens from a dynamic disease outbreak in a native plant population to establish plant-pathogen bioassays for the ecological model plant *Nicotiana attenuata*. *PLoS ONE* **9**: e102915
- Shapiro JA, Steffens JC, Mutschler MA (1994) Acylsugars of the wild tomato *Lycopersicon pennellii* in relation to geographic-distribution of the species. *Biochem Syst Ecol* **22**: 545–561
- Simonovska B, Srbinoska M, Vovk I (2006) Analysis of sucrose esters-insecticides from the surface of tobacco plant leaves. *J Chromatogr A* **1127**: 273–277
- Slocambe SP, Chauvinhold I, McQuinn RP, Besser K, Welsby NA, Harper A, Aziz N, Li Y, Larson TR, Giovannoni J, et al (2008) Transcriptomic and reverse genetic analyses of branched-chain fatty acid and acyl sugar production in *Solanum pennellii* and *Nicotiana benthamiana*. *Plant Physiol* **148**: 1830–1846
- Snook ME, Johnson AW, Severson RF, Teng Q, White RA, Sisson VA, Jackson DM (1997) Hydroxygeranylinalool glycosides from tobacco exhibit antibiosis activity in the tobacco budworm *Heliothis virescens* (F). *J Agric Food Chem* **45**: 2299–2308
- Timmer LW, Peever TL, Solel Z, Akimitsu K (2003) *Alternaria* diseases of citrus-novel pathosystems. *Phytopathol Mediterr* **42**: 99–112
- Treutter D (2006) Significance of flavonoids in plant resistance: a review. *Environ Chem Lett* **4**: 147–157
- Van Dam NM, Hare JD (1998) Biological activity of *Datura wrightii* glandular trichome exudate against *Manduca sexta* larvae. *J Chem Ecol* **24**: 1529–1549
- Van Dam NM, Horn M, Mares M, Baldwin IT (2001) Ontogeny constrains systemic protease inhibitor response in *Nicotiana attenuata*. *J Chem Ecol* **27**: 547–568

- Wagner GJ, Wang E, Shepherd RW** (2004) New approaches for studying and exploiting an old protuberance, the plant trichome. *Ann Bot (Lond)* **93**: 3–11
- Waldbauer GP** (1968) The consumption and utilization of food by insects. In JWL Beament, JE Treherne, VB Wigglesworth, eds, *Advances in Insect Physiology*, Vol 5. Academic Press, New York, pp 229–288
- Walters DS, Steffens JC** (1990) Branched chain amino acid metabolism in the biosynthesis of *Lycopersicon pennellii* glucose esters. *Plant Physiol* **93**: 1544–1551
- Weinhold A, Baldwin IT** (2011) Trichome derived O-acyl sugars are a first meal for caterpillars that tags them for predation. *Proc Natl Acad Sci USA* **108**: 7855–7859
- Weinhold A, Shaker K, Wenzler M, Schneider B, Baldwin IT** (2011) Phaseoloidin, a homogentisic acid glucoside from *Nicotiana attenuata* trichomes, contributes to the plant's resistance against *Lepidopteran* herbivores. *J Chem Ecol* **37**: 1091–1098
- Wink M, editor** (2011) *Annual Plant Reviews, Biochemistry of Plant Secondary Metabolism*, Vol 40. John Wiley & Sons, New York
- Wu J, Hettenhausen C, Meldau S, Baldwin IT** (2007) Herbivory rapidly activates MAPK signaling in attacked and unattacked leaf regions but not between leaves of *Nicotiana attenuata*. *Plant Cell* **19**: 1096–1122
- Xia J, Sinelnikov IV, Han B, Wishart DS** (2015) MetaboAnalyst 3.0: making metabolomics more meaningful. *Nucleic Acids Res* **43**: W251–W257

## 1 Supplemental Figures

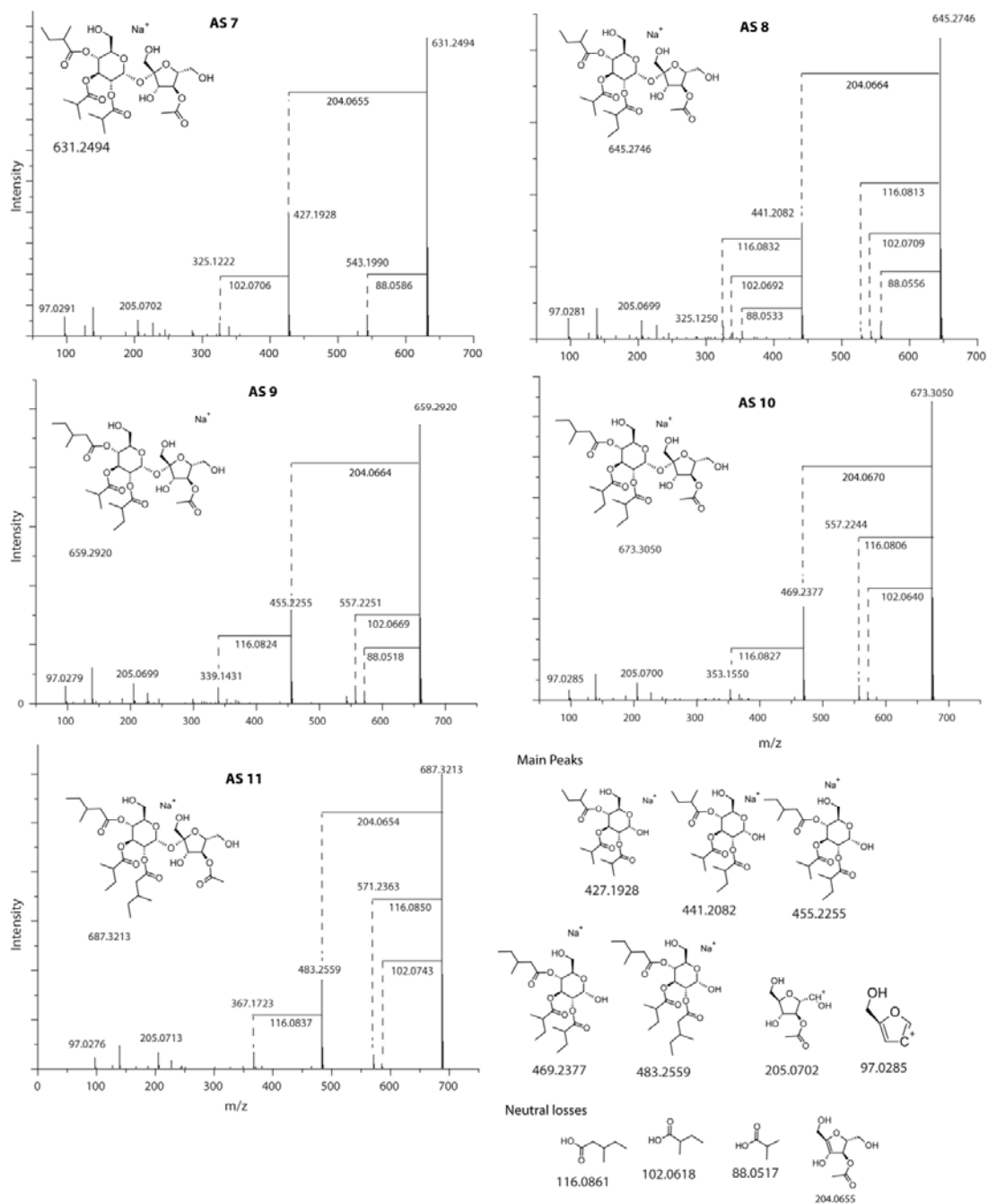


2  
3 **Figure S1.** Total ion chromatogram of a positive mode UHPLC/TOF-MS run (TIC+) of a whole leaf extract  
4 which is compared with an *O*-acyl sugars (*O*-AS) extract. The leaf extract is dominated by nicotine,  
5 phenylpropanoid polyamine conjugates (PPCs), 17-hydroxygeranylinalool diterpene glycosides (DTGs), and  
6 *O*-AS, while the *O*-AS extract was dominated by a mixture of *O*-AS.



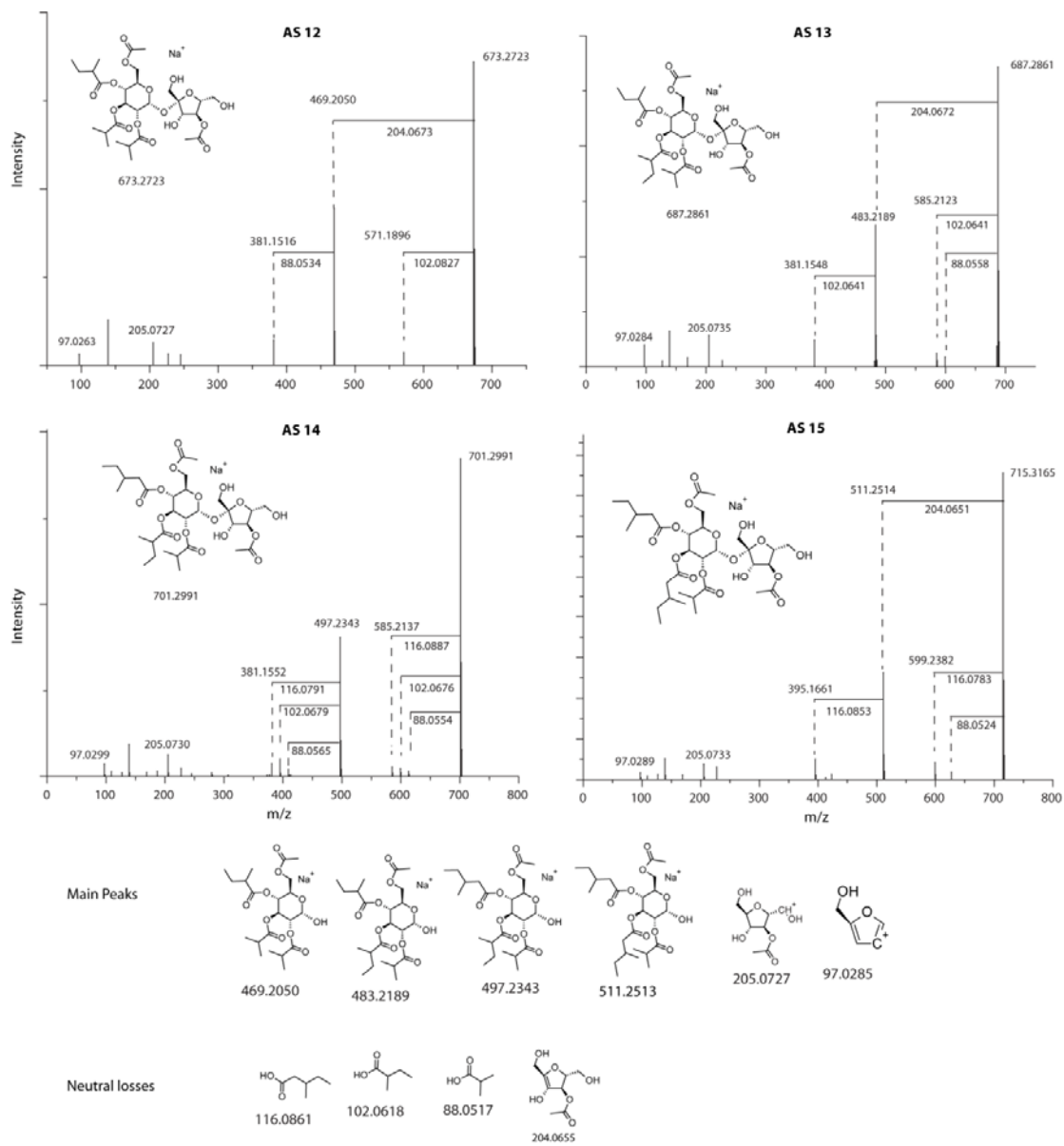
7  
8  
9  
10

**Figure S2:** MS<sup>2</sup> spectra of class 2 *O*-acyl sugars and the annotation of the main fragment peaks (Main peaks) and neutral losses. The position of the branched-chain fatty acids could not be verified and may vary.



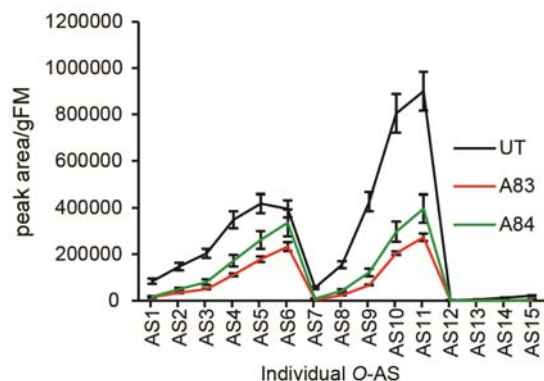
11  
12  
13  
14  
15

**Figure S3:** MS<sup>2</sup> spectra of class 3 *O*-acyl sugars and the annotation of the main fragment peaks (Main peaks) and neutral losses. The position of the branched-chain fatty acids could not be verified and may vary.

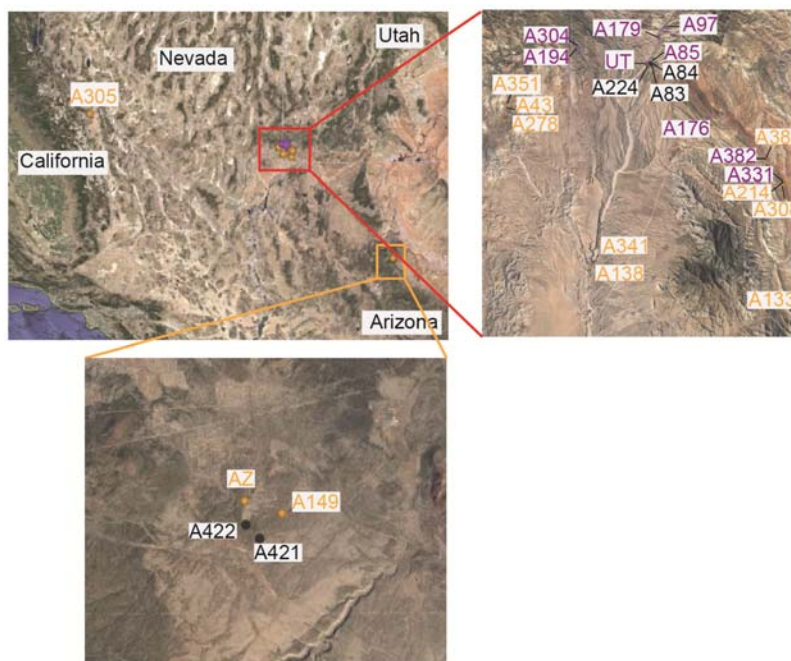


16  
17  
18  
19  
20

**Figure S4:** MS<sup>2</sup> spectra of class 4 *O*-acyl sugars and the annotations of the main fragment peaks (Main peaks) and neutral losses. The position of the branched-chain fatty acids could not be verified and may vary.

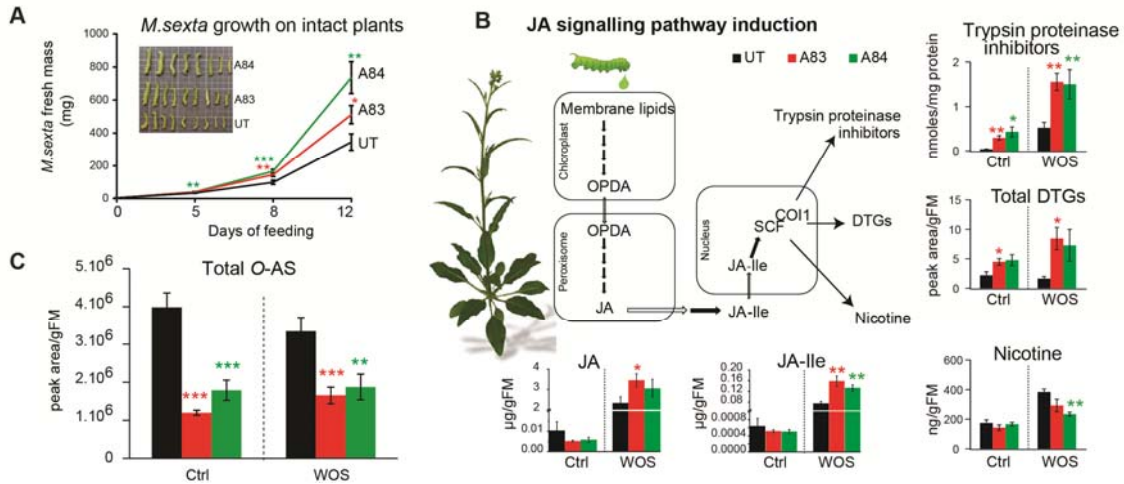


21  
 22 **Figure S5. *O*-acyl sugars composition of A83, A84 and UT plants.** Peak area per gram fresh mass (peak  
 23 area/gFM) of each individual *O*-AS revealing the overall reduction of all 15 *O*-AS in A83 and A84 compared to  
 24 UT.



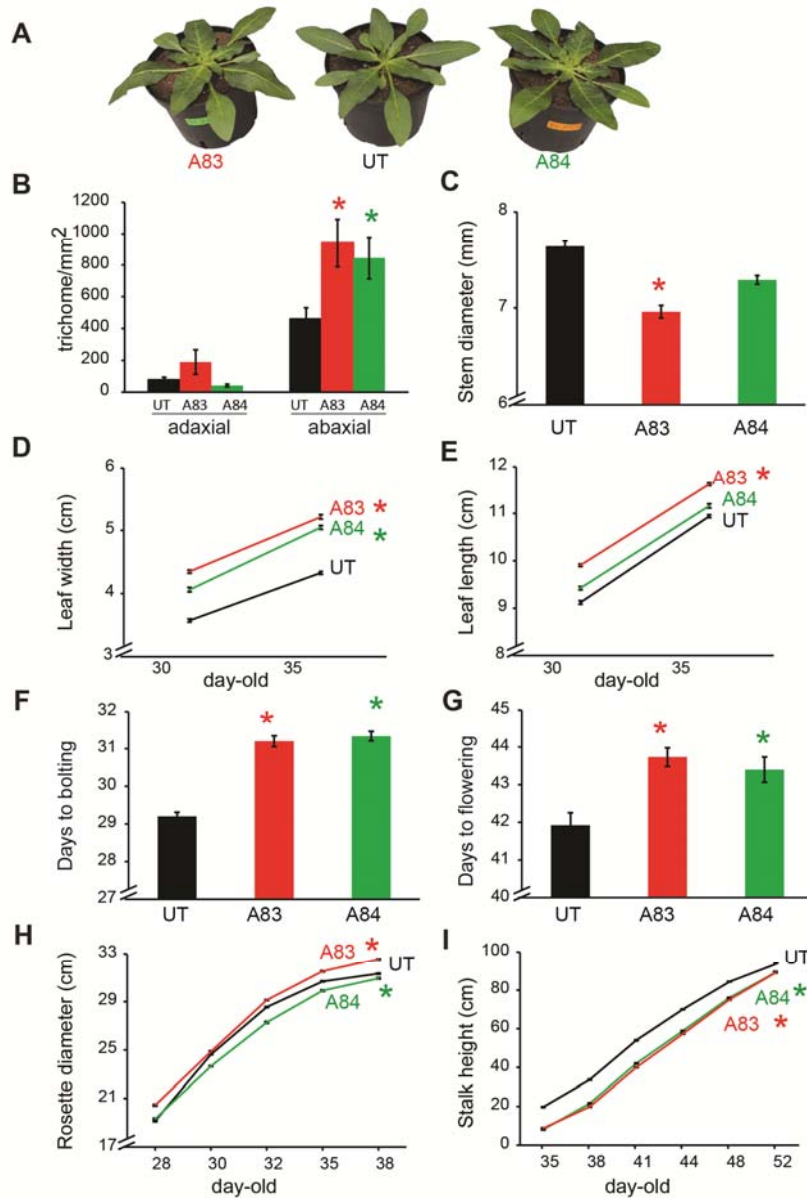
25  
 26 **Figure S6. The location of the 26 accessions collection sites in Utah, Nevada, Arizona, and California.** A  
 27 close-up for the collection sites in Utah and Arizona are presented. Full GPS coordinates are provided in SI  
 28 Appendix, Table S1. Colors were given to accessions according to their cluster based on *O*-AS composition  
 29 (Fig. 2B).

30



31  
 32  
 33  
 34  
 35  
 36  
 37  
 38  
 39  
 40  
 41  
 42  
 43

**Figure S7. Two low *O*-AS accessions are not compromised in JA signaling but more susceptible to the specialist herbivore.** **A.** *M. sexta* larvae fed on A83 (red line) and A84 (green line) plants grew faster than those fed on UT plants. The error bars represent standard errors (n=30). **B.** The JA-induced defenses in two low *O*-AS accessions are intact. A simplified herbivore-induced JA signaling and the defensive responses it activates in *N. attenuata* are shown in the middle and five measured traits are shown as bar plots.  $\mu\text{g/gFM}$ :  $\mu\text{g}$  per gram of fresh mass. Ctrl: control, WOS: wound leaf plus *M. sexta*'s oral secretion. Black bars represent UT while red and green bars represent A83 and A84 plants, respectively. The error bars represent standard error (n= 5- 6). **C.** *O*-AS are not induced after herbivory. In all panels, asterisks indicate significant differences between A83 (red asterisks) or A84 (green asterisks) and UT at a given treatment or a given time point (*t* test, \*\*\*:  $P \leq 0.001$ , \*\*:  $P \leq 0.01$ , \*:  $P \leq 0.05$ ).

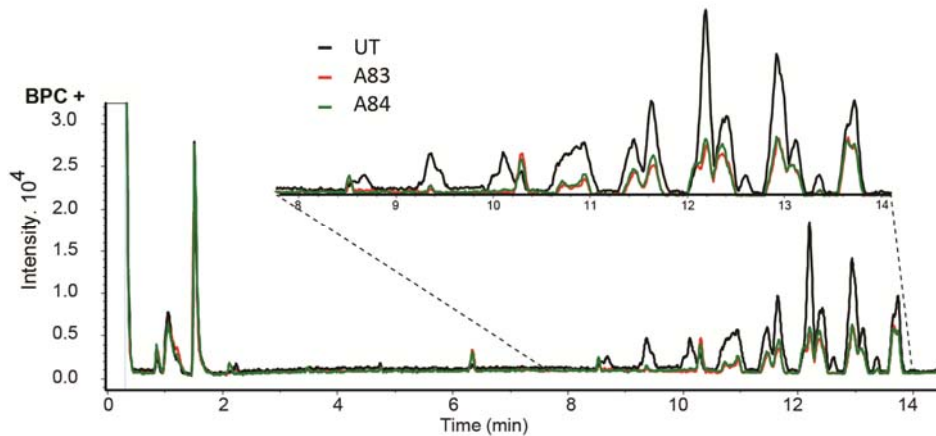


44

45

**Figure S8. Morphological differences between UT, A83 and A84 plants.** A. Representative pictures of UT, A83 and A84 plants at the rosette-stage of growth (30 day-old plants). B. Trichome density on the leaves of UT, A83 and A84 plants (n=5). Stem diameter (C), leaf width (D), leaf length (E), the number of days to bolting (F), the number of days to flowering (G), rosette diameter (H) and stalk height (I) of UT compared to that of A83 and A84. Asterisks indicate significant differences between A83 (red asterisks) or A84 (green asterisks) and UT at a given treatment (*t* test, \*:  $P \leq 0.05$ ). Note the breaks in the Y-axis.

51

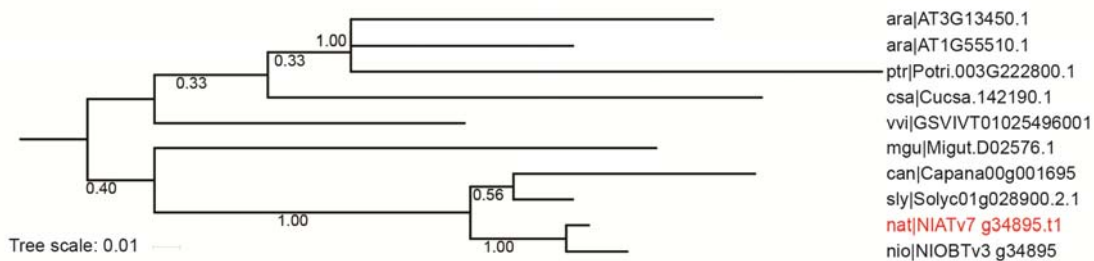


52

53 **Figure S9. A83 and A84 show less *O*-acyl sugars in the water wash compared to UT. Base peak**  
 54 **chromatogram of a positive mode UHPLC/TOF-MS analysis (BPC+) from UT (black line), A83 (red line), A84**  
 55 **(green line) of a 1<sup>st</sup> water leaf wash.**

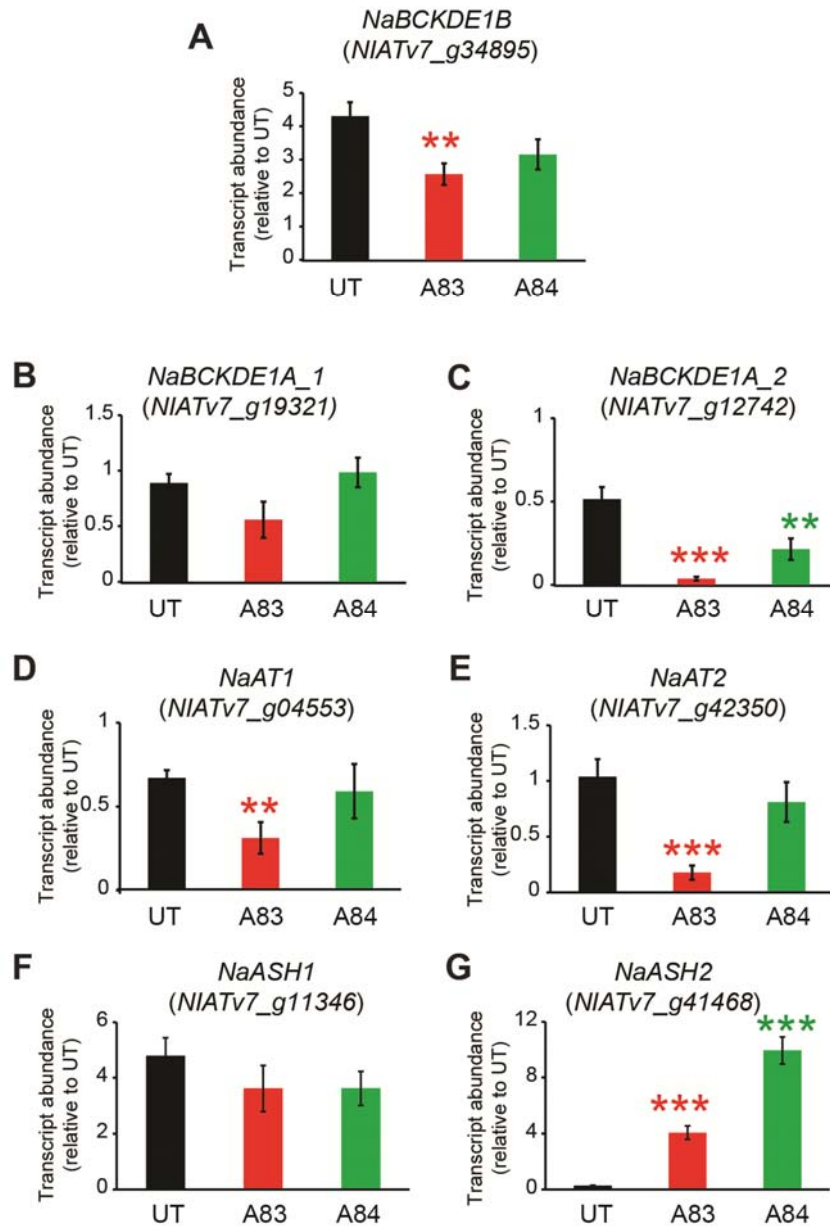
56

57



58

59 **Figure S10. Phylogenetic relationships of genes encoding branched-chain alpha-keto acid dehydrogenase**  
 60 **E1 beta subunit among *N. attenuata* and other closely related species.** The tree was constructed using the  
 61 Maximum Likelihood method based on the whole gene sequences using MEGA5 software with General time  
 62 reversible model. Sequences were aligned using ClustalW algorithm implemented in the MegAlign software.  
 63 The numbers on the nodes indicate bootstrap scores (500 steps) (Tamura et al., 2010). The numbers on the scale  
 64 indicates divergence times with relative units. Species names: ara| *Arabidopsis thaliana* (At); ptr| *Populus*  
 65 *trichocarpa* (Potri.); csa| *Cucumis sativus* (Cucsa); vvi| *Vitis vinifera* (Vi); mgu| *Mimulus guttatus* (Migut); nat|  
 66 *Nicotiana attenuata* (NIAT); nio| *Nicotiana obtusifolia* (NIOBT); sly| *Solanum lycopersicum* (Sl); can| *Capsicum*  
 67 *annuum* (Capana)



68

69 **Figure S11. Gene expression in trichomes of UT in comparison to A83 and A84.** Relative expression of *N.*

70 *attenuata* genes encoding putative branched-chain alpha-ketoacid dehydrogenase *NaBCKDE1B* (A),

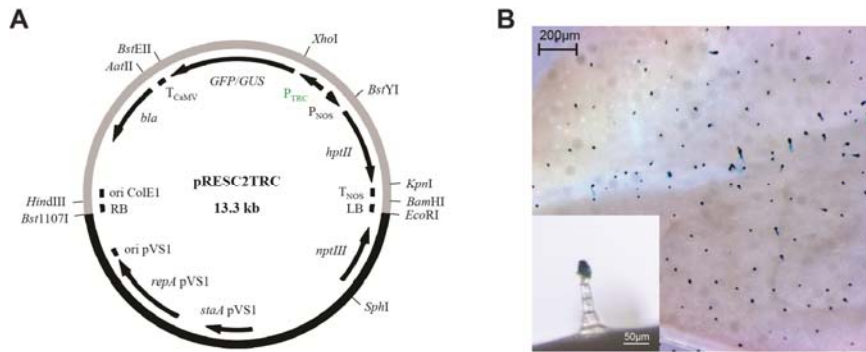
71 *NaBCKDE1A* (B, C), acyltransferases *NaAT1* (D), *NaAT2* (E), acylsugar acyl hydrolase *NaASH1* (F), *NaASH2*

72 (G) in trichomes between A83, 84 compared to UT (n=5-6). Relative gene expression was normalized to the

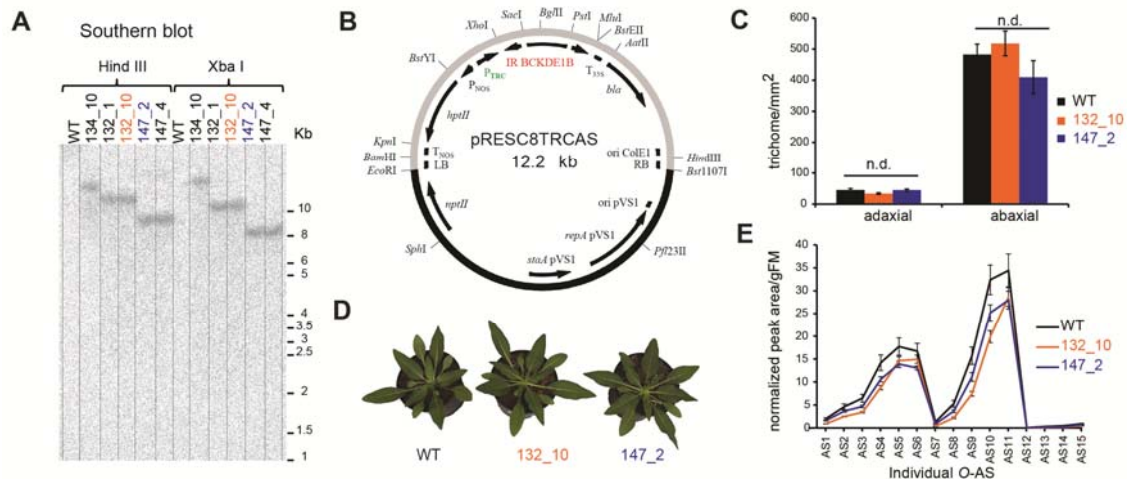
73 expression of the house keeping gene *N. attenuata* actin 7. Asterisks indicate significant differences between

74 A83 (red asterisks) or A84 (green asterisks) and UT at a given treatment (*t* test, \*\*\*:  $P \leq 0.001$ , \*\*:  $P \leq 0.01$ , \*:  $P$

75  $\leq 0.05$ ).

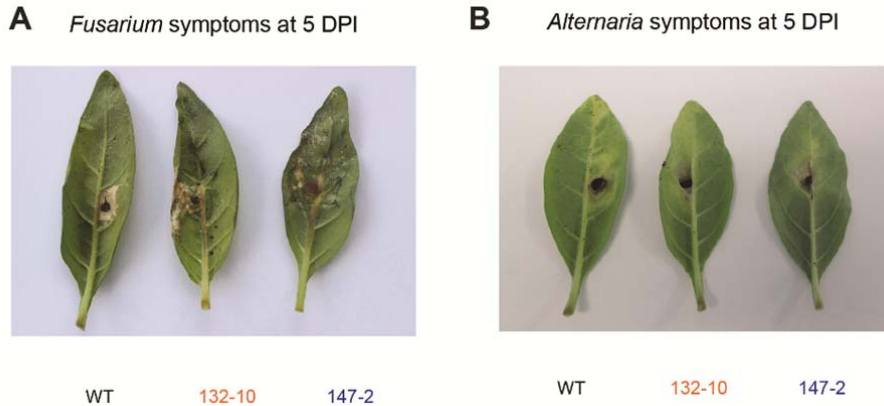


76  
 77 **Figure S12. Expression specificity of *S. lycopersicum* trichome specific promoter (SIAT2) in *N. attenuata*.**  
 78 **A.** The pRES2TRC series binary plant transformation vectors used for expressing SIAT2::GFP/GUS in *N.*  
 79 *attenuata*. The 1495bp of the trichome-specific promoter from *S. lycopersicum* SIAT2 gene was inserted into  
 80 pRES2TRC vector with the hygromycin (*hptII*) resistance gene as a selection marker. Abbreviations: LB/RB,  
 81 left/right border of T-DNA; PNOS/TNOS, promoter/terminator of the nopaline synthase gene from the Ti  
 82 plasmid of *Agrobacterium tumefaciens*; PTRC, trichome specific promoter from *Solanum lycopersicum* SIAT2;  
 83 T35S, 35S terminator from cauliflower mosaic virus; *hptII*, hygromycin phosphotransferase gene from  
 84 pCambia-1301 (AF234297); *nptII*, amino glycoside phosphotransferase class II; ori, origin of replication. **B.**  
 85 SIAT2::GUS is expressed in tip cells of both type C and D trichome of *N. attenuata*. Images obtained using a  
 86 ZEISS stereomicroscope SV 11 with 4x and Axio Zoom.V16 Stereo microscope at 180X magnification.

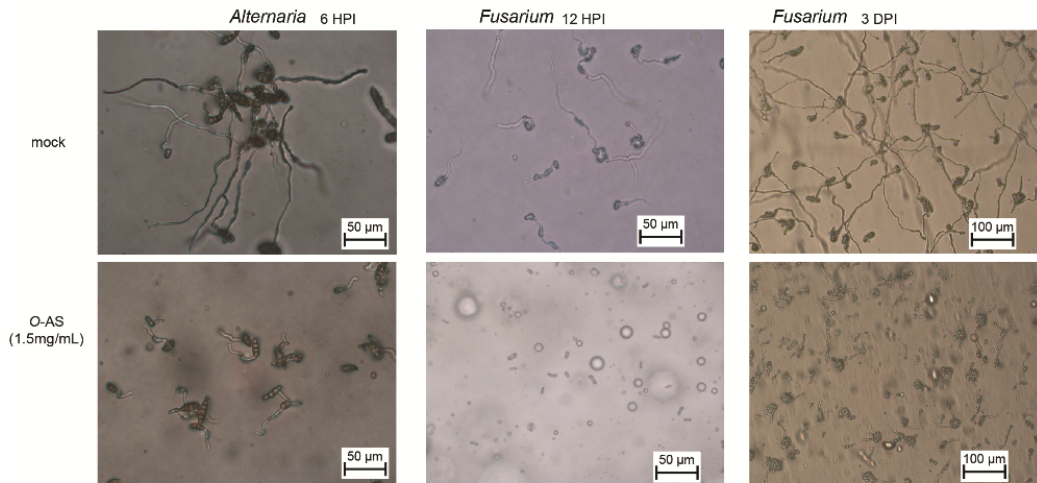


87  
 88 **Figure S13. Creating irBCKDE1B transgenic lines using *Agrobacterium*-transformation.** **A.** Two  
 89 *Agrobacterium*-transformed lines irBCKDE1B-132-10 and irBCKDE1B-147-2 were subjected to Southern blot  
 90 analysis using genomic DNA digested with HindIII and XbaI restriction enzyme and *hptII*-radiolabeled probe.  
 91 Both lines showed single insertions of T-DNA fragment into the genome. **B.** The pRES8TRCAS series binary  
 92 plant transformation vectors used for silencing BCKDE1B encoding gene (*NIATv7\_g34895*). A 351bp of  
 93 NaBCKDE1B gene was inserted into pRES8TRCAS vector as an inverted-repeat construct with *hptII* used as  
 94 plant selection marker gene. Abbreviations: LB/RB, left/right border of T-DNA; PNOS/TNOS, promoter/  
 95 terminator of the nopaline synthase gene from the Ti plasmid of *Agrobacterium tumefaciens*; PTRC, trichome  
 96 specific promoter from *Solanum lycopersicum* SIAT2; T35S, 35S terminator from cauliflower mosaic virus;  
 97 *hptII*, hygromycin phosphotransferase gene from pCambia-1301 (AF234297); i, intron 3 of

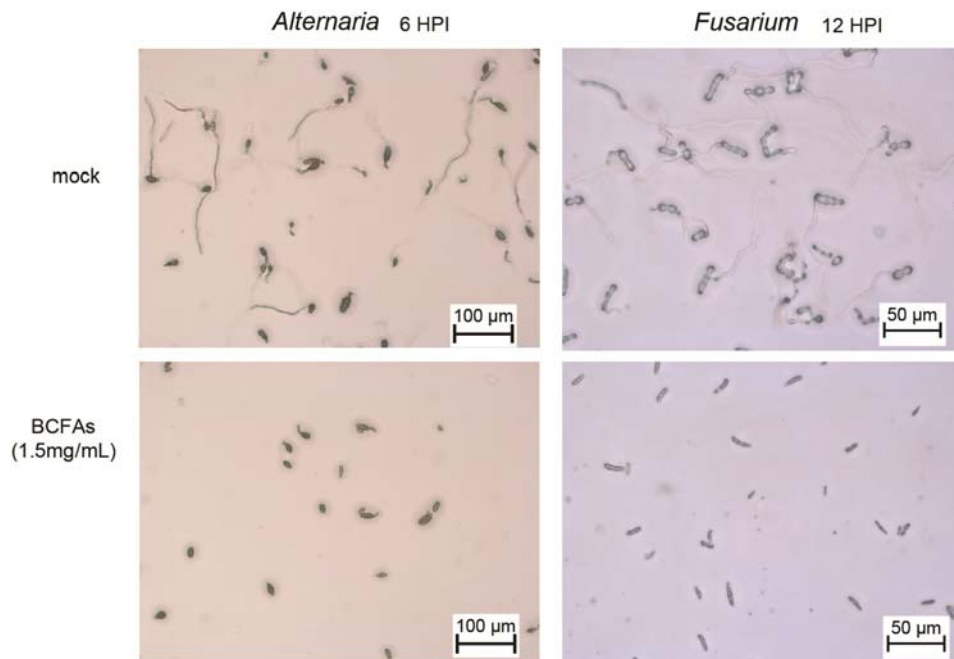
98 *Flaveriatrinerviapdk* gene for pyruvate, orthophosphate dikinase; *nptII*, amino glycoside phosphotransferase  
 99 class II; ori, origin of replication. C. Trichome density of two independently transformed homozygous  
 100 irBCKDE1B lines and wild-type (WT) plants (n=5). D The similarity of the morphology of two *Agrobacterium*-  
 101 transformed lines irBCKDE1B-132-10 and irBCKDE1B-147-2 at the rosette-stage of growth. E. Individual *O*-  
 102 AS in 2 irBCKDE1B independent lines. Error bars represent standard error. Asterisks indicate significant  
 103 differences between WT and individual irBCKDE1B lines (*t* test, \*\*\*:  $P \leq 0.001$ , \*\*:  $P \leq 0.01$ , \*:  $P \leq 0.05$ ).



104  
 105 **Figure S14. Detached leaf assay on irBCKDE1B transgenic lines.** Necrotic lesions caused by *Fusarium* (A)  
 106 and *Alternaria* (B) and on detached leaves of WT, 132-10 and 147-2 at 5 days post inoculation (DPI )



107  
 108 **Figure S15. Effect of *O*-acyl sugars on fungal pathogens.** Spore germination and hyphal length of *Alternaria*  
 109 and *Fusarium* fungal on plain agar supplemented with *O*-AS concentrations 1.5 mg/mL in comparison with  
 110 mock treatment at 6 and 12 h post inoculation (HPI) or 3 days post inoculation (DPI). Pictures were taken under  
 111 the light microscope Axio Observer.D1 with 400 X magnification.



112  
 113 **Figure S16. Effect of branched-chain fatty acids (BCFAs) on fungal pathogens.** Spore germination and  
 114 hyphal length of *Alternaria* and *Fusarium* fungal on plain agar supplemented with BCFAs at concentrations of  
 115 1.5 mg/mL in comparison with mock treatment at 6 and 12 h post inoculation (HPI). Pictures were taken under  
 116 the light microscope Axio Observer.D1 with 400 X magnification.

117

118 **Literature Cited**

119 Tamura K, Peterson D, Peterson N, Stecher G, Nei M, Kumar S. 2011. MEGA5: Molecular evolutionary  
 120 genetics analysis using maximum likelihood, evolutionary distance, and maximum parsimony methods.  
 121 Molecular Biology and Evolution 28(10): 2731-2739.

122 **Supplemental Tables**123 **Table S1:** GPS coordinates of 26 natural accessions

<b>No. of accession</b>	<b>Accession</b>	<b>Latitude</b>	<b>Longitude</b>
1	A84	37°19'35.48"N	113°57'38.28"W
2	A83	37°19'35.48"N	113°57'38.28"W
3	A422	35°12'44.80"N	111°28'24.80"W
4	A421	35°12'31.10"N	111°28'8.38"W
5	A278	37°16'16.22"N	114° 7'39.67"W
6	A305	37°45'19.61"N	118°35'41.82"W
7	A224	37°19'33.89"N	113°57'54.16"W
8	A138	37° 8'19.58"N	114° 1'35.10"W
9	A351	37°17'9.10"N	114° 7'31.50"W
10	UT	37°19'36.26"N	113°57'53.05"W
11	A133	37° 6'12.50"N	113°49'36.60"W
12	Az	35°13'8.62"N	111°28'26.03"W
13	A308	37°13'5.50"N	113°48'24.25"W
14	A149	35°12'56.07"N	111°27'41.29"W
15	A43	37°17'9.10"N	114° 7'31.50"W
16	A214	37°13'15.83"N	113°48'20.86"W
17	A384	37°14'27.05"N	113°49'36.71"W
18	A304	37°20'22.52"N	114° 2'40.86"W
19	A341	37° 9'45.30"N	114° 0'58.52"W
20	A331	37°13'15.83"N	113°48'20.86"W
21	A194	37°20'22.52"N	114° 2'40.86"W
22	A97	37°21'35.24"N	113°56'38.68"W
23	A382	37°14'27.05"N	113°49'36.71"W
24	A176	37°16'38.65"N	113°53'35.18"W
25	A179	37°21'1.04"N	113°57'5.17"W
26	A85	37°19'35.48"N	113°57'38.28"W

124

125 **Table S2.** The list of m/z and retention times (RT) used to identify and measure *O*-acyl sugars (*O*-AS). *O*-AS  
 126 annotation was done as described by Kim et al. (2012) which includes sucrose backbone (S for sucrose), the  
 127 number of acyl chains, the total number of carbons for acyl chains and the expected length of each acyl chain.  
 128 For instance, S3:13(4,5,4): acyl sucrose with 3 acyl chains of 4, 5 and 4 carbons, so in total 13 carbons.

<i>O</i> -acyl sugars	<i>O</i> -AS annotation	m/z	m/z width	RT(min)	RT width
AS1	S3:13(4,5,4)	589.24	0.05	8.6	0.5
AS2	S3:14 (5,4,5)	603.26	0.05	9.4	0.5
AS3	S3:15 (5,5,5)	617.27	0.05	10.1	0.5
AS4	S3:16 (6,5,5)	631.29	0.01	10.9	0.5
AS5	S3:17 (6,5,6)	645.31	0.01	11.7	0.5
AS6	S3:18 (6,6,6)	659.32	0.01	12.3	0.5
AS7	S4:15 (2,4,4,5)	631.25	0.05	9.9	0.5
AS8	S4:16 (2,5,4,5)	645.27	0.01	10.7	0.5
AS9	S4:17 (2,5,4,6)	659.29	0.01	11.3	0.5
AS10	S4:18 (2,5,5,6)	673.3	0.01	12	0.5
AS11	S4:19 (2,6,5,6)	687.32	0.01	12.9	0.5
AS12	S5:17 (2,4,4,5)	673.27	0.01	11.1	0.5
AS13	S5:18 (2,4,5,5,2)	687.28	0.01	11.8	0.5
AS14	S5:19 (2,4,5,6,2)	701.29	0.01	12.6	0.5
AS15	S5:20 (2,4,6,6,2)	715.31	0.01	13.4	0.5

129  
 130 **Table S3:** Branched-chain fatty acids (BCFAs) compositions of *N. attenuata* *O*-acyl sugars (*O*-AS).  
 131 Retention times (RT) and indices (RI) of authentic standards are compared to those found in the extract of  
 132 saponified *O*-AS. The most abundant BCFAs are highlighted (bold).

Acid	RT	RI	RT	RI
	Single Standards		extracthydrolysis	
1 aceticacid	19.386	1456	19.319	1453
2 propionicacid	21.538	1543	21.603	1546
3 <b>2-methyl propanoicacid</b>	22.281	1574	22.124	1567
4 <b>2-methyl butanoicacid</b>	24.679	1678	24.501	1670
5 <b>3-methyl butanoicacid</b>	24.678	1678	24.501	1670
6 <b>3-methyl pentanoicacid</b>	27.393	1802	27.265	1796
7 <b>4-methyl pentanoicacid</b>	27.601	1813	27.46	1806
8 hexanoicacid	28.536	1859	28.426	1853

133

134 **Table S4:** MS<sup>2</sup>-spectral data showing the annotation of class 2 *O*-acyl sugars elemental formulas, their  
 135 calculated monoisotopic mass, the elemental formula of fragment ions, and their annotations, intensity and m/z  
 136 values compared to the calculated m/z values.

ID	Monoisotopic mass El Formula	Elemental Formula Fragments	Annotation	Intensity	m/z Fragment	m/z Calc	Δppm
AS1	566.2926 C <sub>25</sub> H <sub>42</sub> O <sub>14</sub>	C <sub>25</sub> H <sub>42</sub> O <sub>14</sub> Na <sup>+</sup>	[M+Na] <sup>+</sup>	14.68	589.2477	589.2467	1
		C <sub>19</sub> H <sub>32</sub> O <sub>9</sub> Na <sup>+</sup>	[(M -C <sub>6</sub> H <sub>10</sub> O <sub>5</sub> )+Na] <sup>+</sup>	100.00	427.1935	427.1938	0.3
		C <sub>15</sub> H <sub>24</sub> O <sub>7</sub> Na <sup>+</sup>	[(M -C <sub>6</sub> H <sub>10</sub> O <sub>5</sub> - C <sub>4</sub> H <sub>8</sub> O <sub>2</sub> )+Na] <sup>+</sup>	4.36	339.1383	339.1414	3.1
		C <sub>14</sub> H <sub>22</sub> O <sub>7</sub> Na <sup>+</sup>	[(M -C <sub>6</sub> H <sub>10</sub> O <sub>5</sub> - C <sub>5</sub> H <sub>10</sub> O <sub>2</sub> )+Na] <sup>+</sup>	5.88	325.1317	325.1257	6
		C <sub>6</sub> H <sub>10</sub> O <sub>5</sub> Na <sup>+</sup>	[(M -C <sub>19</sub> H <sub>32</sub> O <sub>9</sub> )+Na] <sup>+</sup>	3.33	185.0404	185.042	1.6
AS2	580.2731 C <sub>26</sub> H <sub>44</sub> O <sub>14</sub>	C <sub>26</sub> H <sub>44</sub> O <sub>14</sub> Na <sup>+</sup>	[M+Na] <sup>+</sup>	100.00	603.2663	603.2623	4
		C <sub>20</sub> H <sub>34</sub> O <sub>9</sub> Na <sup>+</sup>	[(M -C <sub>6</sub> H <sub>10</sub> O <sub>5</sub> )+Na] <sup>+</sup>	33.88	441.2048	441.2095	4.7
		C <sub>15</sub> H <sub>24</sub> O <sub>7</sub> Na <sup>+</sup>	[(M -C <sub>6</sub> H <sub>10</sub> O <sub>5</sub> - C <sub>4</sub> H <sub>8</sub> O <sub>2</sub> )+Na] <sup>+</sup>	7.52	353.1583	353.1571	1.2
		C <sub>15</sub> H <sub>24</sub> O <sub>7</sub> Na <sup>+</sup>	[(M -C <sub>6</sub> H <sub>10</sub> O <sub>5</sub> - C <sub>5</sub> H <sub>10</sub> O <sub>2</sub> )+Na] <sup>+</sup>	6.58	339.1448	339.1414	3.4
		C <sub>6</sub> H <sub>10</sub> O <sub>5</sub> Na <sup>+</sup>	[(M -C <sub>20</sub> H <sub>34</sub> O <sub>9</sub> )+Na] <sup>+</sup>	4.36	185.0404	185.042	1.6
AS3	594.2887 C <sub>27</sub> H <sub>46</sub> O <sub>14</sub>	C <sub>27</sub> H <sub>46</sub> O <sub>14</sub> Na <sup>+</sup>	[M+Na] <sup>+</sup>	16.82	617.2756	617.2779	2.3
		C <sub>21</sub> H <sub>36</sub> O <sub>9</sub> Na <sup>+</sup>	[(M -C <sub>6</sub> H <sub>10</sub> O <sub>5</sub> )+Na] <sup>+</sup>	100.00	455.2249	455.2251	0.2
		C <sub>17</sub> H <sub>28</sub> O <sub>7</sub> Na <sup>+</sup>	[(M -C <sub>6</sub> H <sub>10</sub> O <sub>5</sub> - C <sub>4</sub> H <sub>8</sub> O <sub>2</sub> )+Na] <sup>+</sup>	1.83	367.1745	367.1727	1.8
		C <sub>16</sub> H <sub>26</sub> O <sub>7</sub> Na <sup>+</sup>	[(M -C <sub>6</sub> H <sub>10</sub> O <sub>5</sub> - C <sub>5</sub> H <sub>10</sub> O <sub>2</sub> )+Na] <sup>+</sup>	6.13	353.1538	353.157	3.2
		C <sub>15</sub> H <sub>24</sub> O <sub>7</sub> Na <sup>+</sup>	[(M -C <sub>6</sub> H <sub>10</sub> O <sub>5</sub> - C <sub>6</sub> H <sub>12</sub> O <sub>2</sub> )+Na] <sup>+</sup>	4.30	339.1365	339.1414	4.9
		C <sub>6</sub> H <sub>10</sub> O <sub>5</sub> Na <sup>+</sup>	[(M -C <sub>21</sub> H <sub>36</sub> O <sub>9</sub> )+Na] <sup>+</sup>	2.88	185.0406	185.042	1.4
AS4	608.3044 C <sub>28</sub> H <sub>48</sub> O <sub>14</sub>	C <sub>28</sub> H <sub>48</sub> O <sub>14</sub> Na <sup>+</sup>	[M+Na] <sup>+</sup>	18.98	631.2962	631.2926	3.6
		C <sub>22</sub> H <sub>38</sub> O <sub>9</sub> Na <sup>+</sup>	[(M -C <sub>6</sub> H <sub>10</sub> O <sub>5</sub> )+Na] <sup>+</sup>	100.00	469.2403	469.2408	0.5
		C <sub>17</sub> H <sub>28</sub> O <sub>7</sub> Na <sup>+</sup>	[(M -C <sub>6</sub> H <sub>10</sub> O <sub>5</sub> - C <sub>5</sub> H <sub>10</sub> O <sub>2</sub> )+Na] <sup>+</sup>	2.54	367.1625	367.1727	10.2
		C <sub>16</sub> H <sub>26</sub> O <sub>7</sub> Na <sup>+</sup>	[(M -C <sub>6</sub> H <sub>10</sub> O <sub>5</sub> - C <sub>6</sub> H <sub>12</sub> O <sub>2</sub> )+Na] <sup>+</sup>	7.66	353.1575	353.157	0.5
		C <sub>6</sub> H <sub>10</sub> O <sub>5</sub> Na <sup>+</sup>	[(M -C <sub>22</sub> H <sub>38</sub> O <sub>9</sub> )+Na] <sup>+</sup>	2.71	185.0419	185.042	0.1
AS5	622.3201 C <sub>29</sub> H <sub>50</sub> O <sub>14</sub>	C <sub>29</sub> H <sub>50</sub> O <sub>14</sub> Na <sup>+</sup>	[M+Na] <sup>+</sup>	20.23	645.3117	645.3093	2.4
		C <sub>23</sub> H <sub>40</sub> O <sub>9</sub> Na <sup>+</sup>	[(M -C <sub>6</sub> H <sub>10</sub> O <sub>5</sub> )+Na] <sup>+</sup>	100.00	483.2553	483.2564	1.1
		C <sub>18</sub> H <sub>30</sub> O <sub>7</sub> Na <sup>+</sup>	[(M -C <sub>6</sub> H <sub>10</sub> O <sub>5</sub> - C <sub>5</sub> H <sub>10</sub> O <sub>2</sub> )+Na] <sup>+</sup>	2.33	381.1848	381.1883	3.5
		C <sub>17</sub> H <sub>28</sub> O <sub>7</sub> Na <sup>+</sup>	[(M -C <sub>6</sub> H <sub>10</sub> O <sub>5</sub> - C <sub>6</sub> H <sub>12</sub> O <sub>2</sub> )+Na] <sup>+</sup>	9.52	367.1711	367.1727	1.6
		C <sub>6</sub> H <sub>10</sub> O <sub>5</sub> Na <sup>+</sup>	[(M -C <sub>23</sub> H <sub>40</sub> O <sub>9</sub> )+Na] <sup>+</sup>	3.42	185.0412	185.042	0.8
AS6	636.3249 C <sub>30</sub> H <sub>52</sub> O <sub>14</sub>	C <sub>30</sub> H <sub>52</sub> O <sub>14</sub> Na <sup>+</sup>	[M+Na] <sup>+</sup>	25.23	659.324	659.3249	0.9
		C <sub>24</sub> H <sub>42</sub> O <sub>9</sub> Na <sup>+</sup>	[(M -C <sub>6</sub> H <sub>10</sub> O <sub>5</sub> )+Na] <sup>+</sup>	100.00	497.2725	497.2721	0.4
		C <sub>18</sub> H <sub>30</sub> O <sub>7</sub> Na <sup>+</sup>	[(M -C <sub>6</sub> H <sub>10</sub> O <sub>5</sub> - C <sub>6</sub> H <sub>12</sub> O <sub>2</sub> )+Na] <sup>+</sup>	9.24	381.1893	381.1883	1
		C <sub>6</sub> H <sub>10</sub> O <sub>5</sub> Na <sup>+</sup>	[(M -C <sub>24</sub> H <sub>42</sub> O <sub>9</sub> )+Na] <sup>+</sup>	2.54	185.0408	185.042	1.2

137

138 **Table S5:** MS<sup>2</sup>-spectral data showing the annotations of class 3 *O*-acyl sugars elemental formulas, their  
 139 calculated monoisotopic mass, the elemental formula of fragment ions, their annotations, intensity and m/z  
 140 values compared to the calculated m/z values.

ID	Monoisotopic mass EI Formula	Elemental Formula Fragments	Annotation	Intensity	m/z Fragment	m/z Calc	Δppm
AS7	608.2680 C <sub>27</sub> H <sub>44</sub> O <sub>15</sub>	C <sub>27</sub> H <sub>44</sub> O <sub>15</sub> Na <sup>+</sup>	[M+Na] <sup>+</sup>	100.00	631.2554	631.2572	1.8
		C <sub>23</sub> H <sub>36</sub> O <sub>13</sub> Na <sup>+</sup>	[(M - C <sub>4</sub> H <sub>8</sub> O <sub>2</sub> )+Na] <sup>+</sup>	5.99	543.199	543.2048	5.8
		C <sub>19</sub> H <sub>32</sub> O <sub>9</sub> Na <sup>+</sup>	[(M - C <sub>8</sub> H <sub>12</sub> O <sub>6</sub> )+Na] <sup>+</sup>	40.35	427.1928	427.1939	1.1
		C <sub>14</sub> H <sub>22</sub> O <sub>7</sub> Na <sup>+</sup>	[(M - C <sub>8</sub> H <sub>12</sub> O <sub>6</sub> - C <sub>5</sub> H <sub>10</sub> O <sub>2</sub> )+Na] <sup>+</sup>	4.27	325.1222	325.1258	3.6
		C <sub>8</sub> H <sub>13</sub> O <sub>6</sub> <sup>+</sup>	[M - C <sub>19</sub> H <sub>31</sub> O <sub>9</sub> Na] <sup>+</sup>	5.32	205.0702	205.0706	0.4
		C <sub>5</sub> H <sub>5</sub> O <sub>2</sub> <sup>+</sup>	[C <sub>8</sub> H <sub>13</sub> O <sub>6</sub> - C <sub>2</sub> H <sub>4</sub> O <sub>2</sub> - HCHO - H <sub>2</sub> O] <sup>+</sup>	6.32	97.0291	97.0285	0.6
AS8	622.2837 C <sub>28</sub> H <sub>46</sub> O <sub>15</sub>	C <sub>28</sub> H <sub>46</sub> O <sub>15</sub> Na <sup>+</sup>	[M+Na] <sup>+</sup>	100.00	645.2746	645.2729	1.7
		C <sub>24</sub> H <sub>38</sub> O <sub>13</sub> Na <sup>+</sup>	[(M - C <sub>4</sub> H <sub>8</sub> O <sub>2</sub> )+Na] <sup>+</sup>	4.83	557.219	557.2204	1.4
		C <sub>23</sub> H <sub>36</sub> O <sub>13</sub> Na <sup>+</sup>	[(M - C <sub>5</sub> H <sub>10</sub> O <sub>2</sub> )+Na] <sup>+</sup>	2.55	543.2058	543.2048	1
		C <sub>22</sub> H <sub>34</sub> O <sub>13</sub> Na <sup>+</sup>	[(M - C <sub>6</sub> H <sub>12</sub> O <sub>2</sub> )+Na] <sup>+</sup>	1.48	529.1925	529.1891	3.4
		C <sub>20</sub> H <sub>34</sub> O <sub>9</sub> Na <sup>+</sup>	[(M - C <sub>8</sub> H <sub>12</sub> O <sub>6</sub> )+Na] <sup>+</sup>	38.54	441.2082	441.2095	1.3
		C <sub>16</sub> H <sub>26</sub> O <sub>7</sub> Na <sup>+</sup>	[(M - C <sub>8</sub> H <sub>12</sub> O <sub>6</sub> - C <sub>4</sub> H <sub>8</sub> O <sub>2</sub> )+Na] <sup>+</sup>	1.57	353.1538	353.157	3.2
		C <sub>15</sub> H <sub>24</sub> O <sub>7</sub> Na <sup>+</sup>	[(M - C <sub>8</sub> H <sub>12</sub> O <sub>6</sub> - C <sub>5</sub> H <sub>10</sub> O <sub>2</sub> )+Na] <sup>+</sup>	2.22	339.1365	339.1414	4.9
		C <sub>14</sub> H <sub>22</sub> O <sub>7</sub> Na <sup>+</sup>	[(M - C <sub>8</sub> H <sub>12</sub> O <sub>6</sub> - C <sub>6</sub> H <sub>12</sub> O <sub>2</sub> )+Na] <sup>+</sup>	4.11	325.125	325.1258	0.8
		C <sub>8</sub> H <sub>13</sub> O <sub>6</sub> <sup>+</sup>	[M - C <sub>20</sub> H <sub>33</sub> O <sub>9</sub> Na] <sup>+</sup>	6.09	205.0699	205.0706	0.7
C <sub>5</sub> H <sub>5</sub> O <sub>2</sub> <sup>+</sup>	[C <sub>8</sub> H <sub>13</sub> O <sub>6</sub> - C <sub>2</sub> H <sub>4</sub> O <sub>2</sub> - HCHO - H <sub>2</sub> O] <sup>+</sup>	6.79	97.0281	97.0285	0.4		
AS9	636.2993 C <sub>29</sub> H <sub>48</sub> O <sub>15</sub>	C <sub>29</sub> H <sub>48</sub> O <sub>15</sub> Na <sup>+</sup>	[M+Na] <sup>+</sup>	100.00	659.292	659.2885	3.5
		C <sub>25</sub> H <sub>40</sub> O <sub>13</sub> Na <sup>+</sup>	[(M - C <sub>4</sub> H <sub>8</sub> O <sub>2</sub> )+Na] <sup>+</sup>	2.92	571.2342	571.2361	1.9
		C <sub>24</sub> H <sub>38</sub> O <sub>13</sub> Na <sup>+</sup>	[(M - C <sub>5</sub> H <sub>10</sub> O <sub>2</sub> )+Na] <sup>+</sup>	3.64	557.2251	557.2204	4.7
		C <sub>23</sub> H <sub>36</sub> O <sub>13</sub> Na <sup>+</sup>	[(M - C <sub>6</sub> H <sub>12</sub> O <sub>2</sub> )+Na] <sup>+</sup>	2.38	543.2059	543.2048	1.1
		C <sub>21</sub> H <sub>36</sub> O <sub>9</sub> Na <sup>+</sup>	[(M - C <sub>8</sub> H <sub>12</sub> O <sub>6</sub> )+Na] <sup>+</sup>	33.45	455.2255	455.2251	0.4
		C <sub>17</sub> H <sub>28</sub> O <sub>7</sub> Na <sup>+</sup>	[(M - C <sub>8</sub> H <sub>12</sub> O <sub>6</sub> - C <sub>4</sub> H <sub>8</sub> O <sub>2</sub> )+Na] <sup>+</sup>	1.14	367.1748	367.1727	2.1
		C <sub>16</sub> H <sub>26</sub> O <sub>7</sub> Na <sup>+</sup>	[(M - C <sub>8</sub> H <sub>12</sub> O <sub>6</sub> - C <sub>5</sub> H <sub>10</sub> O <sub>2</sub> )+Na] <sup>+</sup>	1.41	353.1542	353.157	2.8
		C <sub>15</sub> H <sub>24</sub> O <sub>7</sub> Na <sup>+</sup>	[(M - C <sub>8</sub> H <sub>12</sub> O <sub>6</sub> - C <sub>6</sub> H <sub>12</sub> O <sub>2</sub> )+Na] <sup>+</sup>	5.64	339.1431	339.1414	1.7
		C <sub>8</sub> H <sub>13</sub> O <sub>6</sub> <sup>+</sup>	[M - C <sub>21</sub> H <sub>35</sub> O <sub>9</sub> Na] <sup>+</sup>	7.08	205.0699	205.0706	0.7
		C <sub>5</sub> H <sub>5</sub> O <sub>2</sub> <sup>+</sup>	[C <sub>8</sub> H <sub>13</sub> O <sub>6</sub> - C <sub>2</sub> H <sub>4</sub> O <sub>2</sub> - HCHO - H <sub>2</sub> O] <sup>+</sup>	6.08	97.0279	97.0285	0.6

141

142

143 Table S5 continued:

144

ID	Monoisotopic mass El Formula	Elemental Formula Fragments	Annotation	Intensity	m/z Fragment	m/z Calc	Appm
AS10	650.315 C <sub>30</sub> H <sub>50</sub> O <sub>15</sub>	C <sub>30</sub> H <sub>50</sub> O <sub>15</sub> Na <sup>+</sup>	[M+Na] <sup>+</sup>	100.00	673.305	673.3041	0.9
		C <sub>25</sub> H <sub>40</sub> O <sub>13</sub> Na <sup>+</sup>	[(M - C <sub>5</sub> H <sub>10</sub> O <sub>2</sub> )+Na] <sup>+</sup>	2.72	571.2365	571.2361	0.4
		C <sub>24</sub> H <sub>38</sub> O <sub>13</sub> Na <sup>+</sup>	[(M - C <sub>6</sub> H <sub>12</sub> O <sub>2</sub> )+Na] <sup>+</sup>	4.80	557.2244	557.2204	4
		C <sub>22</sub> H <sub>38</sub> O <sub>9</sub> Na <sup>+</sup>	[(M - C <sub>8</sub> H <sub>12</sub> O <sub>6</sub> )+Na] <sup>+</sup>	31.03	469.2377	469.2408	3.1
		C <sub>17</sub> H <sub>28</sub> O <sub>7</sub> Na <sup>+</sup>	[(M - C <sub>8</sub> H <sub>12</sub> O <sub>6</sub> - C <sub>5</sub> H <sub>10</sub> O <sub>2</sub> )+Na] <sup>+</sup>	1.95	367.1767	367.1727	4
		C <sub>16</sub> H <sub>26</sub> O <sub>7</sub> Na <sup>+</sup>	[(M - C <sub>8</sub> H <sub>12</sub> O <sub>6</sub> - C <sub>6</sub> H <sub>12</sub> O <sub>2</sub> )+Na] <sup>+</sup>	3.46	353.155	353.157	2
		C <sub>8</sub> H <sub>13</sub> O <sub>6</sub> <sup>+</sup>	[M - C <sub>22</sub> H <sub>37</sub> O <sub>9</sub> Na] <sup>+</sup>	5.67	205.07	205.0706	0.6
		C <sub>5</sub> H <sub>5</sub> O <sub>2</sub> <sup>+</sup>	[C <sub>8</sub> H <sub>13</sub> O <sub>6</sub> - C <sub>2</sub> H <sub>4</sub> O <sub>2</sub> - HCHO - H <sub>2</sub> O] <sup>+</sup>	3.36	97.0276	97.0285	0.9
AS11	664.3306 C <sub>31</sub> H <sub>52</sub> O <sub>15</sub>	C <sub>31</sub> H <sub>52</sub> O <sub>15</sub> Na <sup>+</sup>	[M+Na] <sup>+</sup>	100.00	687.3213	687.3198	1.5
		C <sub>26</sub> H <sub>42</sub> O <sub>13</sub> Na <sup>+</sup>	[(M - C <sub>5</sub> H <sub>10</sub> O <sub>2</sub> )+Na] <sup>+</sup>	1.69	585.2495	585.2517	2.2
		C <sub>25</sub> H <sub>40</sub> O <sub>13</sub> Na <sup>+</sup>	[(M - C <sub>6</sub> H <sub>12</sub> O <sub>2</sub> )+Na] <sup>+</sup>	4.84	571.2363	571.2361	0.2
		C <sub>23</sub> H <sub>40</sub> O <sub>9</sub> Na <sup>+</sup>	[(M - C <sub>8</sub> H <sub>12</sub> O <sub>6</sub> )+Na] <sup>+</sup>	30.06	483.2559	483.2565	0.6
		C <sub>17</sub> H <sub>28</sub> O <sub>7</sub> Na <sup>+</sup>	[(M - C <sub>8</sub> H <sub>12</sub> O <sub>6</sub> - C <sub>6</sub> H <sub>12</sub> O <sub>2</sub> )+Na] <sup>+</sup>	5.62	367.1723	367.1727	0.4
		C <sub>8</sub> H <sub>13</sub> O <sub>6</sub> <sup>+</sup>	[M - C <sub>23</sub> H <sub>39</sub> O <sub>9</sub> Na] <sup>+</sup>	5.41	205.0713	205.0706	0.7
		C <sub>5</sub> H <sub>5</sub> O <sub>2</sub> <sup>+</sup>	[C <sub>8</sub> H <sub>13</sub> O <sub>6</sub> - C <sub>2</sub> H <sub>4</sub> O <sub>2</sub> - HCHO - H <sub>2</sub> O] <sup>+</sup>	3.72	97.0285	97.0285	0

145

146

147 **Table S6:** MS<sup>2</sup>-spectral data showing the annotations of class 4 *O*-acyl sugars elemental formulas, their  
 148 calculated monoisotopic mass, the elemental formula of fragment ions, and their annotations, intensity and m/z  
 149 values compared to the calculated m/z values.

ID	Monoisotopic mass EI Formula	Elemental Formula Fragments	Annotation	Intensity	Fragment Mass	Calc	Appm
AS 12	650.2786 C <sub>29</sub> H <sub>46</sub> O <sub>16</sub>	C <sub>29</sub> H <sub>46</sub> O <sub>16</sub> Na <sup>+</sup>	[M+Na] <sup>+</sup>	100.00	673.2723	673.2678	4.5
		C <sub>25</sub> H <sub>38</sub> O <sub>14</sub> Na <sup>+</sup>	[(M - C <sub>4</sub> H <sub>8</sub> O <sub>2</sub> )+Na] <sup>+</sup>	3.31	585.2072	585.2153	8.1
		C <sub>24</sub> H <sub>36</sub> O <sub>14</sub> Na <sup>+</sup>	[(M - C <sub>5</sub> H <sub>10</sub> O <sub>2</sub> )+Na] <sup>+</sup>	4.42	571.1896	571.1997	10.1
		C <sub>21</sub> H <sub>34</sub> O <sub>10</sub> Na <sup>+</sup>	[(M - C <sub>8</sub> H <sub>12</sub> O <sub>6</sub> )+Na] <sup>+</sup>	51.73	469.205	469.2044	0.6
		C <sub>17</sub> H <sub>26</sub> O <sub>8</sub> Na <sup>+</sup>	[(M - C <sub>8</sub> H <sub>12</sub> O <sub>6</sub> - C <sub>4</sub> H <sub>8</sub> O <sub>2</sub> )+Na] <sup>+</sup>	8.37	381.1516	381.1519	0.3
		C <sub>8</sub> H <sub>13</sub> O <sub>6</sub> <sup>+</sup>	[M - C <sub>21</sub> H <sub>33</sub> O <sub>10</sub> Na] <sup>+</sup>	7.53	205.0727	205.0706	2.1
		C <sub>5</sub> H <sub>5</sub> O <sub>2</sub> <sup>+</sup>	[C <sub>8</sub> H <sub>13</sub> O <sub>6</sub> - C <sub>2</sub> H <sub>4</sub> O <sub>2</sub> - HCHO - H <sub>2</sub> O] <sup>+</sup>	3.72	97.0263	97.0285	2.2
AS 13	664.2942 C <sub>30</sub> H <sub>48</sub> O <sub>16</sub>	C <sub>30</sub> H <sub>48</sub> O <sub>16</sub> Na <sup>+</sup>	[M+Na] <sup>+</sup>	100.00	687.2861	687.2835	2.6
		C <sub>26</sub> H <sub>40</sub> O <sub>14</sub> Na <sup>+</sup>	[(M - C <sub>4</sub> H <sub>8</sub> O <sub>2</sub> )+Na] <sup>+</sup>	3.36	599.2303	599.231	0.7
		C <sub>25</sub> H <sub>38</sub> O <sub>14</sub> Na <sup>+</sup>	[(M - C <sub>5</sub> H <sub>10</sub> O <sub>2</sub> )+Na] <sup>+</sup>	4.52	585.2123	585.2153	3
		C <sub>22</sub> H <sub>36</sub> O <sub>10</sub> Na <sup>+</sup>	[(M - C <sub>8</sub> H <sub>12</sub> O <sub>6</sub> )+Na] <sup>+</sup>	47.27	483.2189	483.2201	1.2
		C <sub>17</sub> H <sub>26</sub> O <sub>8</sub> Na <sup>+</sup>	[(M - C <sub>8</sub> H <sub>12</sub> O <sub>6</sub> - C <sub>5</sub> H <sub>10</sub> O <sub>2</sub> )+Na] <sup>+</sup>	8.99	381.1548	381.1519	2.9
		C <sub>8</sub> H <sub>13</sub> O <sub>6</sub> <sup>+</sup>	[M - C <sub>22</sub> H <sub>35</sub> O <sub>10</sub> Na] <sup>+</sup>	10.54	205.0735	205.0706	2.9
		C <sub>5</sub> H <sub>5</sub> O <sub>2</sub> <sup>+</sup>	[C <sub>8</sub> H <sub>13</sub> O <sub>6</sub> - C <sub>2</sub> H <sub>4</sub> O <sub>2</sub> - HCHO - H <sub>2</sub> O] <sup>+</sup>	7.30	97.0284	97.0285	0.1
AS 14	678.3098 C <sub>31</sub> H <sub>50</sub> O <sub>16</sub>	C <sub>31</sub> H <sub>50</sub> O <sub>16</sub> Na <sup>+</sup>	[M+Na] <sup>+</sup>	100.00	701.2973	701.2991	1.8
		C <sub>27</sub> H <sub>42</sub> O <sub>14</sub> Na <sup>+</sup>	[(M - C <sub>4</sub> H <sub>8</sub> O <sub>2</sub> )+Na] <sup>+</sup>	1.58	613.2455	613.2467	1.2
		C <sub>26</sub> H <sub>40</sub> O <sub>14</sub> Na <sup>+</sup>	[(M - C <sub>5</sub> H <sub>10</sub> O <sub>2</sub> )+Na] <sup>+</sup>	2.58	599.2348	599.231	3.8
		C <sub>25</sub> H <sub>38</sub> O <sub>14</sub> Na <sup>+</sup>	[(M - C <sub>6</sub> H <sub>12</sub> O <sub>2</sub> )+Na] <sup>+</sup>	2.90	585.2137	585.2153	1.6
		C <sub>23</sub> H <sub>38</sub> O <sub>10</sub> Na <sup>+</sup>	[(M - C <sub>8</sub> H <sub>12</sub> O <sub>6</sub> )+Na] <sup>+</sup>	43.62	497.2343	497.2357	1.4
		C <sub>19</sub> H <sub>30</sub> O <sub>8</sub> Na <sup>+</sup>	[(M - C <sub>8</sub> H <sub>12</sub> O <sub>6</sub> - C <sub>4</sub> H <sub>8</sub> O <sub>2</sub> )+Na] <sup>+</sup>	2.15	409.1778	409.1832	5.4
		C <sub>18</sub> H <sub>28</sub> O <sub>8</sub> Na <sup>+</sup>	[(M - C <sub>8</sub> H <sub>12</sub> O <sub>6</sub> - C <sub>5</sub> H <sub>10</sub> O <sub>2</sub> )+Na] <sup>+</sup>	5.48	395.1664	395.1676	1.2
		C <sub>17</sub> H <sub>26</sub> O <sub>8</sub> Na <sup>+</sup>	[(M - C <sub>8</sub> H <sub>12</sub> O <sub>6</sub> - C <sub>6</sub> H <sub>12</sub> O <sub>2</sub> )+Na] <sup>+</sup>	4.11	381.1552	381.152	3.2
		C <sub>8</sub> H <sub>13</sub> O <sub>6</sub> <sup>+</sup>	[M - C <sub>23</sub> H <sub>37</sub> O <sub>10</sub> Na] <sup>+</sup>	6.83	205.0703	205.0706	0.3
C <sub>5</sub> H <sub>5</sub> O <sub>2</sub> <sup>+</sup>	[C <sub>8</sub> H <sub>13</sub> O <sub>6</sub> - C <sub>2</sub> H <sub>4</sub> O <sub>2</sub> - HCHO - H <sub>2</sub> O] <sup>+</sup>	3.96	97.0299	97.0285	1.4		
AS 15	692.3225 C <sub>32</sub> H <sub>52</sub> O <sub>16</sub>	C <sub>32</sub> H <sub>52</sub> O <sub>16</sub> Na <sup>+</sup>	[M+Na] <sup>+</sup>	100.00	715.3165	715.3148	1.7
		C <sub>28</sub> H <sub>44</sub> O <sub>14</sub> Na <sup>+</sup>	[(M - C <sub>4</sub> H <sub>8</sub> O <sub>2</sub> )+Na] <sup>+</sup>	2.46	627.2641	627.2623	1.8
		C <sub>26</sub> H <sub>40</sub> O <sub>14</sub> Na <sup>+</sup>	[(M - C <sub>6</sub> H <sub>12</sub> O <sub>2</sub> )+Na] <sup>+</sup>	5.74	599.2382	599.231	7.2
		C <sub>24</sub> H <sub>40</sub> O <sub>10</sub> Na <sup>+</sup>	[(M - C <sub>8</sub> H <sub>12</sub> O <sub>6</sub> )+Na] <sup>+</sup>	34.86	511.2514	511.2513	0.1
		C <sub>18</sub> H <sub>28</sub> O <sub>8</sub> Na <sup>+</sup>	[(M - C <sub>8</sub> H <sub>12</sub> O <sub>6</sub> - C <sub>6</sub> H <sub>12</sub> O <sub>2</sub> )+Na] <sup>+</sup>	6.68	395.1661	395.1676	1.5
		C <sub>8</sub> H <sub>13</sub> O <sub>6</sub> <sup>+</sup>	[M - C <sub>24</sub> H <sub>39</sub> O <sub>10</sub> Na] <sup>+</sup>	5.07	205.0733	205.0706	2.7
		C <sub>5</sub> H <sub>5</sub> O <sub>2</sub> <sup>+</sup>	[C <sub>8</sub> H <sub>13</sub> O <sub>6</sub> - C <sub>2</sub> H <sub>4</sub> O <sub>2</sub> - HCHO - H <sub>2</sub> O] <sup>+</sup>	2.24	97.0289	97.0285	0.4

150

151 **Table S7:** The concentration of each branched-chain fatty acids (BCFAs) released from *Manduca sexta*'s frass  
 152 and bodies as described by Weinhold and Baldwin (2011) and in the reconstructed mixture for the artificial diet  
 153 and spore germination medium.

	2-methyl butanoic acid	3-methyl butanoic acid	3-methyl pentanoic acid	4-methyl pentanoic acid	Total 4 BCFAs
ng/g frass within 2h	199.6	660.12	5110.2	248.72	6218.64
% in frass within 2h	3.2	10.6	82.2	4.0	
ng/ 3rd instar caterpillar within 2h	44.06	212.32	1210.57	37.17	1504.12
% in 3rd instar caterpillar within 2h	2.9	14.1	80.5	2.5	
mg/g diet	0.04	0.13	0.99	0.05	1.2
% in diet	3.2	10.6	82.2	4.0	
mg/mL medium	0.1	0.32	2.47	0.12	3
% in medium	3.2	10.6	82.2	4.0	

154

155

156 **Literature Cited**

157 Brockmüller T, Ling Z, Li D, Gaquerel E, Baldwin IT, Xu S. 2017. *Nicotiana attenuata* Data Hub (NaDH): an  
 158 integrative platform for exploring genomic, transcriptomic and metabolomic data in wild tobacco.  
 159 BMC Genomics 18(1): 79.

160 Kim J, Kang K, Gonzales-Vigil E, Shi F, Jones AD, Barry CS, Last RL (2012) Striking natural diversity in  
 161 glandular trichome acylsugar composition is shaped by variation at the acyltransferase2 locus in the  
 162 wild tomato *Solanum habrochaites*. Plant Physiology 160: 1854-1870

163 Weinhold A, Baldwin IT (2011) Trichome derived *O*-acyl sugars are a first meal for caterpillars that tags them  
 164 for predation. Proceedings of the National Academy of Sciences of the United States of America 108:  
 165 7855-7859

166

167

168 **Supplemental Methods**

169

170 ***O*-AS isolation and characterization**

171 To isolate *O*-AS from *N. attenuata* plants, we used a protocol similar to that of Van Dam and Hare  
172 (1998). All plant parts except the flowers were harvested. The stem was cut into small pieces (approx. 10cm).  
173 Around 1 kg of tissue was combined in a 5 L glass beaker (Schott) and soaked in 3 L of chloroform for 1h of  
174 stirring. Afterwards, the plant tissue was removed and the solvent was dried over sodium sulfate (anhydrous  
175 Sigma-Aldrich). The chloroform was removed in a rotary evaporator and the residue was resolved in acetonitrile  
176 (ACN) (VWR International) and sonicated. The ACN phase was partitioned 3 times against n-hexane (VWR  
177 International) (ACN: n-Hexane 1:2). The hexane phase was discarded and the ACN was removed in a rotary  
178 evaporator. The residue was solved in dichloromethane (DCM) (VWR) and partitioned 3 times against 1N  
179 tartaric acid (Sigma-Aldrich) 2 times against distilled water. Afterward, the DCM was removed and the glue-  
180 like, brownish yellow residue was kept under argon at 4°C until further use for bioassay and for MS<sup>2</sup>  
181 experiment. A small portion was dissolved in 40% methanol and analyzed by ultra-high performance liquid  
182 chromatography/ time-of-flight mass spectrometry (UHPLC/TOF-MS) to verify the extraction.

183 To fragment the *O*-AS for MS<sup>2</sup> experiment, extracted *O*-AS was dissolved in acetonitrile to a  
184 concentration of 1mg/mL. We used an Agilent 1100 HPLC system equipped with a DAD detector. Separation  
185 was achieved on a preparative Luna 5n C18 column (250 x 10 mm, 5µm, Phenomenex) connected to a Luna 5n  
186 C-18 guard column (50 x 10 mm, 5 µm) with a mixture of deionized water (0.1 % (v/v) formic acid + 0.1%  
187 (v/v) ammonia) (solvent A) and methanol (solvent B) at a flow rate of 3 mL/min. We used an isocratic gradient  
188 with 80 % of solvent B for 20 min and then increased to 95% of solvent B in 5 min. The post-run time was 7  
189 min. We collected fractions with a Foxy fraction collector (Isco) in 20 mL glass reaction tubes (Schott). 40  
190 fractions of 30 s were cut starting 5 min. after injection. The fractions were transferred to scintillation vials and  
191 the solvent was evaporated in a vacuum centrifuge (Eppendorf). The single fractions were then analyzed for  
192 their content by injection into an UHPLC/TOF-MS system (BrukerDaltonik, Bremen, Germany) with conditions  
193 described in Weinhold and Baldwin (2011).

194 For MS<sup>2</sup> experiments, 1µL of each fraction was separated using a Dionex RSLC system (Dionex,  
195 Sunnyvale, USA) with a Dionex Acclaim RSLC 120 C-18 column (150 x 2.1 mm, 2.2 µm). The following  
196 binary gradient was applied: 0 to 1 min isocratic 90% A (deionized water, 0.1% (v/v) acetonitrile (Baker, HPLC  
197 grade), and 0.05% formic acid), 10% B (acetonitrile and 0.05%formic acid); 1 to 9 min linear gradient to 80%  
198 B; isocratic for 2 min. The flow rate was 400 µL/min. MS detection was carried out with an ultra-high  
199 performance liquid chromatography/quadrupole time-of-flight mass spectrometry (UHPLC/Q-TOF-MS)  
200 (BrukerDaltonik, Bremen, Germany) operated in positive electrospray mode. Typical instrument settings were  
201 as follows: capillary voltage, 4500 V; dry gas temperature, 180 °C; dry gas flow, 10 L/min. Ions were detected  
202 from m/z 50 to 1400 at a repetition rate of 1 Hz. The instrument was operated in autoMS/MS mode at various  
203 CID voltages from 5 to 75 eV for sodium adducts. Mass calibration was performed using sodium formate  
204 clusters (10 mM solution of NaOH in 50/50% v/v isopropanol/water containing 0.2% formic acid). Elemental  
205 formula and mass were calculated with the ACD/Labs 12 ChemSketch calculating tool (ACD/Labs, Frankfurt,  
206 Germany).

207

208 **Analysis of *O*-AS acid composition**

209 One mg of an *O*-AS extract, obtained as described above, was saponified by adding 1 mL of a 0.2 M  
210 aqueous potassium hydroxide solution (Sigma-Aldrich). The solution was sonicated and kept in a sealed vial for  
211 24 h. The mixture was neutralized by adding 1 mL of a 0.2 M hydrochloric acid solution and then partitioned  
212 against 1.5 mL dichloromethane (VWR). One  $\mu$ L of the dichloromethane phase was then injected into a Varian  
213 3800 gas chromatograph equipped with a ZB-Wax-plus column (30m x 0.25mm x 0.25 $\mu$ m, Restek) and a flame  
214 ionization detector (GC-FID) (Agilent). The injector temperature was set to 230°C and the flow was 1 mL/min  
215 (constant flow). The oven was kept at 40°C for 5 min, then heated to 185°C at a rate of 5°C/min and finally with  
216 a rate of 30°C/min to 250 °C. The FID was operated at 250°C with 25 mL/min make up gas flow and 30  
217 mL/min hydrogen and 300 mL/min compressed air flow. The identities of the carboxylic acids were verified by  
218 the injection of authentic standards at a concentration of 50ng/ $\mu$ L. Retention indices were calculated in reference  
219 to an alkane standard mixture (C8-C20, Sigma-Aldrich).

220

221 ***O*-AS relative comparison analysis**

222 To cross-compare *O*-AS levels among different accessions or genotypes, we extracted leaf or trichome  
223 *O*-AS using a method described by Gaquerel et al. (2010). Briefly, approximately 100 mg of ground leaf  
224 materials (without the midvein) or 50mg trichome materials were homogenized with 2 steel beads by  
225 GenoGrinder 2000 (SPEX SamplePrep) at 1100 strokes per minute for 30 seconds and then extracted with 1 mL  
226 extraction solution (50 mM acetate buffer, pH 4.8, containing 40% methanol spiked with sucrose monolaurate  
227 (Sigma) with final concentration of 10 ng/ $\mu$ L as an internal standard. The extraction was done using  
228 GenoGrinder 2000 (SPEX SamplePrep) with 1100 strokes per min for 15 minutes. After centrifugation at  
229 13,200 rpm for 20 min at 4°C, the supernatant was collected and centrifuged again. 100  $\mu$ L of the supernatant  
230 was transferred to a HPLC vial and 1  $\mu$ L supernatants were separated using a HPLC Dionex RSLC system  
231 (Dionex, Sunnyvale, USA) with a Dionex Acclaim RSLC 120 C-18 column (150 x 2.1 mm, 2.2  $\mu$ m). The  
232 following binary gradient was applied: 0.5 min isocratic 90% A (deionized water, 0.1% (v/v) acetonitrile  
233 (Baker, HPLC grade), and 0.05% formic acid), 10% B (acetonitrile and 0.05%formic acid); 13 min linear  
234 gradient to 80% B; isocratic for 1.5 min. The flow rate was 400  $\mu$ L/min. MS detection was carried out with the  
235 UHPLC/TOF-MS system (Bruker Daltonik, Bremen, Germany) operated in positive electrospray mode. Typical  
236 instrument settings were described by Gilardoni et al. (2011) with some modification: capillary voltage, 4500 V;  
237 dry gas temperature, 200 °C; dry gas flow, 10 L/min. Ions were detected from m/z 50 to 1400 at a repetition rate  
238 of 2 Hz. Mass calibration was performed using sodium formate clusters (10 mM solution of NaOH in 50/50%  
239 v/v isopropanol/water containing 0.2% formic acid). The peak areas were integrated using extracted ion traces  
240 for the sodium adduct  $[M+Na]^+$  of each individual *O*-AS in the QuantAnalysis software version 2.0 SP1  
241 (Bruker Daltonics).The amount of each *O*-AS in plant tissue was normalized internal standard and the fresh  
242 weight of the tissue. Total *O*-AS was calculated by summing the normalized peak area of all 15 *O*-AS. The  
243 annotated 15 *O*-AS together with its m/z value and retention time (RT) is listed in Table S2.

244

245 **Extraction and analysis of phytohormones, secondary metabolites**

246 Phytohormone extraction was carried out as described previously by Gilardoni et al. (2011). Briefly,  
247 0.1 g of frozen leaf tissue was homogenized with a Genogrinder 2000 (BTC and OPS Diagnostics). One

248 milliliter of ethylacetate spiked with [9,10-<sup>2</sup>H<sub>2</sub>]-dihydro-JA and [<sup>13</sup>C<sub>6</sub>]-JA-Ile was added to the samples. After  
249 vortexing, the samples were centrifuged for 20 min at 12,000g (4°C). The organic phase was collected and  
250 evaporated to dryness, which were subsequently reconstituted in 300 mL of 70% (v/v) methanol/water for  
251 analysis on a Bruker Elite EvoQ Triple quad-MS equipped with a HESI (heated electrospray ionization) ion  
252 source using the MRM transitions described in (Schäfer et al., 2016). Each phytohormone (JA, JA-Ile) was  
253 quantified by comparing its peak area with the peak area of its respective internal standard as described in Wu et  
254 al. (2007). Phytohormone levels were quantified per gram fresh mass (µg/gFM).

255

256 Nicotine and hydroxygeranylinalool diterpene glycosides (HGL-DTGs) were extracted as described  
257 above for *O*-AS extraction. Analysis of these metabolites was done using an HPLC-DAD method described by  
258 Keinänen et al. (2001) with some modification. Briefly, after extraction, 1 µL of the supernatants were injected  
259 into an Agilent 1100 HPLC (Agilent HPLC 1100 Series, Palo Alto, CA) installed with a Chromolith  
260 FastGradient RP-18 (5032 mm; Merck, Darmstadt, Germany) endcapped 50 x 2 mm HPLC column (Lot No.  
261 HX802433 Merck, Darmstadt, Germany) attached to a Gemini NX RP18, 3µm, 2 x 4.6 mm precolumn  
262 (Phenomenex, Aschaffenburg, Germany) with a column oven set at 40°C. The mobile phase consisted of a mix  
263 of solvent A (0.1 % formic acid and 0.1 % ammonium hydroxide solution in water (pH 3.5) and solvent B  
264 (methanol) was used in a gradient mode (time/concentration min/% for A: 0:00/100; 0.50/100; 6.50/20;  
265 10:00/20; 15:00/100) with a flow rate 0.8 mL/min. Under these conditions, nicotine eluted at a retention time  
266 (RT) of 0.5 min (detected by UV absorbance at 260 nm. HGL-DTGs were detected by evaporative light  
267 scattering detector (ELSD) after HPLC separation at RT from 7.15 to 8.31 min. The peak areas were integrated  
268 using the Chromeleon software (ThermoFisher) and nicotine in plant tissue was quantified using external  
269 dilution series of standard mixtures of nicotine. The peak areas were quantified to estimate total HGL-DTGs  
270 contents and normalized it to tissue fresh mass. The method was described previously by Kaur et al. (2010)

271

#### 272 **Ir-construct sequence of *NaBCKDE1***

273 GAAGATGTTGGTTTCGGTGGTGTCTTTCGTTGCACTACTGGATTAGCTGACCGATTGGAAAACAG  
274 AGAGTTTTTAACTCCTTTATGTGAGCAGGGCATAGTTGGATTTGCTATTGGTCTGGCTGCAATG  
275 GACAATCGAGCTATAGCAGAAATTC AATTTGCAGATTATATTTTTTCCTGCTTTCGATCAGATCGTCA  
276 ATGAAGCTGCGAAATTCAGATATAGGAGTGGTAATCAGTTCAACTGCGGAGGCTTA ACTATAAGA  
277 GCACCTTATGGAGCTGTTGGACATGGCGGGCATTACCACTCACAAATCCCCTGAATCTTCTCTGCC  
278 ATGTTCCCTGGTATAAAGGTG

279

#### 280 **RNA extraction, cDNA synthesis and quantitative real-time PCR**

281 Total RNA was extracted from approximately 50 mg of frozen leaf or trichome tissue with Trizol  
282 (Thermo scientific, 15596-026), followed by DNase-I treatment (Thermo Scientific) according to the  
283 manufacturer's instructions. The cDNA was synthesized from 2 µg of total RNA using RevertAid First Strand  
284 cDNA Synthesis Kit (Thermo scientific, K162). Quantitative real-time PCR was conducted with synthesized  
285 cDNA using the Takyon™ qPCR Kits for SYBR® assays (Eurogentec) and gene-specific primer pairs using  
286 Mx3005P PCR cycler (Stratagene). Relative gene expression was calculated from calibration curves obtained by  
287 analysis of dilution series of cDNA samples, and the values were normalized by the expression of housekeeping

288 gene *N. attenuata* actin 7. All reactions were performed using the following qPCR conditions: initial  
289 denaturation step of 95°C for 3 min, followed by 40 cycles each of 95°C for 10 s, 60°C for 20s and 72°C for  
290 40s, followed by melting curve analysis of PCR products.

291

#### 292 **Primer sequences for SYBR-qPCR**

293 NaBCKDE1B\_For: 5'- GTATAAAGGTGGTCATCC-3'

294 NaBCKDE1B\_Rev: 5'- GCAACATATAATCATCTTCA-3'

295 Na\_Actin 7\_For: 5'- TTCTTCGTCTGGACCTTGCT-3'

296 Na\_Actin 7\_Rev: 5'- ATCATGGATGGCTGGAAGAG-3'

297 NaBCKDE1A\_1\_For: 5'- CAATACATTATGGCTCTAAC -3'

298 NaBCKDE1A\_1\_Rev: 5'- GTCCATTTTCAGAGAATAAG -3'

299 NaBCKDE1A\_2\_For: 5'- GACCCAGTAACTAGATTCAG -3'

300 NaBCKDE1A\_2\_Rev: 5'- GTAAATACATGCTTAATTGG -3'

301 NaAT1\_For: 5'- CTTATTCATCCAAGCAGTA -3'

302 NaAT1\_Rev: 5'- AAGATAGTACCTCTTCTGG -3'

303 NaAT2\_For: 5'- GTTCATCCAAAAGTTTTAC -3'

304 NaAT2\_Rev: 5'- TCACAGCATGGACTAATG -3'

305 NaASH1\_For: 5'- GAACTTTATGGCATAGTTG -3'

306 NaASH1\_Rev: 5'- GTAGTAAACTAAGACGGGTAG -3'

307 NaASH2\_For: 5'- GTTTTCTCTAAAGACGTCAC -3'

308 NaASH2\_Rev: 5'- TGACGTAAACAGTGATTCC -3'

309

#### 310 **Literature Cited**

311 Gaquerel E, Heiling S, Schoettner M, Zurek G, Baldwin IT (2010) Development and validation of a liquid  
312 chromatography-electrospray ionization-time-of-flight mass spectrometry method for induced changes  
313 in *Nicotiana attenuata* leaves during simulated herbivory. *Journal of Agricultural and Food Chemistry*  
314 58: 9418-9427

315 Gilardoni PA, Hettenhausen C, Baldwin IT, Bonaventure G (2011) *Nicotiana attenuata* LECTIN RECEPTOR  
316 KINASE1 suppresses the insect-mediated inhibition of induced defense responses during *Manduca*  
317  *sexta* herbivory. *The Plant Cell* 23: 3512-3532

318 Kaur H, Heinzel N, Schottner M, Baldwin IT, Galis I (2010) R2R3-NaMYB8 regulates the accumulation of  
319 phenylpropanoid-polyamine conjugates, which are essential for local and systemic defense against  
320 insect herbivores in *Nicotiana attenuata*. *Plant Physiology* 152: 1731-1747

321 Keinanen M, Oldham NJ, Baldwin IT (2001) Rapid HPLC screening of jasmonate-induced increases in tobacco  
322 alkaloids, phenolics, and diterpene glycosides in *Nicotiana attenuata*. *Journal of Agricultural and Food*  
323 *Chemistry* 49: 3553-3558

324 Schäfer M, Brütting C, Baldwin IT, Kallenbach M (2016) High-throughput quantification of more than 100  
325 primary- and secondary-metabolites, and phytohormones by a single solid-phase extraction based  
326 sample preparation with analysis by UHPLC-HESI-MS/MS. *Plant Methods* 12: 30

327 Van Dam NM, Hare JD (1998) Biological activity of *Datura wrightii* glandular trichome exudate against

328 *Manduca sexta* larvae. Journal of Chemical Ecology 24: 1529-1549  
329 Weinhold A, Baldwin IT (2011) Trichome derived *O*-acyl sugars are a first meal for caterpillars that tags them  
330 for predation. Proceedings of the National Academy of Sciences of the United States of America 108:  
331 7855-7859  
332 Wu J, Hettenhausen C, Meldau S, Baldwin IT (2007) Herbivory rapidly activates MAPK signaling in attacked  
333 and unattacked leaf regions but not between leaves of *Nicotiana attenuata*. The Plant Cell 19: 1096-  
334 1122  
335